Doctoral school in Health Sciences

Doctoral Programme in Drug Research

Development and biological characterization of novel ligands for protein-protein interaction-based effects of prolyl oligopeptidase

Tommi Kilpeläinen

Division of Pharmacology and Pharmacotherapy

Faculty of Pharmacy

University of Helsinki

Finland

DOCTORAL DISSERTATION

To be presented with the permission of the Faculty of Pharmacy,
University of Helsinki for public examination
in Viikki Biocenter 2, auditorium 1041, on 4th of June, 2021 at 12 o´clock
Helsinki 2021

Supervisors   Docent Timo T. Myöhänen, PhD
                   Division of Pharmacology and Pharmacotherapy
                   Faculty of Pharmacy
                   University of Helsinki
                   Finland

                   Docent Erik Wallén, PhD
                   Division of Pharmaceutical Chemistry and Technology
                   Faculty of Pharmacy
                   University of Helsinki
                   Finland

Reviewers   Professor Ingrid De Meester, PhD
                   Department of Pharmaceutical Sciences
                   University of Antwerp
                   Belgium

                   Professor Kai Kaarniranta, PhD, MD
                   School of Medicine/Institute of Clinical Medicine
                   Faculty of Health Sciences,
                   University of Eastern Finland
                   Finland

Opponent   Professor Ullamari Pesonen, PhD
                   Institute of Biomedicine
                   Faculty of Medicine
                   University of Turku
                   Finland

Custos   Professor Raimo K. Tuominen, PhD, MD
                   Division of Pharmacology and Pharmacotherapy
                   Faculty of Pharmacy
                   University of Helsinki
                   Finland

The Faculty of Pharmacy uses the Urkund system (plagiarism recognition) to examine all doctoral dissertations.

"The greatest enemy of knowledge is not ignorance, it is the illusion of knowledge"
-Stephen Hawking

ABSTRACT

Most neurodegenerative diseases (NDD) are characterized by accumulation of toxic protein species leading to the loss of movement and cognitive disorders. In the two most common NDD Parkinson´s disease (PD) and Alzheimer´s disease (AD), there are almost 60 million patients worldwide. In the U.S, there were one million PD patients and an estimated economic burden of 51.9 billion dollars in 2017. As there is no disease-modifying therapy available, NDD lead to loss of life quality and eventually to untimely death. Current drug therapies for PD can only relieve symptoms of the disease by increasing dopaminergic activity in the brain but they do not address the underlying mechanisms of the disease such as clearance of detrimental protein aggregates.

In previous studies, prolyl oligopeptidase (PREP) has been shown to negatively regulate autophagy and enhance the aggregation of alpha-synuclein (αSyn). Thus, PREP inhibitors have been shown to reduce aggregation and increase clearance of αSyn aggregates via enhanced autophagy. These mechanisms are mediated by protein-protein -interactions (PPI) of PREP with other proteins. Several small molecular inhibitors of PREP have been developed to target memory disorders, cancer, and NDD. However, none of these PREP inhibitors are in therapeutical use. The aim of this study was to investigate the effect of these inhibitors in two neurodegeneration-related functions of PREP: autophagy and αSyn dimerization. A further aim was to synthesize novel PREP ligands targeted to modulate these PPI-mediated functions of PREP. In the first part of this study, a structurally diverse set of 12 potent PREP inhibitors were tested in *in vitro* assays of autophagy and αSyn dimerization. The study revealed that the least potent inhibitor with IC_{50}-value of 1010 nM had the most prominent effect on reduction of αSyn dimers and enhancing autophagy, while some of the highly potent inhibitors with IC_{50}-value ranging from 0.32 to 1.2 nM did not have an effect on autophagy or αSyn dimerization.

In the second part of the study, novel 4-phenylbutanoyl-α-aminoacyl-2(*S*)-tetrazolyl-pyrrolidines were designed and synthesized to target αSyn dimerization. Synthesized compounds had IC_{50}-values ranging from 12 nM to 200 000 nM, but they all reduced αSyn dimerization in a cellular assay. Furthermore, molecular docking studies showed that these novel compounds have another putative binding mode to PREP compared to typical PREP inhibitors. These findings combined with the findings from the first part of the study suggest that the PREP mediated reducing effect on αSyn dimerization and enhancing effect on autophagy is not dependent on the magnitude of PREP inhibition but more likely due to conformational stabilization in PREP caused by ligand binding. Another speculative explanation is that PREP has another binding site, which modulates the conformation of PREP and thereby the PPI mediated functions of PREP.

In the third part of the study, a human αSyn transgenic mouse, carrying A30P and A53T point mutations in αSyn was characterized and evaluated as a model for early onset PD. The model displayed behavioral alternations at an early age with differences in dopaminergic neurotransmission in the nigrostriatal pathway and accumulation of oligomeric αSyn leading to decreased tyrosine hydroxylase in the striatum and substantia nigra. Furthermore, we evaluated the effect of seven days treatment by the novel PREP inhibitor, HUP-55, in this model. Results in this study showed that HUP-55 was able to decrease the level of oligomeric αSyn in the striatum and substantia nigra.

In summary, this study revealed and highlighted the disconnected structure-activity relationships between inhibition of the proteolytic activity and the PPI mediated functions of PREP. Moreover, this finding led to the development of a novel PREP ligand that was successfully tested in a PD mouse model.

TIIVISTELMÄ

Useimmissa keskushermostoa rappeuttavissa sairauksissa havaitaan haitallisten proteiinien kertymistä aivoihin, mikä johtaa kognitiivisiin oireisiin sekä tahdonalaisten liikkeiden häiriöihin. Yleisimmät keskushermostoa rappeuttavat sairaudet ovat Alzheimerin tauti ja Parkinsonin tauti, joita sairastaa lähes 60 miljoona ihmistä maailmassa. Keskushermostoa rappeuttaviin sairauksiin ei ole parantavaa tai taudin etenemistä hidastavaa hoitoa, joten ne johtavat väistämättä elämänlaadun heikentymiseen ja lopulta ennenaikaiseen kuolemaan. Tällä hetkellä Parkinsonin taudin oireita pystytään lievittämään lisäämällä keskushermoston dopamiinin aktiivisuutta aivoissa, mutta tämä ei vaikuta taudin taustalla oleviin mekanismeihin kuten haitallisten proteiinikertymien poistumiseen aivoista.

Aikaisemmissa tutkimuksissa on osoitettu, että prolyyli oligopeptidaasi (PREP) vähentää autofagiaa sekä lisää haitallisten alfasynukleiini-proteiinikertymien muodostumista. Toisaalta, PREP:n estämisen on osoitettu vähentävän alfasynukleiinin kertymistä keskushermostoon ja lisäävän sen puhdistumista autofagian avulla. Nämä prosessit johtuvat PREP:n ja muiden proteiinien välisistä suorista proteiini-proteiini vuorovaikutuksista. Lukuisia pienimolekyylisiä PREP-estäjiä onkin kehitetty muistihäiriöiden, syövän ja keskushermostoa rappeuttavien sairauksien hoitoon, mutta mikään näistä ei ole päätynyt markkinoille. Tämän tutkimuksen tarkoituksena oli tutkia PREP-estäjien vaikutusta kahteen keskushermoston rappeutumiseen liittyvään mekanismiin: autofagian säätelyyn ja alfasynukleiinin kertymiseen. Tämän tutkimuksen ensimmäisessä osassa selvitettiin 12 tehokkaan PREP-estäjän vaikutuksia autofagiaan ja alfasynukleiinin kertymiseen in vitro. Suurin vaikutus autofagiaan sekä alfasynukleiinikertymien vähentymiseen saatiin heikoimmalla PREP-estäjällä, samalla osa tehokkaista PREP-estäjistä eivät saaneet aikaan haluttuja vaikutuksia.

Toisessa osassa tätä tutkimusta suunniteltiin ja syntetisoitiin uudenlaisia PREP-ligandeja, joilla pyrittiin vähentämään alfasynukleiinin kertymistä. Osa näistä yhdisteistä olivat heikkoja PREP-estäjiä, mutta kaikki yhdisteet vähensivät kuitenkin alfasynukleiinin kertymistä solukokeessa. Lisäksi molekyylien telakointi tietokoneavusteisesti osoitti, että nämä yhdisteet sitoutuvat eri tavalla PREP:iin kuin tyypilliset PREP-estäjät. Yhdistettynä ensimmäisen osakokeen havaintoihin, voidaan todeta, että PREP-välitteinen alfasynukleiinin kertymisen vähentyminen ja autofagian kiihtyminen ei ole riippuvainen PREP eston voimakkuudesta vaan todennäköisesti ligandin sitoutumisen aiheuttamasta stabilisaatiosta tiettyyn PREP konformaatioon. On myös mahdollista, että PREP:ssa on toinen sitoutumispaikka ligandeille, mikä säätelee PREP:in konformaatiota ja näin ollen proteiini-proteiini-vuorovaikutuksisten säätelemiä mekanismeja.

Kolmannessa osakokeessa karakterisoitiin siirtogeenisen hiirilinjan, joka kantoi A30P ja A53T pistemutaatioita alfasynukleiinigeenissä, ominaisuuksia mallintaa aikaisen vaiheen Parkinsonin tautia. Hiirillä havaittiin muutoksia käytöksessä sekä dopaminergisessa signaalinvälityksessä sekä alfasynukleiinin kertymisessä, joka johti hermosolujen vähentymiseen aivojuoviossa ja mustatumakkeessa. Lisäksi tutkimme uuden PREP-ligandi HUP-55:en vaikutuksia näihin hiiriin seitsemän päivän hoidon jälkeen. Havaittiin, että HUP-55 vähensi kertyneen alfasynukleiinin määrää aivojuoviossa sekä mustatumakkeessa.

Yhteenvetona, tämä tutkimus paljasti epäjohdonmukaisuuden rakenneaktiivisuussuhteessa PREP:n aktiivisuuden estämisen sekä proteiini-proteiini-vuorovaikutus välitteisten PREP-vaikutusten välillä. Lisäksi tässä tutkimuksessa löytyi kokonaan uudenlainen PREP-ligandi, joka testattiin onnistuneesti Parkinsonin taudin hiirimallissa.

CONTENTS

LIST OF ORIGINAL PUBLICATIONS

This thesis is based on the following publications:

I   **Kilpeläinen TP**, Hellinen L, Vrijdag J, Yan X, Svarcbahs, R, Vellonen K.-S, Lambeir A-M, Huttunen H, Urtti A, Wallen, EAA, Myöhänen TT. The effect of prolyl oligopeptidase inhibitors on alpha-synuclein aggregation and autophagy cannot be predicted by their inhibitory efficacy. Biomed Pharmacother:128:110253, 2020

II   **Kilpeläinen TP**, Tyni JK, Lahtela-Kakkonen MK, Eteläinen TS, Myöhänen TT, Wallén EAA: Tetrazole as a Replacement of the Electrophilic Group in Characteristic Prolyl Oligopeptidase Inhibitors. ACS Med Chem Lett 10: 1635-1640, 2019

III   **Kilpeläinen TP**, Julku UH, Svarcbahs R, Myöhänen TT: Behavioural and dopaminergic changes in double mutated human A30P*A53T alpha-synuclein transgenic mouse model of Parkinson´s disease. Sci Rep 9: 17382, 2019

The publications are referred to in the text by their roman numerals. Reprints were made with the permission of the copyright holders. Supplementary results for study III are also presented.

Author's contribution to the original publications included in the Thesis:

Study I. The author participated in experimental design and wrote the first version of the manuscript. The author performed αSyn protein complementation assays, Western blot, and native gel electrophoresis with other authors, and performed all autophagy cell line assays. Data analysis of Western blot, αSyn protein complementation assays, and autophagy cell line assays was done by the author.

Study II. The author participated in experimental design and wrote the first version of the manuscript. The author synthesized novel compounds, measured IC_{50}-values, and performed the αSyn protein complementation assay. Data analysis was done by the author.

Study III. The author participated in experimental design and wrote the first version of the manuscript. The author performed behavioral testing with other authors, and conducted the analysis of behavioral tests and immunohistochemistry.

ABBREVIATIONS

5-HIAA	5-Hydroxyindole acid
5-HT	5-Hydroxydopamine
6-OHDA	6-hydroxydopamine
α-MSH	Alpha-melanocyte-stimulating hormone
αSyn	Alpha-synuclein
Aβ	Amyloid beta
ab	Antibody
AAV	Adeno-associated virus
Ach	Acetylcholine
Ac-SDKP	N-acetyl-serinyl-asparginyl-lysyl-proline
AD	Alzheimer´s disease
Aib	2-amino-isobutyricacid
ALP	Autophagy-lysosome pathway
ALS	Amyotrophic lateral sclerosis
AMC	7-Amido-4-methylcoumarin
ANOVA	Analysis of variance
APP	Amyloid precursor protein
AVP	Arginine vasopressin
BBB	Blood brain barrier
BCA	Bicinchoninic acid
CNS	Central nervous system
COPD	Chronic obstructive pulmonary disease
DAergic	Dopaminergic
DA	Dopamine
DAB	3,3'-Diaminobenzidine
DAT	Dopamine transporter
DMSO	Dimethyl sulfoxide
DMEM	Dulbecco's modified Eagle's medium
DPP	dipeptidyl peptidase
DOPAC	3,4-Dihdydroxyphenyl acetic acid
ELISA	Enzyme-linked immunosorbent assay
EM	Electron microscopy
ER	Endoplasmic reticulum
FBS	Fetal bovine serum
GABA	Gamma-aminobutyric acid
GAP-43	Growth cone associated protein 43
GAPDH	Glyceraldehyde-3-phosphate dehydrogenase
GFP	Green fluorescent protein
HD	Huntington´s disease
HEK	Human embryonic kidney
HPLC	High-performance liquid chromatography
HVA	Homovanillic acid
IHC	Immunohisto-chemistry

INFγ	Interferon gamma
IC$_{50}$	50 % inhibitory concentration
IP$_3$	Inositol 1,4,5-triphosphate
LB	Lewy bodies
LC3	Microtubule-associated protein light chain 3
LC3B-II	Microtubule-associated protein light chain 3 2B
LPS	Lipopolysaccharide
MeAla	*N*-Methyl-*L*-alanine
mHTT	Mutant huntingtin
mRNA	Messenger ribonucleic acid
MS	Multiple sclerosis
N2A	Mouse Neuro-2A
NDD	Neurodegenerative diseases
NMR	Nuclear magnetic resonance
OD	Optical density
PCA	Protein-fragment complementation assay
PD	Parkinson´s disease
PFA	Paraform-aldehyde
PGP	Prolyl-glycyl-proline
PI3K	Phosphoinositidie 3-kinase
PP2A	Protein phosphatase 2A
PPI	Protein-protein interaction
PREP	Prolyl oligopeptidase
PREPko	PREP knock-out
RFP	Red fluorescent protein
ROS	Reactive oxygen species
SAR	Structure-activity relationship
SAXS	Small-angle-X-ray scattering
SEM	Standard error of mean
SN	Substantia nigra
SNCA	Alpha synuclein coding gene
SP	Substance P
STR	Striatum
TDP-43	TAR DNA-binding protein 43
tg	Transgenic
TH	Tyrosine hydroxylase
TRH	Thyrotropin releasing hormone
UPS	ubiquitin–proteasomal system
WB	Western blot
wt	Wild-type
ZIP	Z-pro-prolinal-insensitive peptidase

1 INTRODUCTION

Neurodegenerative diseases (NDD) represent a growing public health challenge as the average age of people is increasing. NDD are a broad spectrum of disorders characterized by progressive loss of neurons in certain parts of the CNS (central nervous system). Depending on the part of the brain affected by neurodegeneration, the symptoms vary from cognitive and behavioral impairment to motor dysfunction and non-motor symptoms and combinations of these, all of which has been described previously in (Dugger and Dickson 2017). However, NDD are progressive by nature leading to a decreased quality of life and eventually to death, as there are no disease-modifying therapies available. The most common NDD are Alzheimer's disease (AD), Parkinson's disease (PD), amyotrophic lateral sclerosis (ALS), and Huntington's disease (HD).

Worldwide, there were 43.8 million patients with AD and other dementias and 6.1 million patients with PD in 2016 (Collaborators 2015). These diseases led to 2.4 and 210 000 deaths, respectively. In Finland, approximately 1 % of over 65 year old people have PD, with at total number of 16 000 patients (Atula 2018). In the U.S only, there were one million PD patients linked to an economic burden of 51.9 billion dollars in 2017 and the numbers are expected to grow to 1.6 million and 79 billion, respectively, during the next 20 years (Yang et al. 2020). Thus, much of the research effort is dedicated to finding therapeutic approaches for these disorders. The causes of NDD such as PD are not fully known and, the risk increases at the age above 60 years. The causes involve a range of factors from genetic mutations in different proteins to environmental factors such as oxidative stress causing neuroinflammation and dysfunction in protein processing and recycling eventually leading to cell death. In PD, dopaminergic (DAergic) neurons in the substantia nigra (SN) start to gradually degenerate leading to decreased dopamine (DA) levels and abnormal DAergic signaling in the nigrostriatal tract (DeMaagd and Philip 2015). Thus, clinical features of PD include bradykinesia, resting tremor, and rigidity of movements. In addition, non-motor symptoms such as constipation, fatigue, autonomic symptoms, and dementia at the later stage of the disease are known clinical features of PD. The treatment of PD relies on drugs that increases DA levels or acts as agonists of DA receptors. These approaches cannot reverse or even slow down PD and despite various research efforts, there is no disease-modifying therapy available for the disease. One reason for this might be that most therapies under development target only one pathological pathway behind NDD. As an example, targeting only alpha-synuclein (αSyn) protein aggregates with humanized IgG monoclonal antibody prasinezumab failed to achieve the primary therapeutic outcome in phase II although it was deemed to be safe and tolerable (Jankovic et al. 2018).

These diseases are usually diagnosed rather late as the symptoms occur only after advanced cell death has occurred. Therefore, specific *in vivo* biomarkers that could be detected from biofluids for detecting early onset of the diseases have a high priority among the research efforts. On the other hand, a drug therapy reviving degenerated neurons or merely stopping the progression of degeneration would be a breakthrough in the field of NDD. One promising drug development target for achieving this goal could be prolyl oligopeptidase (PREP) as it has been shown to regulate several pathways behind NDD such as protein processing via autophagy (Savolainen et al. 2014; Svarcbahs et al. 2020) and aggregation of αSyn (Brandt et al. 2008; Savolainen et al. 2015) via protein-protein interactions (PPI). Modulation of PPIs by small molecules is an emerging mechanism of action in drug discovery. In cells, PPIs form a complex network that regulates e.g. signal transduction (Arkin

and Whitty 2009), cell growth and differentiation (Loregian and Palù 2005) and protein processing and aggregation (Ballatore et al. 2011). Therefore, modulation of PPIs provides a drug target for NDD and cancer. As there are estimated to be 650 000 different PPIs in the human body and the interface of PPI is much larger than for example, interface in the active site of an enzyme in a protein-ligand interaction, identifying and studying PPIs is more difficult than classic small molecule drug discovery (Lu et al. 2020). Small molecules can affect these strong interactions by binding to the PPI interface enhancing or disrupting the interaction or by binding to the allosteric site, triggering conformational change, which can increase the affinity of two proteins or decrease it. Despite the challenging task of identifying PPIs and modulating them with small molecules, some small molecule modulators of PPIs have entered clinical trials for infectious diseases, such as HIV and several types of cancer and tumors (Lu et al. 2020). This thesis explores the role of PREP inhibitors as potential disease-modifying therapies for NDD. The aim is to clarify how PREP inhibitors modulate PPI mediated functions of PREP such as autophagy and αSyn aggregation.

2 REVIEW OF THE LITERATURE

2.1 ABNORMAL PROTEIN AGGREGATION IN NEURODEGENERATION

The pathophysiology of NDD involve common abnormalities in the conformation of different proteins that are typical for each disease. In PD, the hallmark protein is αSyn, in AD tau and beta-amyloid (Aβ), in amyotrophic lateral scleorsis (ALS) TAR DNA-binding protein 43 (TDP-43), and in HD mutant huntingtin protein (mHTT). Moreover, protein aggregation in these disorders is not limited to the hallmark protein only; Tau aggregates are seen in PD and in dementia with Lewy bodies (LB) and αSyn accumulation can be seen also in AD (Galpern and Lang 2006). In PD, one histopathological finding is formation of LB that are formed from over 300 proteins (Leverenz et al. 2007) while the main component is αSyn (Spillantini et al. 1997). αSyn is a 140 amino acid long protein mainly localized in pre-synaptic terminals (Iwai et al. 1995). Function of αSyn is not fully known but it has several functions e.g. in regulation of calmodulin activity, neuronal differentiation, DA biosynthesis, and vesicle trafficking (Emamzadeh 2016) . In addition, it has interactions with several proteins important for cell function such as tubulin (Chen et al. 2007) and dopamine transporter (DAT) (Lee et al. 2001). LB are also found in other NDD such as dementia with LB. LB are used as pathological hallmark of PD, but it is not fully known if LB contribute to neuronal death or if the formation of LB is a protective mechanism. It has been suggested that smaller pre-synaptic αSyn aggregates promote neurodegeneration instead of LBs (Kramer and Schulz-Schaeffer 2007) by causing synaptic dysfunction (Schulz-Schaeffer 2010). Additionally, these proteins can interact and enhance aggregation of other proteins (Li et al. 2016). Growing experimental evidence suggests that abnormal protein conformers are able to spread from cell-to-cell along neuronal pathways. Impairments in protein processing and degradation are also common features among NDD. Dysfunctional ubiquitin–proteasomal system (UPS) and autophagy-lysosome pathway (ALP) lead to accumulation of toxic proteins. Besides aggregation and clearance of abnormal proteins, NDD share other processes behind the progressive neuronal death such as oxidative stress, elevated programmed cell death, and neuroinflammation (Dugger and Dickson 2017).

As protein misfolding leading to cellular dysfunction is common for several NDD, it is important to understand the underlying mechanisms behind the process. Protein misfolding is a cascade of events where natively unfolded proteins form fibrils (Ogen-Shtern et al. 2016). This process is called aggregation. In physiological conditions, a protein folds to their lowest energy state where the hydrophobic residues are inside the protein and hydrophilic residues are on the surface of the protein. This folding process can be disrupted by different factors e.g. genetic mutations or environmental stress factors including endoplasmic reticulum (ER) and oxidative stress. Misfolding can lead to a situation where hydrophobic residues are exposed and able to interact with other proteins leading to aggregation. As an example, αSyn is an intrinsically disordered protein and duplications, triplications and point mutations in the αSyn coding gene SNCA are linked to early onset PD (Chartier-Harlin et al. 2004; Polymeropoulos et al. 1997; Singleton et al. 2003). Indeed, A53T, A30P and E46K mutations are shown to be more prone to aggregation and fibril formation using cryo-electron microscopy (EM) compared to the wild-type (wt) protein due to their different surface properties (de Oliveira and Silva 2019). However, cellular homeostasis aims to tackle these misfolded proteins via UPS and ALP which are the main degradation pathways for abnormal proteins (Rubinsztein 2006). Autophagy is a conserved intracellular degradation process regulated by the mammalian target of

rapamycin complex (mTORC1), which inhibits autophagy initiation by phosphorylating unc-like kinase 1 (ULK1). Activation of ULK1 leads to autophagosome formation from cellular membranes after activating it's downstream targets such as beclin-1 and phosphoinositide 3-kinase (PI3K). The autophagosome is formed from double membraned phagophore where LC3-II (light chain protein 3) is a key player. The autophagosome envelops the cargo and fuses with lysosomes in order to degrade the cargo. Autophagic receptors recognize specific cargos such as aggregated αSyn via p62. Also, APP (amyloid precursor protein), TDP-43, and mHTT are targets for autophagy (Frake et al. 2015). On the other hand genetic mutations in autophagic receptors, such as p62 or optineurin, have often been associated with neurodegeneration (Scrivo et al. 2018).

In conclusion, there are at least two main factors that lead to accumulation of harmful protein aggregates: environmental factors or mutations leading to misfolding of the protein and impairments in protein clearance.

2.2 OVERVIEW OF PROLYL OLIGOPEPTIDASE (PREP)

PREP (EC 3.4.21.26, also abbreviated PO, PE, PEP and POP) is a post-proline cleaving enzyme, found mainly in the cytosol (Dresdner et al. 1982; Polgár 1992). PREP is highly conserved in eukaryotes and is found in nearly all organisms from bacteria to mammals (Venäläinen et al. 2004). Proline (Pro) residues are present in many bioactive peptides, but most peptidases are unable to cleave those Pro containing residues due to the cyclic structure of Pro. However, PREP is one of the few proteases able to cleave peptides containing Pro. PREP has different limitations for its proteolytic activity; it is able to cleave only peptides shorter than 30 amino acids at the carboxyl side of an internal Pro, excluding Pro-Pro bonds (Koida and Walter 1976; Moriyama et al. 1988). PREP can also cleave peptide bonds with alanine, but with a much slower rate (Polgar 1992). In addition, PREP is shown to cleave bonds with other amino acids *in vitro* such as valine in octadecaneuropeptide (Leprince et al. 2006) and cystein in humanin (Bär et al. 2006). PREP belongs to the family of serine proteases (clan SC, family S9) including also dipeptidyl peptidase 4 (DPP4), oligopeptidase B, acylaminoacyl peptidases and tripeptidyl peptidases (Venäläinen et al. 2004). Other closely related peptidases to PREP are DPP2, DPP8, DPP9, and fibroblast activation protein (FAP) (Maes et al. 2005; Park et al. 1999). DPP enzymes are exopeptidases cleaving dipeptides while PREP is an endopeptidase and FAP shares both abilities.

2.2.1 PREP structure and dynamics

The crystal structure of porcine PREP with an inhibitor revealed that the enzyme is a cylinder shaped 80 kDa soluble protein of 710 amino acids consisting of two domains (**Fig 1.**) (Fülöp et al. 1998). Notably, porcine PREP has a 97 % identical amino acid sequence with human PREP. The catalytic domain consists of residues 1-72 and 428-710, which displays a characteristic α/β-hyrdolase fold with catalytic triad Ser554, His680, and Asp641. Residues 73-427 form a 7-bladed β-propeller domain arranged around the central tunnel and hides the active site. This β-propeller structure is the likely explanation for why PREP is unable to hydrolyze peptides longer than 30 amino acid residues. The β-propeller domain also contains several flexible loops such as loop A 189-209, loop B 577-608, and loop C 636-646, which are associated with substrate entry to the active site (Kaszuba et al. 2012; Szeltner et al. 2013). The two domains are covalently connected only from one side of PREP with a hinge in residues 72-79 and 424-434. The hinge is formed by the peptide chain passing twice from

one domain to the other. However, the crystal structure of PREP with an inhibitor does not explain how peptides can enter the active site. Although the cavity leading to the active site is large enough to accommodate peptides, the pore leading to the cavity is too small for peptide substrates (Rea and Fülöp 2006). Hence, it is necessary that the conformation of the enzyme changes during the substrate entry. It has been shown that the rate-limiting step of peptidase catalysis is not chemical but physical, most likely the conformational change needed for substrate binding (Polgár 1992).
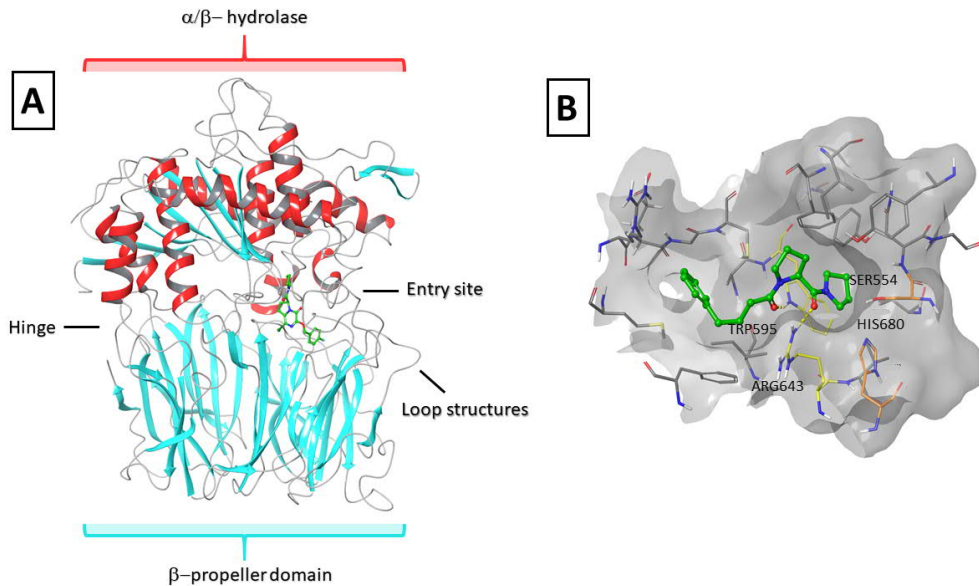

Figure 1. Structure of PREP. **A** 3D structure of PREP. **B** PREP inhibitor SUAM-1221 bound to the active site of PREP using molecular docking (Figures kindly provided by Henri Pätsi).

PREP exists in different conformations in cells which can be seen on native gel electrophoresis. Both native PREP and catalytically inactive S554A-PREP separates in to three distinctive bands believed to represent an open and a closed conformer, and an oligomer (Savolainen et al. 2015). It was shown by nuclear magnetic resonance (NMR) spectroscopy and small-angle X-ray scattering (SAXS) experiments that there is a slow equilibrium between the open and closed conformers and that the equilibrium could be shifted to a closed form by PREP inhibitors (López et al. 2016). The conformational dynamics of PREP involved in domain motions and the gating mechanism that allows the substrate to access the active site have been under intense investigation. Molecular dynamics simulations suggest that bilateral opening of the two domains around the hinge allows substrate entry (Kaushik et al. 2014). ^{15}N relaxation NMR studies proved that PREP is in equilibrium between an open and a closed form in solution (Kichik et al. 2011). Different PREP mutants have been created to study conformational changes of the enzyme. As an example, a PREP mutant where residue T597C forms a disulfide bond with Cys255 residue to keep the enzyme permanently closed leads to inactivation of the proteolytic activity indicating that a conformational change is required for the substrate entry as well (Szeltner et al. 2004). In addition, the movement of the flexible loops on the interface of PREP has a role in the function of the enzyme. When the active site is occupied, loop A forms a stronger interaction with loop B, compared to the situation when the active site is empty (Kaszuba et al. 2012). Furthermore, when loop A is locked to loop B with a disulfide bridge the enzyme activity is abolished. A recent study used hydrogen/deuterium exchange mass spectrometry to show that the binding of a PREP inhibitor stabilizes a network of loops, increasing the

conformational stability (Tsirigotaki et al. 2017). These findings suggest that the conformational state of PREP is crucial for the function of the enzyme and interaction with other proteins.

2.2.2 PREP expression and activity

Although PREP is mainly a cytosolic enzyme, significant PREP activities have been found in extracellular fluids such as cerebrospinal fluid, serum, urine, and seminal fluid (Goossens et al. 1996). In addition, a membrane bound type of the enzyme has been identified (Tenorio-Laranga et al. 2008). In the periphery, PREP is also found in the cell nuclei, indicating that PREP could have a role in cell proliferation and/or differentiation (Myöhänen et al. 2008b). However, in neuronal cells PREP is not present in cell nuclei (Myöhänen et al. 2008a; Myöhänen et al. 2008b), but instead in cytosol or bound to the rough ER and Golgi apparatus (Myöhänen et al. 2008a).

Expression of PREP has typically been studied by measuring PREP activity, determining mRNA levels, and by using immunostainings. Interestingly, expression levels do not always correlate with the enzymatic activity of PREP. As an example, IHC with a PREP-specific antibody shows high PREP levels in the SN of rats (Myöhänen et al. 2007). However, in another study no PREP activity was found in the SN (Gallegos et al. 1999). This may indicate that endogenous regulation of PREP activity occurs in certain areas of the body. In fact, a PREP-specific endogenous inhibitor has been identified (Salers 1994; Yoshimoto et al. 1982). This inhibitor has molecular weight of 6.5 kDa and is localized in the cytosol, but no further studies of its physiological role have been done. In 2013, α-2-macroglobulin was identified as an endogenous PREP inhibitor, but it is a large protein, so it is not likely the same inhibitor that was identified before (Tenorio-Laranga et al. 2013). On the other hand, hormones such as estradiol-17β, progesterone (Ohta et al. 1992), and cortisol (Yasuda et al. 1992) increase PREP activity in the periphery. Studies on rodents have shown that age affects the expression of PREP mRNA levels in the CNS in the way that they are lowest during adulthood and highest during embryogenesis and old age (Agirregoitia et al. 2007; Rampon et al. 2000).

In mammalian tissues, PREP is expressed throughout the body with the highest protein levels in the brain, kidney, testis, and thymus (Goossens et al. 1996; Myöhänen et al. 2008b). The highest PREP activities in peripheral organs have been reported from liver and testis (Myöhänen et al. 2008b). Recent studies have evaluated the role of PREP in spermatogenesis and fertility by WB and immunofluorescent analysis showing that infertile men have decreased PREP expression compared to fertile men (Venditti et al. 2020b) and cadmium-induced toxicity increased PREP expression in the testis of rats (Venditti et al. 2020a). In addition, human proliferating cells and various tumors have high PREP activities in the periphery (Goossens et al. 1996). PREP expression is also higher in malignant tumors compared to benign tumors indicating a role for PREP in formation of metastasis of tumors (Myöhänen et al. 2012b).

Generally, PREP activity is higher in the CNS than in the periphery and PREP is expressed in all regions of the brain, except in the corpus callosum, and mainly in neuronal cells rather than glial cells (Männisto et al. 2007). However, differences between brain regions in activity and levels of PREP do exist. In the rat brain, high PREP protein levels are found in SN, hippocampus, cerebellum, and caudate putamen; and in humans in caudate putamen hippocampus and cortex (Irazusta et al. 2002; Myöhänen et al. 2007). In the rat brain, PREP protein levels were also high in glutamatergic pyramidal neurons in cerebral primary motor and somatosensory cortices and GABAergic and cholinergic interneuron of thalamus and cortex (Myöhänen et al. 2008a).

2.2.3 Physiological role of PREP

PREP has been under keen investigation after its discovery in 1971. Several labs have been trying to solve the physiological role of PREP, but the mystery remains, in many aspects, still unsolved. In this chapter, different physiological roles of PREP are discussed in general.

2.2.3.1 Substrates of PREP

PREP was first discovered as an oxytocin cleaving enzyme (Walter et al. 1971). Later on, several endogenous substrates for PREP were identified. *In vitro* peptidase assays have shown that PREP is able to cleave most of the naturally occurring proline-containing small peptides (for review see (García-Horsman et al. 2007)). In addition, as PREP also cleaves alanine-containing bonds, but with a lower rate, octadecaneuropeptide was identified to be cleaved from alanine residue *in vitro*. However, the physiological relevance of these *in vitro* assays with purified PREP and substrate are debatable. The *in vitro* situation may not correlate with *in vivo* situation due the fact that the tested substrate may not be in the same cellular compartment with PREP in a physiological state. For some neuropeptides, such as substance P (SP) (Bellemère et al. 2003), arginine-vasopressin (AVP) (Bellemère et al. 2005; Toide et al. 1995b), thyrotropin releasing hormone (TRH) (Bellemère et al. 2003; Shinoda et al. 1995), α-melanocyte-stimulating hormone (α-MSH) (Bellemère et al. 2003), and angiotensin II (Serfozo et al. 2020) evidence of physiological relevance of peptide cleavage by PREP in *in vivo* setups is reported.

Maybe the most extensively studied neuropeptide as a PREP substrate is SP, the most abundant tachykinin in the CNS, which has a selective neurokinin 1 receptor (NK-1R) modulating inflammatory responses such as endothelial cell retraction, vascular smooth muscle dilation and cytokine release (Maggi 1995; 1997). SP is also associated with learning and memory (Schlesinger et al. 1986). PREP has shown to decrease the concentration of intracellular signaling molecule inositol 1,4,5-triphosphate (IP_3) in astroglioma cell line and PREP inhibition was found to amplify SP-mediated stimulation of IP_3 (Schulz et al. 2002). Administration of PREP inhibitors are reported to increase SP immunoreactivity in cortex and striatum of young rats (Toide et al. 1995a). Furthermore, PREP inhibition has been shown to improve results in memory trials in rats (Morain et al. 2002; Toide et al. 1997a; Toide et al. 1997b). However, this is in contrast to the findings that PREP inhibition does not alter SP immunoreactivity in the hippocampus, particularly for old rats (Bellemère et al. 2003; Toide et al. 1995b).

Similar findings have been reported with TRH, a neuropeptide connected to depression and cognition, among other functions. PREP inhibition increased TRH immunoreactivity in the hippocampus and cortex in rats (Bellemère et al. 2005; Shinoda et al. 1995; Toide et al. 1995a). In addition, PREP inhibition is reported to increase arginine-vasopressin (AVP) immunoreactivity in several brain areas in rats (Shinoda et al. 1995; Toide et al. 1995a; Toide et al. 1995b) and potentiate effects of AVP on memory and learning (Toide et al. 1997a). One report described single administration of a PREP inhibitor to increase α-MSH (also linked to learning and memory) immunoreactivity in the frontal cortex and hypothalamus in rats (Bellemère et al. 2003). However, chronic administration with the same PREP inhibitor failed to increase α-MSH immunoreactivity. These reports conclude that PREP might be involved with metabolism of neuropeptides. On the other hand, some results are inconsistent, and it would be important to see how overexpression or deletion of PREP *in vivo* changes these neuropeptide levels rather than investigate how treatment with a particular PREP

inhibitor alters the levels. In addition, most of the results were obtained by using immunostainings. Measurement of short-lived neuropeptides by immunostainings may not be a robust way to evaluate neuropeptide levels. Mass-spectrometry analysis might give results that are more reliable. However, a recent study showed that PREP is the main enzyme responsible for angiotensin II conversion to other angiontensins by using PREP knock out (ko) mice combined to pharmacological inhibition of PREP in wt animals (Serfozo et al. 2020). Other peptides that are suggested to have physiological relevance as PREP substrates according to *in vitro* tissue homogenate or cell assays are oxytocin, bradykinin, β-endorphin and neurotensin (García-Horsman et al. 2007).

PREP has also been suggested to be involved in cleaving of Aβ from APP (Ishiura et al. 1990). As APP is a 110 kDa protein and Aβ is a 34.7 kDa peptide, it is unlikely that PREP is able to cleave Aβ from APP. However, treatment with a PREP inhibitor has been reported to decrease Aβ in a senescence-accelerated mouse (Kato et al. 1997), but the mechanism of action remained unclear. The question remains if PREP is able to cleave already formed Aβ peptides or able to modulate the PPI needed for aggregation of Aβ. There are also reports showing that PREP is involved in the digestion of thymosin β4 in the formation of the tetrapeptide N-acetyl-Ser-Asp-Lys-Pro (Ac-SDKP), which promotes angiogenesis, reduces fibrosis and apoptosis, and has an anti-inflammatory effect (Kumar et al. 2016). Thymosin β4 is also a 43 residues long peptide and therefore too large for PREP to cleave directly. However, meprin-α metalloprotease first cleaves thymosin β4 and thereafter PREP can release Ac-SDKP from thymosin β4 and the formation of Ac-SDKP was blocked by using a PREP or a meprin-α inhibitor *ex vivo*.

2.2.3.2 Inflammation response

Neuronal inflammation is currently gaining more attention as a pathological factor behind NDD during recent years. PREP is also involved in several inflammatory diseases including obstructive pulmonary diseases (O'Reilly et al. 2009) and rheumatoid arthritis (Kamori et al. 1991) indicating a role in peripheral inflammation response. PREP was suggested to have a central role in the mechanism of neutrophilic inflammation in a pulmonary system (Gaggar et al. 2008). Indeed, PREP was shown to be involved in the formation of Pro-Gly-Pro (PGP), which is a pro-neutrophilic mediator, and PREP inhibition was able to reduce this neutrophilic response *ex vivo*. A recent study showed that high-fat-diet mice with disrupted PREP had decreased proinflammatory response and inflammation-associated factors in their liver tissue compared to wt high-fat-diet mice (Jiang et al. 2020). PREP expression levels respond to systemic inflammation and neuroinflammation when proinflammatory markers were measured from the brain and plasma of rats with portacaval shunt and ibuprofen treatment (Tenorio-Laranga et al. 2015). Despite the fact that PREP is not significantly expressed in microglia (Myöhänen et al. 2007), stimulation of microglia by lipopolysaccharide (LPS) and interferon γ (INFγ) leads to reduced intracellular and increased extracellular PREP activity, indicating that PREP is implicated in the inflammation response (Natunen et al. 2019). In addition, the tail-suspension test and IHC analysis showed that PREPko mice do not have a response in LPS treatment suggesting that PREP could have a role in the inflammatory response (Höfling et al. 2016). Moreover, inhibition of PREP leads to dose-dependent protection against LPS-stimulated human THP-1 and microglia cell supernatants, which are toxic for neuroblastoma cells, in human neuroblastoma SH-SY5Y cells (Klegeris et al. 2008).

2.2.3.3 Interaction partners for PREP

Although PREP is classified as a serine protease and has been mostly studied for its proteolytic activities, several interaction partners for PREP have been identified over the years. Interaction partners with evidence of physiological relevance are presented in **Table 1**. These PPI-mediated functions of PREP are not directly related to the proteolytic activity of PREP.

Table 1. Known interaction partners for PREP.

PREP interaction partners	Role of PREP	Function	Method	Reference
Tubulin	Binds to the C-terminus of α-tubulin	Axonal, transport, intracellular trafficking, protein secretion	Co-localization and yeast two-hybrid assays	(Schulz et al. 2005)
αSyn	Increases interaction of αSyn-αSyn	Aggregation of αSyn	*In vitro* aggregation assay with purified proteins (Brandt et al. 2008), Protein fragment complementation assay (PCA) with mouse neuroblastoma cells	(Brandt et al. 2008) (Savolainen et al. 2015)
GAP-43	Binds to GAP-43	Regulation of synaptic plasticity and growth cone mobility	Yeast-two-hybrid assay, co-localization, co-precipitation	(Di Daniel et al. 2009), (Szeltner et al. 2010)
GAPDH	Nuclear translocation of GAPDH	Cell death	Affinity column, Co-immunoprecipitation	(Matsuda et al. 2013)
PP2A	Negative regulation of PP2A	Autophagy induction and regulation of proliferation	Co-immunoprecipitation and PCA	(Svarcbahs et al. 2020)

One of the first found interaction partners for PREP was α-tubulin (Schulz et al. 2005). α-Tubulin is a part of the cytoskeleton structure involved in cell proliferation, intracellular transport, and vesicle secretion. PREP was shown to co-localize with α-tubulin and interact with it using a yeast two-hybrid screen. PREP inhibition did not alter the co-localization of PREP and α-tubulin, but interestingly it increased protein and peptide release in U-343 cells.

One important interaction partner of PREP is αSyn. αSyn is a 140 amino acids long protein found abundantly in the brain and it is the main component of LB and Lewy neurites which are considered to contribute to the pathophysiology of PD (Spillantini et al. 1997). It was shown *in vitro* using purified proteins that incubation of αSyn with PREP induced aggregation of αSyn (Brandt et al. 2008). Even though the effect was reversed by the inhibition of proteolytic activity of PREP, it is not related to the ability of PREP to hydrolyze αSyn due to the enzyme restrictions of substrate size. Later on it was shown that PREP increases αSyn dimerization by direct PPI with protein fragment complementation assay (PCA) in mouse neuroblastoma cells (Savolainen et al. 2015). Interestingly, the same effect was seen with the catalytically inactive PREP S554A mutant. PREP inhibition decreased the αSyn-αSyn interaction, but as expected, a PREP inhibitor did not have an effect on the ability of S554A mutant PREP to decrease the interaction. Interestingly, PREP inhibition also increased the interaction between αSyn and PREP, suggesting that PREP is involved in the αSyn-αSyn interaction process by having a certain conformation or allowing a dynamic equilibrium between different conformations that is favorable for the αSyn aggregation, which is then abolished when a PREP inhibitor stabilizes the conformation of the enzyme in another way.

PREP is shown to interact with GAP-43 (growth cone associated protein 43) (Di Daniel et al. 2009), which is considered as a regulator of synaptic plasticity, growth cone formation, and axon guidance. Both native and catalytically inactive PREP are able to bind to GAP-43. In addition, PREPko cells had altered growth cone dynamics and it could be restored with either wt PREP or catalytically inactive S554A-PREP. A later study proposed that PREP is involved in the regulation of neural cell adhesion molecules, but interaction with these molecules was not seen (Jaako et al. 2016). PREP overexpression in SH-SY5Y neuroblastoma cells reduced the levels of different species of neural cell adhesion molecules related to growth cone formation and axonal sprouting. Another study found that PREP co-localizes with GAP43 in the cell body and growth cones in differentiated HeLa cells (Szeltner et al. 2010). However, the authors suggests that the interaction between PREP and GAP-43 in physiological conditions is likely to be weak and indirect based on results acquired by several different methods such as native gel electrophoresis, enzyme-linked immunosorbent assay (ELISA), and co-precipitation.

Another protein that binds to PREP is glyceraldehyde-3-phosphate dehydrogenase (GAPDH). GAPDH is involved in energy production pathways but also initiates apoptosis. Binding of GAPDH to PREP was confirmed with an affinity column using recombinant human PREP in NB-1 cell extracts and confirmed with co-immunoprecipitation both *in vitro* and *in vivo* (Matsuda et al. 2013). Furthermore, PREP inhibition and deletion blocked the translocation of GAPDH to the nucleus and increased the survival of cytosine arabinoside promoted cell death in NB-1 cells. Another study showed that PREP inhibition prevented GAPDH translocation to mitochondria and nuclei and formation of reactive oxygen species (ROS) in toxin-treated monkey fibroblast cells CV1-P and SH-SY5Y cells (Puttonen et al. 2006).

Recently, the interaction of PREP with protein phosphatase 2A (PP2A) was established (Svarcbahs et al. 2020). PP2A is a holoenzyme known to regulate several physiological processes including the cell cycle and regulation of cell growth, phosphorylation of several kinases and proteins such as tau, and e.g. autophagy (Wong et al. 2015). Co-immunoprecipitation showed that PREP forms an interaction with the PP2A complex (Svarcbahs et al. 2020) to negatively regulate the activity of PP2A. In the PP2A complex, PREP regulates the interaction between the catalytic subunit of PP2A and its regulatory proteins, protein phosphatase methylesterase 1 (PME1) and protein phosphatase 2 phosphatase activator (PTPA). Deletion of PREP and PREP inhibition lead to increased PP2A

activity, while PREP overexpression or restoration reduced PP2A activity from cell culture to *in vivo*, emphasizing the importance of PREP in PP2A regulation (Svarcbahs et al. 2020). When the flexible loop B of PREP was mutated, the interaction with the subunit PP2Ac was decreased when assessing this by PCA. Additionally, PREP inhibition was shown to increase activity of PP2A leading to increased autophagy, as shown in earlier studies (Myöhänen et al. 2012a; Savolainen et al. 2014).

In conclusion, several interaction partners for PREP have been identified, suggesting that PREP has actions beyond its proteolytic functions. Interestingly, some of these interactions are not abolished when proteolytically inactive mutations of PREP were used. These reports and findings taken together strongly indicate that PREP has a physiologically relevant role as an interacting modulator of its protein partners which is distinct form its proteolytic activity on physiologically active peptides.

2.2.3.4 Other roles of PREP

There are also several other roles for PREP which might be related to the afore-mentioned roles of PREP, but as the mechanisms are not fully understood they cannot be confirmed. Evidence that PREP is also involved in cellular signaling via IP$_3$ and cell proliferation was reported with human neuroblastoma SH-SY5Y cells (Moreno-Baylach et al. 2011). In this study, PREP activity was decreased after induction of differentiation in the nucleus but increased in the cytoplasm. PREP inhibition, however, was able to postpone the onset of differentiation.

Dopamine-transporter (DAT) is an important part of the DAergic system. It transports extracellular DA to the cytosol and plays a role in DA depletion. PREP was found to regulate the phosphorylation of DAT in the nigrostriatal pathway of mouse, leading to elevated extracellular levels of DA in the striatum (Julku et al. 2018). PREP might also play a role in reproductive functions. PREPko mice had a smaller testes tubule and lumen diameter compared to wt mice. Furthermore, percentage of spermiated tubules, total sperm count and sperm motility is much higher in wt mice compared to PREPko mice (Dotolo et al. 2016). Another study showed that PREPko HEK-293 cells did not produce ROS as a response to oxidative stress compared to normal PREP expressing HEK-293 cells (Svarcbahs et al. 2018). Based on this, it seems likely that PREP is involved in the oxidative stress response of the cell.

2.2.4 PREP in disease

The above-mentioned features of PREP opens a road for connecting PREP to several diseases and physiological conditions. PP2A, inflammation, protein aggregation, autophagy, and ROS-production are interesting targets for drug discovery since they play a significant role in several diseases. In this chapter, the role of PREP in certain conditions relevant for this thesis is discussed.

2.2.4.1 Altered PREP levels in disease

Alternations in PREP levels and activity have been found in several disorders. In 1987, it was shown by fluorescence high performance liquid chromatography (HPLC) that patients with PD have lower PREP activity in the cerebral spinal fluid (CSF) compared to healthy controls (Hagihara and Nagatsu 1987). However, PREP activity in serum was not changed. Later it was shown that PREP activity

from brain samples of cases with PD, AD, HD, and dementia with LB had reduced 30-35 % compared to healthy controls (Mantle et al. 1996). PREP was also shown to co-localize with αSyn, AB, tau protein, and astroglia in post-mortem brain samples with PD and AD (Hannula et al. 2013). In addition, PREP activity was shown to decrease in plasma of patients having relapsed multiple sclerosis (MS), most likely due to the increase of endogenous PREP inhibitor (Tenorio-Laranga et al. 2010). Interestingly, the decreased PREP activity correlated with patient age and disability, suggesting that PREP may have a pathophysiological role in MS as well. Furthermore, the levels of endogenous PREP inhibitor α-2-macroglobulin was significantly decreased in patients with MS (Tenorio-Laranga et al. 2013). However, it is not clear if the decreased α-2-macroglobulin levels are related to pathophysiology of MS or if it is a protective mechanism, but this may give new diagnostic tools for MS.

Alternations in PREP activity have also been reported in mental disorders. Patients with major depression had lower PREP activity in plasma (Maes et al. 1994), and on the other hand patients with mania and schizophrenia had increased PREP activity in plasma (Maes et al. 1995). In depressed subjects, PREP activity in plasma was significantly increased during treatment with fluoxetine, but the treatment with neuroleptics in schizophrenic patients did not alter PREP activity in plasma. Bipolar disorder is also among diseases where alternations in PREP activity has been found. When patients with bipolar disorder were treated with lithium, PREP activity reduces (Maes et al. 1995) while untreated patients had elevated PREP activity levels (Breen et al. 2004). The fact that first line treatment in given mental disorder affects PREP activity is intriguing and indicates that PREP may play a role in the pathophysiology of the disease. It should be noted that these studies do not take into account the role of Z-pro-prolinal insensitive peptidase (ZIP), which is able to cleave similar substrates as PREP, thus some of the afore-mentioned effects might also be caused by ZIP (Breen et al. 2004). However, both PREP and ZIP levels had a significant decrease in patients with bipolar disorder undergoing lithium treatment, but no changes were observed in patients with schizophrenia.

Differences in PREP activities were also found in various tumors. In a study from 2010, PREP activity was analyzed from over one hundred tissue samples of normal and neoplastic tissues (Larrinaga et al. 2010). It was found that PREP activity was increased in colorectal adenomatous polyps, renal cell carcinoma, urothelial carcinoma, and neck squamous cell carcinoma. In another study, increased tissular and intratumoral blood PREP activities were detected in cancer patients (Liu et al. 2008). Increased PREP activity and expression have also been demonstrated in colorectal cancer. It was shown that PREP activity was higher in colorectal cancer patients than in healthy individuals (Larrinaga et al. 2014). More importantly, the high PREP activity was connected to worse overall and disease-free survival suggesting that PREP could be a diagnostic tool for colorectal cancer.

The above discussed altered PREP activities in different diseases or disorders may just be a scratch to the surface for the role of PREP in disease. It is impossible to say if altered PREP activity is due to the stress response caused by the disorder or is it a part of the pathophysiology of disease. In addition, measurements of PREP activity from tissue samples are susceptible to alternations as PREP degrades easily depending on tissue processing and storing. However, PREP activity can be measured from CSF and serum and therefore could potentially be used as a diagnostic tool.

2.2.4.2 Neurodegeneration

PREP was first linked to neurodegeneration as an enzyme degrading neuropeptides. More importantly, later discoveries have shown that PREP is linked in neurodegeneration through several

different pathways such as regulation of apoptosis, reducing toxic effects of aggregated proteins, reducing stress caused by ROS, inflammation, and increasing PP2A activity.

As discussed above, PREP interacts with αSyn leading to oligomerization of αSyn (Brandt et al. 2008; Savolainen et al. 2015). As well, PREP inhibition has been shown to increase cell viability in oxidative stress (Myöhänen et al. 2012a) and rotenone-treated αSyn overexpressing cells (Dokleja et al. 2014). A recent report showed that removal of PREP reduces αSyn toxicity in cells and *in vivo* (Svarcbahs et al. 2018). In this study, adeno-associated virus (AAV) carrying human αSyn was injected unilaterally above the SN of PREPko mice but did not affect on locomotor activity or behaviour in cylinder test compared to wt mice. However, restoration of PREP in PREPko animals led to impaired locomotor activity and paw use in cylinder test similarly to wt mice with αSyn injection. In addition, αSyn phosphorylated at Ser129, proteinase K resistant αSyn levels, and tyrosine hydroxylase (TH) positive cells were decreased in PREPko animals with αSyn and PREP injection compared to PREPko animals without PREP restoration, suggesting that PREP increases toxicity of αSyn. In an A53T/A30P mutant αSyn overexpressing cell line inhibition of PREP was able to reduce aggregation of αSyn induced by oxidative stress (Myöhänen et al. 2012a). Cells treated with a PREP inhibitor had significantly less αSyn inclusions and aggregated αSyn as well as increased cell viability. The effect was confirmed *in vivo* using A30P αSyn mutant mice, where PREP inhibitor treatment reduced αSyn immunoreactivity and soluble αSyn protein. In later studies, PREP inhibitor treatment was shown to restore motor impairment in a PD mouse model (Svarcbahs et al. 2016). In this study, AAV-αSyn viral vector was injected above the SN of wt animals causing reduced DA release and motor impairment in cylinder test. Decreased TH positive immunoreactivity in SN and increased αSyn and oligomeric αSyn particles in striatum (STR) and SN were also observed. Interestingly, four-week treatment with a PREP inhibitor after the behavioral symptoms emerged, restored these pathological findings to the control level. In addition, PREP inhibition was recently demonstrated to increase degradation of pre-formed αSyn fibrils in astroglial cells and neuroblastoma cells, highlighting the potential of PREP inhibition in αSyn aggregation-related diseases (Rostami et al. 2020).

Another protein related to NDD that has been studied in PREP research is tau. PREP localizes in microtubules (Schulz et al. 2005) similar to tau, and PREP inhibition has been shown to increase the small tau peptide sequence in rat CNS (Nolte et al. 2009). PREP and tau also have a similar association in the AD post-mortem brain as αSyn in the PD post-mortem brain (Hannula et al. 2013). In addition, PP2A, an interaction partner of PREP, regulates tau phosphorylation directly and in directly via activating glycogen synthase kinase 3β (Qian et al. 2010). Thus, it can be hypothesized that increased PP2A activity via PREP inhibition could lead to decreased tau hyperphosphorylation and aggregation. However, in order to confirm the role of PREP in the tau aggregation process, PREP inhibitors need to be studied in preclinical tau models.

Dysfunctional protein degradation systems UPS and ALP also have an important role in pathophysiology leading to proteinopathies and neurodegeneration. Interestingly, the above-mentioned effects on αSyn aggregation may be better explained by the ability of PREP inhibitors to increase autophagy rather than reduce αSyn dimerization (Myöhänen et al. 2012a; Savolainen et al. 2014). PREP inhibition induces autophagy via PP2A activation that activates the class III PI3K beclin1 pathway leading to increased clearance of αSyn (Savolainen et al. 2014; Svarcbahs et al. 2018). The effect of PREP inhibition on autophagy is significant since it is able to overcome the effect of proteosomal inhibitor lactacystin (Myöhänen et al. 2017). In this study, A53T or A30P mutant αSyn overexpressing cells were treated with lactacystin with or without a PREP inhibitor. PREP

inhibition reduced insoluble αSyn particles and the levels of protein accumulation marker p62 while the level of autophagosome marker LC3B-II was increased.

Oxidative stress leading to mitochondrial damage, changes in energy metabolism and eventually to protein aggregation is another common feature of several NDD. PREP seems to have a role in redox regulation as well. HEK-293 PREPko cells did not show increased ROS production after oxidative stress compared to wt cells (Svarcbahs et al. 2018). In addition, reduced oxidative stress was observed in PREP inhibitor-treated CV1-P cells exposed to 6-hydroxydopamine (6-OHDA), a common mitochondrial toxin (Puttonen et al. 2006) and in αSyn overexpressing cells (Dokleja et al. 2014). Puttonen et al. (2006) suggested that the mechanism behind this is reduced GAPDH translocation as described earlier, but PP2A has also been connected with the oxidative stress response (Elgenaidi and Spiers 2019). Regulation of neuronal apoptosis is another NDD-related function suggested where PREP is involved. PREP inhibitor ONO-1603 has been shown to protect age-induced apoptosis and suppress GAPDH overexpression in rat cerebral cortical primary neurons (Katsube et al. 1999). However, other reports indicate that at least some PREP inhibitors such as JTP-4819 and Fmoc-Pro-Pro-CN are not able to modulate apoptosis in neurotoxin models (Fiedorowicz et al. 2001; Puttonen et al. 2006).

As discussed above, PREP is involved in several pathological pathways behind neurodegeneration. In addition, inhibition of PREP by small molecule inhibitors is able to tackle most of these pathological routes. These routes include reduction of neuroinflammation, oxidative stress, harmful protein aggregation and increased clearance of abnormal proteins leading to reduced toxicity and increased neuronal survival. PREP inhibition have been verified to be an effective treatment in *in vivo* models of PD, and these mechanisms are also present in other NDD such as AD and HD. Indeed, PREP inhibitor KYP-2047 was able to attenuate mutant Htt aggregation and toxicity in lactacystin-treated HeLa cells (Norrbacka et al. 2019). Thus, PREP inhibitors have therapeutic potential in several different NDD.

2.1.4.3 Other diseases

The role of PREP in several other disorders has been studied extensively. Besides neurodegeneration, PREP has been suggested to be a therapeutic target for cognitive and, mental disorders, several types of cancers and tumors, chronic obstructive pulmonary disease (COPD), parasite infections, hypertension, and celiac disease.

Memory enhancement and cognitive improvement by increased levels of certain neuropeptides suggested to be cleaved mainly by PREP was thought to be the main function of PREP. Several PREP inhibitors improve memory and learning in animal models as discussed in chapter 2.3.2 and some of these compounds have also advanced to clinical trials as memory enhancers (Morain et al. 2002; Umemura et al. 1997). Although these PREP inhibitors were proven safe and orally bioavailable, the clinical trials were discontinued, probably due to the lack of effect.

Altered PREP activity levels have been observed in mental disorders, but the exact physiological role of PREP in these disorders is not fully understood. In 1999, a study showed that *dictyostelium* mutants lacking PREP do not respond to lithium treatment by reducing intracellular IP_3 concentration (Williams et al. 1999). Later, it was shown that PREP modulates the inositol phosphate signaling and has been shown to negatively modulate multiple inositol polyphosphate phosphatase activity increasing IP_3 levels (Schulz et al. 2002). In addition, it was shown that PREP acts via multiple

inositol polyphosphate phosphatase to control gene expression of the inositol monophosphatase gene, which is associated with risk of bipolar disorder (King et al. 2010). However, more studies are required to confirm the role of PREP in the inositol signaling pathway and mood disorders.

Particularly elevated PREP activity is also linked to several types of cancers and tumors. PREP inhibition by small molecules or siRNA has been reported to suppress cancer cell growth in human neuroblastoma cells (Sakaguchi et al. 2011) and in gastric cancer cells (Suzuki et al. 2013). More recently, it was found that PREP inhibition inhibited proliferation of human breast cancer cells by interrupting the G_1-phase (Tanaka et al. 2017). These effects are hypothesized to be mediated by the interaction of PREP with GAPDH leading to decreased energy metabolism in cancer cells. Tumor growth suppression by PREP inhibition is also reported in mice (Jackson et al. 2015). In this study, PREP inhibition led to reduced tumor growth and reduced number of microvessels in tumors in mice with human colon cancer tumors.

The role of PREP in the inflammation process in the periphery led to investigation of a connection between PREP and COPD. PREP increases the formation of PGP, which leads to increased neutrophil migration to the area and an increased inflammatory response typical of COPD (Gaggar et al. 2008). In addition, PREP activity, along with PGP, was shown to increase in epithelial and neutrophilis cells in lung tissue of mice that were exposed to cigarette-smoke (Braber et al. 2011). PREP inhibition was shown to decrease neutrophil elastase levels in a simulated extracorporeal circulation model (Yoshimura et al. 2003) and reduce inflammation chemotaxis in mouse and human neutrophils (Russell et al. 2019). However, the effects of PREP inhibitors in lung inflammation models need to be studied further.

PREP was also found to be an essential part of the ability of the parasite *Trypanosome cruzi* to cause Chagas disease. The PREP of *T.cruzi* degrades the collagens and extracellular matrix in host cells allowing the parasite to spread (Santana et al. 1997). Moreover, it was shown that inhibitors for PREP of *T.cruzi* were able to prevent the *in vitro* invasion of rodent muscle cells by trypomastigotes in a concentration dependent manner (Grellier et al. 2001).

In hypertension, PREP is responsible for angiotensin II conversion to angiotensin (1-7) (Serfozo et al. 2020). Angiotensin II is the main component in the renin-angiotensin-system and angiotensin (1-7) is a downstream peptide of angiotensin II. PREP-deficient mice had decreased angiotensin (1-7) levels and delayed recovery of hypertension compared to wt mice after angiotensin II infusion-induced hypertension. PREP inhibition also reduced angiotensin (1-7) formation in serum and in lung lysates of wt mice. The physiological importance of PREP in angiotensin II conversion is based on the reduction of the overactivity of angiotensin II and on the positive effects mediated by angiotensin (1-7).

PREP has also been studied in the context of celiac disease. PREP from *Flavobacterium meningosepticum*, *Sphingomonas capsulate* and *Myxococcus xanthus* was shown to degrade immunogenic gluten (Shan et al. 2004). Immunogenic gluten is Pro-rich but its size is over 30 amino acids, and therefore, mammalian PREP cannot cleave it. As proteolysis-resistant gluten peptides are the culprits for immunotoxic reactions in celiac disease, the PREP enzyme might be potential treatment.

2.3 PREP AS A TARGET OF DRUG DISCOVERY

PREP plays a role in several different physiological and pathophysiological processes related to neurodegeneration, tumor growth, and inflammation (**Fig. 2**) PREP has been a fascinating target for drug discovery for the past 30 years, however, no PREP inhibitors are in use for any therapeutic area. Modulation of PREP mediated PPIs could be a new strategy for treatment of NDD and other previously described disorders. In this chapter, PREP inhibitors are discussed from the view of drug design, structure-activity relationship (SAR), and biological effects.
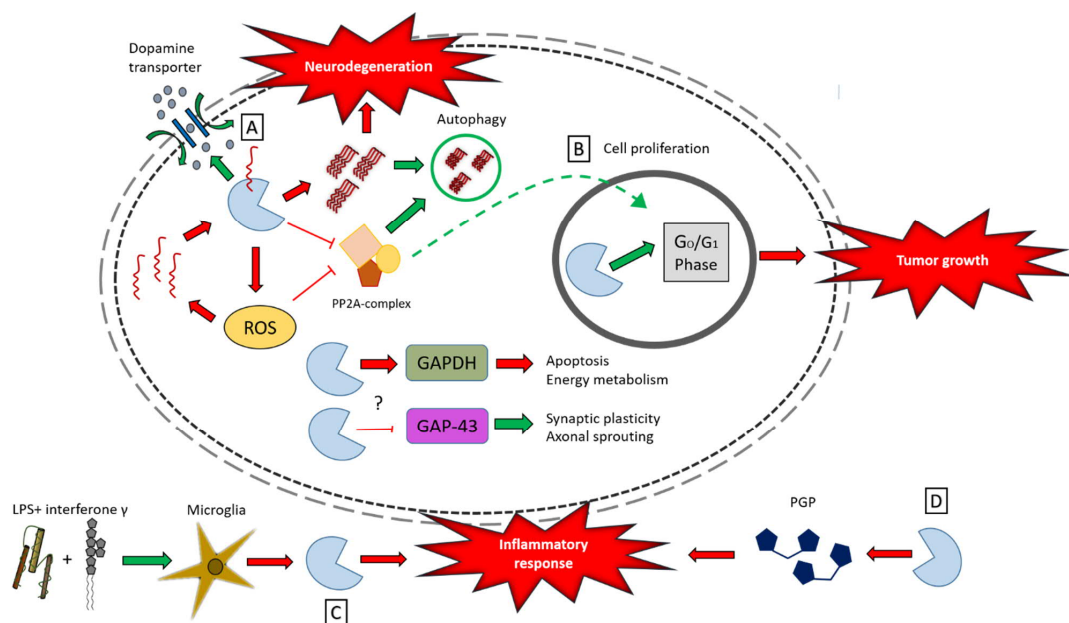

Figure 2. Summary of pathophysiological processes where PREP has a regulatory role. **A.** PREP has several roles in neurodegeneration. PREP increases the aggregation of αSyn and reduces the activity of protein phosphatase 2A (PP2A) via direct protein-protein interaction leading to e.g., declined autophagy. Decreased clearance of abnormal proteins such as αSyn, mutant huntingtin, or tau leads to toxicity and neuronal death. Furthermore, PREP increases the production of reactive oxygen species (ROS), which accelerates the aggregation of abnormal proteins and damages energy metabolism, creating a vicious cycle. In addition, PREP regulates the dopamine transporter phosphorylation rate, which leads to decreased extracellular and increased intracellular dopamine levels. **B.** PREP regulates cell proliferation and is connected to several types of tumors in the periphery. PREP inhibition is able to reduce tumor growth by modulating the G0/G1 phase of cell cycle. In addition, PP2A, an interaction partner of PREP, also modulates cell cycle. **C.** PREP is involved in the inflammatory process in the central nervous system as stimulation of microglia leads to increased extracellular PREP activity. **D.** PREP is also part of the neutrophil pathway in systemic inflammation by increasing the amount of pro-neutrophilic mediator Pro-Gly-Pro (PGP). Additionally, PREP is involved in energy metabolism and apoptosis by activating GAPDH via direct interaction. The interaction with GAP-43 is linked to synaptic plasticity and axonal sprouting, but the relevance of this interaction is not fully known. All of these pathological routes are potential targets for drug development and PREP ligands modulating these functions of PREP could have therapeutic potential.

2.3.1 PREP inhibitors

Typical PREP inhibitors are peptidic compounds with an acyl-L-prolyl-pyrrolidine framework, where the C-terminal pyrrolidine ring binds to the same subsite of the active site of the enzyme as the important L- proline residue of the substrate. (**Fig. 3**). The PREP inhibitor Z-pro-prolinal (ZPP; **Fig. 3**) has been crystallized with porcine PREP and analysis of the resulting structure using molecular modelling showed that the carbonyl groups of ZPP form hydrogen bonds to Arg643 and Trp595 residues of the enzyme (Van Der Veken et al. 2012). In addition, the electrophilic aldehyde group in the 2*S*-position in the pyrrolidine ring forms a reversible covalent hemiacetal adduct with the Ser554 residue of the enzyme, resulting in slow tight binding inhibition. The electrophile is in the corresponding position on the pyrrolidine ring as the carboxyl group in L-proline. The formed reversible covalent bond "anchors" the inhibitor to the active site.
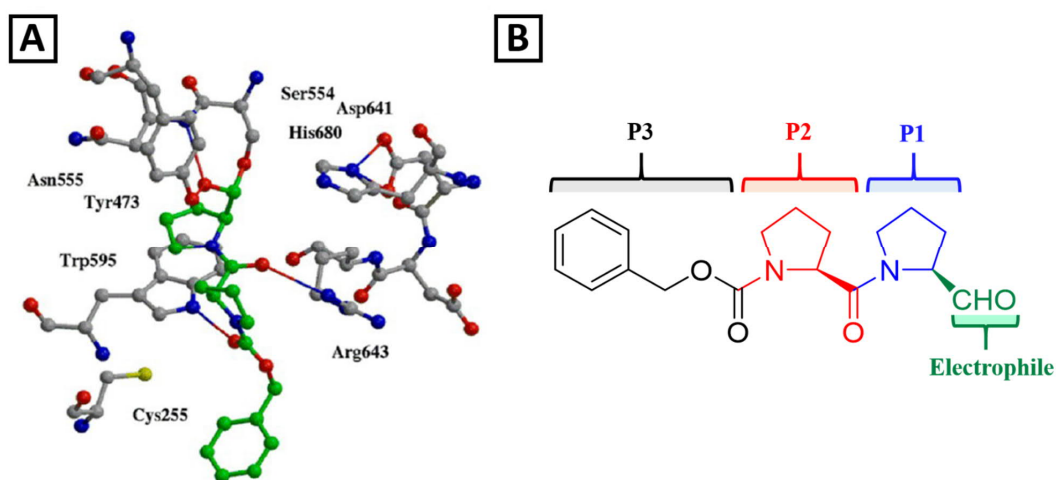

Figure 3. Binding of the PREP inhibitor ZPP to the active site of the enzyme (**A**). For the peptidic PREP inhibitors three distinctive parts named P1, P2 and P3, can be identified, corresponding to the amino acid residues in the peptidic substrate that binds to the binding pockets S1, S2 and S3 in the active site of the enzyme (**B**). Typical PREP inhibitors have the acyl-L-prolyl-pyrrolidine framework where the carbonyl groups form hydrogen bonds to the Arg643 and Trp595 residues of the enzyme. P3 mimics the essential L-proline residue of the substrate having a pyrrolidine ring with an electrophilic group in its 2*S*-position. The most commonly applied electrophiles are aldehyde, nitrile, or hydroxyacetyl. These groups can form a reversible covalent interaction with the catalytic Ser554 residue of the enzyme, resulting in slow tight binding inhibition. Modified from (Van Der Veken et al. 2012)

2.3.2 Structure activity relationship and selectivity for PREP inhibitors

When it comes to designing enzyme inhibitors there are two important factors: selectivity and efficacy. Efficacy can be measured by determining IC_{50}-value or Ki against enzymatic activity *in vitro* using tissue homogenates or purified protein. The IC_{50}-value is measured by determining the concentration of drug where the enzyme activity is 50 % of the full capacity. The substrate usually has a fluorescent part, which is then released for measurement by the enzyme. Several different fluorescent substrates for PREP are commercially available such as 7-amido-4-methylcoumarin (AMC) containing peptides Z-Gly-Pro-AMC or Suc-gyl-Pro-AMC. K_i, on the other hand, is the

dissociation equilibrium constant of the enzyme-inhibitor complex meaning the concentration where half of the enzyme is occupied with the drug. K_i can be determined using similar setups as for measuring IC_{50}-values, but the enzyme reaction needs to be monitored in certain time intervals after the initiation. K_i can also give information about the nature of the inhibition. Recombinant human PREP is the best choice for enzyme source when developing drugs for clinical use. However, porcine PREP is also a commonly used source of protein as it has 97% similar amino acid sequence compared to human and the active site is completely identical (Vanhoof et al. 1994), and it also appears to be more stable in laboratory use than human recombinant PREP. Brain homogenates from different species such as rat, mouse, bovine, pig and canine have been used, most likely due to easy accessibility. In addition, the source and concentration of PREP can affect the inhibitory activity of a tested drug, as the concentration of the inhibitory effect cannot be lower than the amount of PREP used. Due to these variables, inhibition activity between different compounds from different assays may not be fully comparable if the values are close to each other. However, these values gives a good order of magnitude when comparing different inhibitors and can be used to evaluate what kind of structures are potential as a PREP inhibitor.

The structure-activity relationship (SAR) for typical peptidic PREP inhibitors have been studied fairly thoroughly during the years. Some PREP inhibitors are described as a slow tight-binding inhibitors due the reversible covalent binding of the electrophile to the Ser554 residue (Venäläinen et al. 2006). The binding of slow tight-binding inhibitors lasts approximately four to five times longer than the binding of competitive PREP inhibitors lacking the electrophile. The potent inhibitors in the most commonly used assays for PREP activity have low nanomolar IC_{50}-values, and covalently interacting slow tight-binding inhibitors have subnanomolar K_is. Discussion of molecular structures is based on the breakdown of the structure in **Fig 2.** Slow tight-binding PREP inhibitors usually have an electrophilic aldehyde, a nitrile, or a hydroxyacetyl at the 2*S*-position of the P1 pyrrolidine ring that can form a covalent interaction with the catalytic Ser554 residue of the enzyme (Kahyaoglu et al. 1997). However, several other groups that increase the potency of inhibitor compared to the unsubstituted pyrrolidine ring have been reported. Examples of these functionalities are phosphonate esters, α-keto heterocycles, terminal boronates, and hydroxymethyl ketones (Lawandi et al. 2010). L-stereochemistry for the P1 ring substituent is also desired when the group points toward the active Ser554 residue.

The S1 pocket contains hydrophobic residues, allowing the proline ring in the substrate to fit in a stack with the indole ring of Trp595 (Fülöp et al. 1998). Thus, structures mimicking proline are usually optimal. Thiazolidine, thiazolidine S-oxide, oxazolidine, pyrrole and isoxazolidine at the P1 site give reasonable inhibitors but only thiazaolidine gives similar IC_{50}-values compared to pyrrolidine.

The S2 pocket does not have any specific features which would be important for substrate selectivity. The P2 moiety is usually L-Pro or its derivative. However, the amino acid can be varied and still have IC_{50}-values below 10 nM. Amino acids with hydrophobic side chains L-Ala, L-Val, L-Ile, L-Leu, L-Met, and L-Phe at the P2 site do not give inhibitors with drastically decreased inhibitor activity (Saito et al. 1990). This finding indicates that there is space in the S2 pocket for larger groups as well. Thus, larger modifications such as a 5-*tert*-butyl substituent in L-proline do not decrease the potency (Wallén et al. 2003b). In addition, the rigidified structure at the P2 site as cyclopent-2-enecarbonyl gives good potency. The importance of the carbonyl group connecting the P2 and P1 sites was demonstrated by removal of the carbonyl group, which led to an inactive compound (Yoshimoto et al. 1991). Stereochemistry at the P2 site is another crucial part for achieving good activity. L-

stereoisomers of the amino acid at the P2 site are highly favored and using D-stereoisomers led to a 10 000 fold decrease in activity as demonstrated with compounds having thizaolidine in P2 (Arai et al. 1993).

The hydrophobic groups at the P3 site are usually preferred since it interacts with the hydrophobic S3 pocket constituted with nonpolar aminoacid residues (Fülöp et al. 1998). The benzyloxycarbonyl group from ZPP can be replaced with a phenylacyl group and the optimal chain length seems to be three carbons to gain low nanomolar IC_{50}-values (Arai et al. 1993; Portevin et al. 1996). It seems also that simple alkyl chains give a low nanomolar IC_{50}-value when shorter than eight carbons (Arai et al. 1993). However, these modifications do not improve water solubility. To counter that, pyridine was introduced into the P3 moiety to decrease log P value while the IC_{50}-value remained in the low nanomolar range (Jarho et al. 2006). Other heterocycles, larger groups, and rigidified structures have also been used at the P3 site yielding nanomolar IC_{50}-values (Lawandi et al. 2010). Overall, the P3 site seems to be quite freely modifiable in terms of binding to the active site of PREP.

In general, when designing enzyme inhibitors, selectivity over other proteases and peptidases is important for a drug candidate. Close relatives of PREP such as DPP2 and DPP4, aminopeptidase P, prolyl-carboxypeptidase, and FAP are structurally and functionally similar to PREP and therefore it is important to focus drug discovery efforts on selective compounds for PREP. Lawandi et al. 2010 presented aspects to increase PREP inhibitor selectivity over the DPP family enzymes and FAP in their review (Lawandi et al. 2010). They found that the best option to gain selectivity over these enzymes is to have bulky P2 amino acid and hydrophobic aromatic P3.

2.3.3 Review of selected PREP inhibitors

Close to one thousand PREP inhibitors have been described in the literature and PREP inhibitors have been studied in a wide variety of disease and animal models *in vitro* and *in vivo*. Many PREP inhibitors have also been patented for their therapeutic potential in NDD, cognitive diseases, and neuropsychiatric diseases (López et al. 2011). Selected PREP inhibitors and their IC_{50}-values against PREP and biological findings are presented in **Table 2**.

2.3.3.1 Z-Pro-prolinal (ZPP)

ZPP is one of the first PREP inhibitors and it was for many years a model compound for inhibitors (Wilk and Orlowski 1983). It is also the first patented PREP inhibitor and the compound where most of the other patented inhibitors were derived. ZPP is a low tight binding inhibitor with an IC_{50}-value of 0.4 nM against porcine PREP (Wallén et al. 2002). ZPP also inhibits prolyl carboxypeptidase with high concentrations but it is 1000-fold more selective towards PREP (Rabey et al. 2012). ZPP has long-lasting effects in mice after low dose (5 mg/kg) i.p injection. After six hours, PREP inhibition was seen in most tissues, especially in brain (Friedman et al. 1984). In 1986, ZPP was found to increase neurotensin levels by inhibiting PREP in neuroblastoma and colon cancer cell lines (Checler et al. 1986). In addition, oral administration of ZPP increased the levels of AVP in rats (Miura et al. 1995). ZPP also protected the neurons from delayed death in rats with four-vessel-occlusion ischemia (Shishido et al. 1999). Since vasopressin V2 receptor antagonist reversed the neuroprotective effect of ZPP, it was concluded that this effect is most likely AVP-mediated. ZPP was also able to prevent amnesia in scopolamine treated mice in the passive avoidance learning test (Yoshimoto et al. 1987). Despite the promising results on neuropeptide levels, ZPP did not have an effect on Aβ-1-40/1-42

production in a human cell line (Petit et al. 2000) and did not affect TRH degradation in rat serum (Friedman and Wilk 1985). Since ZPP is a specific and orally active PREP inhibitor, these results suggests that the proteolytic activity of PREP does not play a role in Aβ and TRH metabolism.

More recently, the effect of ZPP outside the CNS has been studied with promising results. ZPP was found to have a role in neutrophil inhibition via PREP inhibition *in vitro* and *in vivo*, suggesting potential in treatment of cystic fibrosis and COPD (Russell et al. 2019). ZPP was also able to inhibit generation of Ac-SDKP *ex vivo* (Cavasin et al. 2004). In ex vivo studies, PREP inhibition with ZPP reduced Angiotensin (1-7) formation from Angiotensin II in serum and in lung lysates, expanding the role of PREP inhibitors in the circulation of lungs and kidneys (Serfozo et al. 2020).

2.3.3.2 S17092

S17092 is a potent PREP inhibitor with unnatural amino acid in the peptidic structure. The main difference to typical PREP inhibitors is that S17092 has a large P2 group and the lack of electrophile in 2S-position of the P1 ring. It has Ki of 1.5 nM against human PREP and 1.3 nM against rat cortex homogenate (Barelli et al. 1999). S17092-1 does not have an inhibitory effect on several other peptidases including aminopeptidases and dipeptidylaminopeptidases. Similar to ZPP, S17092 did not have an effect on Aβ levels (Petit et al. 2000). However, S17092 had promising results in other memory and PD-related *in vivo* models. It improved the learning and memory in young and aged scopolamine-treated mice most likely by increasing neuropeptide levels in the brain (Marighetto et al. 2000). Supporting the role of increased neuropeptide levels, single i.p. injection of S17092 (30 mg/kg) in rats caused a significant increase in SP and α-MSH levels in frontal cortex and hypothalamus (Bellemère et al. 2003). S17092 improved performance in an early PD model in monkeys (Schneider et al. 2002). A seven day chronic oral administration in MPTP-treated monkeys led to improvement in variable delayed response delayed matching to sample, and delayed alternation tasks. Due to the promising findings in preclinical memory models S17092 advanced to clinical trials as a therapeutic for memory impairment (Morain et al. 2002). Clinical studies demonstrated that S17092 can be safely administrated to humans with a daily dose of 1200 mg for 14 days, without serious adverse effects. 13-day administration of a 1200 mg dose resulted in a favorable effect on verbal memory compared to placebo. The clinical trials with S17092 were discontinued due to unclear reasons.

More recently, S17092 was studied as a treatment option for liver fibrosis and hypertension. PREP inhibition by S1709 attenuates steatosis in the L02 human liver cell line (Zhou et al. 2016). S17092 was shown to decrease cell proliferation of hepatic stellate cells *in vitro* and increase expression of collagen 1 and α-smooth muscle actin (Zhou et al. 2017). Long-term administration of S17092 decreased Ac-SDKP levels in plasma, heart, and kidneys in hypertensive rats (Cavasin et al. 2004).

2.3.3.3 JTP-4819

JTP-4819 is one of the most studied PREP inhibitors, a slow tight binding inhibitor with an IC$_{50}$ value of 0.83 nM against rat brain homogenate (Toide et al. 1995a). JTP-4819 follows the structure of a typical PREP inhibitor but it has a hydroxyacetyl group in P1 instead of aldehyde or nitrile group. First, the effect of JTP-4819 on neuropeptide levels was tested *in vitro* followed by cognitive tests in rats, as many other early PREP inhibitors. JTP-4819 inhibited the degradation of SP, AVP, TRH, neurotensin, oxytocin, bradykinin, and angiotensin II when incubated with purified PREP *in vitro*

(Toide et al. 1995b). Oral doses of 1 and 3 mg/kg of JTP-4819 increased the performance of rats with scopolamine-induced amnesia in one-trail passive avoidance test (Toide et al. 1995a). However, this result could not be repeated with another similar PREP inhibitor, KYP-2047 (Jalkanen et al. 2007). JTP-4819 increased acetylcholine (Ach) release. Two years later, 14 days administration (1 mg/kg p.o.) of JTP-4819 improved spatial memory in different memory tasks in aged rats (Toide et al. 1997a). In the same year, JTP-4819 was able to suppress the generation of Aβ in neuroblastoma cells (Shinoda et al. 1997). It was also suggested that JTP-4819 might have potential in treatment of AD due to the JTP-4819-induced increase in Ach release from the frontal cortex and hippocampus, regions closely associated with memory, in both young and aged rats (Toide et al. 1997b). Supporting the role of JTP-4819 in treatment of AD, it has improved the performance of aged rats in Morris water maze and in middle cerebral artery occluded rats in a passive avoidance test.

Repeated administration of JTP-4819 in rats with a lesion in the nucleus basalis magnocellularis, which is the major source of cholinergic projections, revealed that the treatment did not have an effect on cholinergic parameters but treatment significantly increased the levels of SP, TRH, and AVP, indicating that JTP-4819 ameliorates memory impairment due to increased neuropeptide levels (Shinoda et al. 1999). However, a more recent study showed with microdialysis that JTP-4819 decreased hippocampal Ach level by 30 % with a 50 µmol/kg dose, suggesting that memory enhancement is not due increased cholinergic transmission (Jalkanen et al. 2014b). In addition, these models may not model AD pathology but only a memory and cognitive impairment. Off-target analysis was performed for JTP-4819 and it did not reveal any off-targets in General Side Effect Profile II or inhibition against other serine proteases and Pro-specific proteases, except for 24 % inhibition of prolyl carboxypeptidase at 10 µM (Jalkanen et al. 2012). JTP-4819 has also been patented for its ability to enhance recovery in rats with unilateral focal forebrain ischemia (Sirviö and Lehtimäki 2005), where systemic daily administration increased the performance in the limb placing task. JTP-4819 made it to phase 1 clinical trials as an orally active memory enhancer (Umemura et al. 1997) where it had acceptable pharmacodynamic and pharmacokinetic profiles. No serious adverse effects were found with 3, 10, 30 and 60 mg doses. In a multiple-dose study 60 mg was administrated thrice daily for 7 days. The plasma cholinesterase activity was gradually increased above the normal level in all subjects during the multiple-dose study, but it returned to normal after completion of dosing. Despite the success in phase 1 clinical trials no further clinical data is found, most likely due to the lack of efficacy.

2.3.3.4 Z-321

Z-321 is a typical PREP inhibitor with an indanylacetyl group as the P3 moiety and L-thioprolyl as the P2 moiety with an IC_{50}-value of 10 nM against canine brain homogenate (Tanaka et al. 1994). Z-321 potentiated synaptic transmission *ex vivo* with a high 100 µM concentration in rat hippocampal slices (Miura et al. 1997). Interestingly, the enantiomer of Z-321 had no such effect, highlighting the importance of the correct stereochemistry for PREP inhibitors. The authors concluded that the effect is most likely mediated by inhibited degradation of AVP since an AVP V1 receptor antagonist reversed the effect. Z-321 made it to phase 1 clinical trials as an orally active memory enhancer (Umemura et al. 1999). Similar to the JTP-4819 clinical trials, it was indicated that Z-321 had suitable pharmacodynamic and pharmacokinetic profiles for clinical use. No serious adverse effects were found in healthy volunteers with 3.75, 7, 15, 30, and 60 mg doses. Z-321 had the same effect on the plasma cholinesterase activity as JTP-4819 during the multiple-dose study. The cholinesterase activity was increased above the normal range on day 8 in 50 % of subjects. However, again similarly

to JTP-4819, Z-321 did not advance to the next stage of clinical trials most likely due to lack of efficacy in memory.

2.3.3.5 ONO-1603

ONO-1603 is one of the early PREP inhibitors with a distinctive structure. ONO-1603 differs from typical PREP inhibitors since it lacks the proline as the P2 moiety. ONO-1603 has also been tested in several memory models *in vivo* and *in vitro*. ONO-1603 inhibits PREP with a Ki value of 12 nM and effectively protects against the scopolamine-induced learning and memory dysfunction in rats (Katsube et al. 1996). ONO-1603 also increased neuronal survival and neurite outgrowth in differentiating cerebellar granule cells, indicating it as a potential treatment for NDD (Katsube et al. 1996). ONO-1603 was also shown to delay age-induced apoptosis in rat primary cerebral cortical cells and suppress GAPDH overexpression, indicating a neuroprotective role (Katsube et al. 1999). Recently, no further studies with this compound have been conducted.

2.3.3.6 SUAM-1221

SUAM-1221 is an archetype of a patented PREP inhibitor (Saito et al. 1991). Similar to S17092, SUAM-1221 lacks the electrophile in the 2*S*-position of P1 moiety suggesting impaired interaction with the S554 residue. Inhibitor activity of SUAM-1221 has been tested against many different sources of PREP in many different assays. Results range from an IC_{50} value of 2.0 nM (Wallén et al. 2002) against porcine PREP to 190 nM against bovine PREP (Portevin et al. 1996). Even though this inhibitor has not been tested in biological models or assays according to the literature, it has gained interest as a model inhibitor for assessing SAR of PREP inhibition.

2.3.3.7 KYP-2047

KYP-2047 was synthesized in 2000 (Jarho 2000) at the University of Kuopio, Finland and has been studied extensively ever since *in vivo* and *in vitro* and particularly in the context of PD models. KYP-2047 is based on the structure of SUAM-1221 but it has an additional electrophilic nitrile group in the 2*S*-poisition of the pyrrolidine ring. KYP-2047 has an IC_{50}- value of 0.2 nM against porcine PREP and it is one of the most potent inhibitors found so far (Jarho et al. 2005). KYP-2047 was more potent compared to ZPP in a PREP activity assay in neuroblastoma cells and rat primary cortical neurons (Klimaviciusa et al. 2012). KYP-2047 penetrates the mouse brain and effectively inhibits mouse PREP with a long-lasting effect (Jalkanen et al. 2014a). When a 9 μmol/kg i.p. dose of KYP-2047 was administered to rats, PREP was still inhibited in brain and liver after six hours (Venäläinen et al. 2006). In addition, KYP-2047 was in the same off-target screen as JTP-4819, showing similar results with no off-targets and high specificity against PREP (Jalkanen et al. 2012). As with many other PREP inhibitors, KYP-2047 was also tested first in memory models and found to improve performance in memory tasks in young scopolamine-treated rats (Jalkanen et al. 2007). However, no significant differences in neuropeptide levels were found in this study, leaving the memory enhancing effect of KYP-2047 unclear. In another study, KYP-2047 did not have an effect on memory in scopolamine-treated rats but it increased locomotor activity compared to vehicle-treated rats (Peltonen et al. 2010). It was also shown later that KYP-2047 fails to increase neurotensin and SP

levels in rat striatum by microdialysis, suggesting that PREP does not actually have a significant role in cleavage of neuropeptides *in vivo* (Jalkanen et al. 2011).

These results urged researchers to find other possible explanations for beneficial results in animal models of memory. After Brandt et al. (2008) revealed that PREP induces aggregation of αSyn, KYP-2047 was tested in αSyn-based PD models and was indeed found to significantly decrease αSyn aggregation in cells overexpressing A30P/A53T mutant αSyn and A30P αSyn transgenic mice (Myöhänen et al. 2012a). This result was supported by another study with A30P αSyn transgenic mice where KYP-2047 increased αSyn clearance and induced autophagy compared to vehicle-treated mice (Savolainen et al. 2014). KYP-2047 did not only decrease αSyn oligomers and increase autophagosome marker LC3B-II but it also significantly increased striatal DA levels. Later, KYP-2047 was tested in a unilateral AAV-αSyn viral vector model (Svarcbahs et al. 2016). In this study, KYP-2047 restored motor deficits caused by unilateral αSyn overexpression and decreased oligomeric αSyn in the STR and SN of the mice compared to vehicle-treated controls. KYP-2047 also had a trend to enhance striatal DAergic system activity. The mechanisms behind these biological effects have also been studied *in vitro*. First, KYP-2047 was able to enhance survival of αSyn overexpressing cells in an oxidative stress induced αSyn aggregation model (Dokleja et al. 2014). In this study, ROS production was also decreased with KYP-2047. KYP-2047 reduced αSyn dimerization in PREP-expressing cells but not in PREPko cells, indicating that the effect on αSyn is PREP-related. In another study, αSyn dimerization was also enhanced by inactive S554A mutant PREP, but this effect could not be reversed by KYP-2047 (Savolainen et al. 2015). KYP-2407 also increases αSyn fibril degradation in neuron-like cells (Rostami et al. 2020). The effect was based on reduced calpain activity and induction of autophagy. Furthermore, KYP-2047 attenuated αSyn toxicity in a lactacystin-treated αSyn overexpressing cell line by enhancing autophagy (Myöhänen et al. 2017). These results suggest that KYP-2047 could have potential as a treatment for PD.

In addition, KYP-2047 was found to reverse PREP-induced angiogenesis both *in vitro* and *in vivo* (Myöhänen et al. 2011). A recent study showed that 7 days 10 mg/kg i.p injection of KYP-2047 had beneficial effects in a mouse model of chronic venous insufficiency (Casili et al. 2020). KYP-2047 treated mice had reduced histological abnormalities of the venous wall combined with reduced expression of vascular growth factors and inflammation mediators compared to control mice. These results suggests that KYP-2047 could also have therapeutic potential in vascular diseases.

2.3.3.8 UAMC-00021

UAMC-00021 differs from the typical PREP-inhibitors by having a larger group with an isoxazole ring in the R-position of the P1 moiety (Bal et al. 2003). It has an IC_{50} value of 1.6 nM against porcine PREP, indicating that a larger P1 group does not disrupt the interaction with the enzyme (Brandt et al. 2008). UAMC-00021 was able to decrease the aggregation of αSyn in *in vitro* measurements with purified proteins similarly to ZPP. Despite these results, no further studies with this compound have been reported.

2.3.3.9 SUAM-14746

SUAM-14746 is a specific PREP inhibitor with the typical structure. A difference compared to other typical inhibitors is that it has a polar secondary alcohol group in the L-proline group in the P2-site. SUAM-14746 has an IC_{50}-value of 16 nM against porcine PREP (Yasuhiko 2011). Interestingly,

SUAM-14746 has been tested mainly in cell proliferation and cancer models but not in memory and neuropeptide models, as with other typical older inhibitors. The reason for that may very well be the fact that SUAM-14746 is commercially available. SUAM-14746 treatment for 24-72 h suppressed the growth of human neuroblastoma cells (Sakaguchi et al. 2011). This effect was mediated by G_0/G_1 arrest, increased levels of cell growth associated proteins, and decreased levels of tumor suppressors p53 and cyclin-dependent kinase inhibitor and inhibited S and G_2/M phase progression. SUAM-14746-mediated cell cycle arrest in KATO III human gastric cells as well, suggesting that SUAM-14746 could have potential in cancer treatment (Suzuki et al. 2013). Similar effects were seen in human breast cancer cell lines *in vitro* (Tanaka et al. 2017).

2.3.3.10 IPR19

IPR19 is an interesting PREP inhibitor with a larger 4-(benzyloxy)-3,5-dimethoxybenzoyl-group in the P3 moiety compared to other reported PREP inhibitors (Giralt et al. 2014). Despite the larger P3 group, IPR19 has an IC_{50}-value of 80 nM (Prades et al. 2017). Another interesting factor is that IPR19 was tested in cognitive performance models. Acute administration (5 mg/kg i.p) of IPR19 reversed cognitive performance deficits in novel object recognition, T-maze and the eight-arm radial maze in three mouse models modelling the cognitive deficits of schizophrenia (Prades et al. 2017).

2.3.3.11 Y-29794

Y-29794 is a potent and selective PREP inhibitor reported in 1992 as having an IC_{50}-value of 0.95 nM against rat brain homogenate (Nakajima et al. 1992). Y-29794 is an intriguing PREP inhibitor since it lacks the peptidic structure common to all other known potent PREP inhibitors. An *ex vivo* study demonstrated that Y-29794 could penetrate into the rat brain to exhibit dose-dependent and long-lasting inhibition. The effect of this inhibitor was first tested on PREP substrates and it had an increasing effect of THR-mediated Ach release in the rat hippocampus (Nakajima et al. 1992). Later, repeated i.p. treatment with Y-29794 was shown to decrease Aβ like deposits in the hippocampus of senescence accelerated mice (Kato et al. 1997). A more recent study proved that Y-29794 inhibited proliferation and induced death in the multiple triple negative breast cancer cell line by blocking the IRS1-AKT-mTORC1 pathway (Perez et al. 2020). In addition, Y-29794 inhibited tumor growth when tested in triple-negative breast cancer models in mice. Despite the promising results on decreasing Aβ deposits and tumor growth, only a few studies with this compound have been conducted.
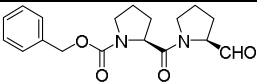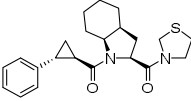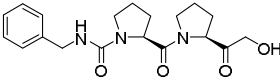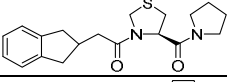
2.3.3.12 J94
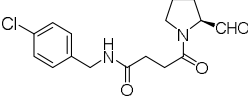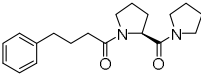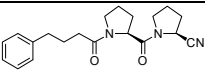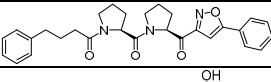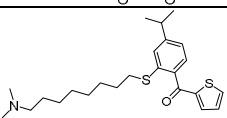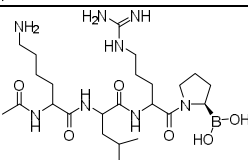
More recently, some potent and specific peptidic PREP inhibitors, lacking the lipophilic P3 group were discovered (Jackson et al. 2015). One of these was J94 which is composed of L-prolyl boronic acid as the P1 group and inhibits PREP totally at 100 nM. J94 did not have an effect against FAP or DPP4 with 10 μM concentration. J94 was tested in a tumor growth mice mod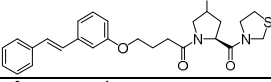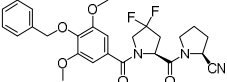el and was able to reduce colon cancer tumors in the 28-day treatment period (Jackson et al. 2015) J94 was tested with M83, which is an inhibitor of FAP and PREP. Interestingly, both inhibitors gave similar effects despite the fact that J94 is a specific PREP inhibitor and M83 inhibits FAP and PREP, indicating that the tumor suppression effect are mostly PREP mediated.

2.3.3.13 Other PREP inhibitors

Most of the developed PREP inhibitors are peptidic structures with some modifications, the only excluding compound is Y-29794. Non-peptidic PREP inhibitors have been difficult to develop since the role of both carbonyl groups in the structure seems to be important for specific binding. Some natural products such as berberine have weak PREP inhibitor properties with IC_{50}-values as high as 145 000 nM. However, these kind of polyaromatic compounds have a tendency to have mild effect on several different enzymes and receptors. Other natural products with selective and slightly better ability to inhibit PREP are baicalin and baicalein, with IC_{50}-values above 10 000 nM (Tarragó et al. 2008a). More recently, polyozellin from mushroom *Polyozellus multiplex* was synthesized (Takahashi et al. 2018). This compound has a *p*-terphenyl structure and IC_{50}-value of 1200 nM. Despite the weak inhibitory activity, polyozellin and its derivate were able to moderately inhibit the growth of cancer cell lines HL60 and MCF-7.

In addition, benzimidazolium salts are found to be weak blood brain barrier (BBB) permeable PREP inhibitors with IC_{50}-values of 65 000 nM (Tarragó et al. 2008b). Potent PREP inhibitors from pyrrolidinyl pyridone and pyrazinone analogues at the P2 site have also been synthesized (Haffner et al. 2008). Most of these compounds have low nanomolar IC_{50}-values against recombinant human PREP. Even though these compounds have a more rigid P2 moiety than typical PREP inhibitors, the carbonyl groups are still present, which might be the reason for lower IC_{50}-values compared to other nonpeptidic inhibitors.

Table 2. Selected PREP inhibitors with extensive studies

Name	Structure	Inhibition	Effect *in vitro*	Effect *in vivo*	Reference
ZPP		Ki=0.35 nM (porcine PREP)	Increased neurotensin and AVP levels, decreased PREP induced αSyn aggregation	Protection from delayed cell death, amnesia prevention, neutrophil inhibition, inhibition of Ac-SDKP and Ang II levels (ex vivo)	(Checler et al. 1986) (Wilk and Orlowski 1983) (Miura et al. 1997) (Russell et al. 2019; Serfozo et al. 2020; Shishido et al. 1999; Yoshimoto et al. 1987)
S17092		Ki=1.5 nM (human PREP)	Attenuates liver steatosis and decreases proliferation of hepatic stellate cells, decreased Ac-SDKP levels	Improved learning and memory, increases SSP and a-MSH levels, improved performance in memory tasks of early PD model, clinical trials in memory impairment	(Barelli et al. 1999; Cavasin et al. 2004; Marighetto et al. 2000; Morain et al. 2002; Schneider et al. 2002; Zhou et al. 2016)
JTP-4819		IC$_{50}$= 0.83 (rat brain homogenate)	Increased neuropeptide levels, reduced generation of AB,	Increased memory in scopolamine treated rats and aged rats, enhanced recovery from ischemia in rats, clinical trials as a memory enhancer	(Shinoda et al. 1995; Sirviö and Lehtimäki 2005; Toide et al. 1995a; Toide et al. 1995b; Toide et al. 1997a; Toide et al. 1997b)
Z-321		IC$_{50}$= 10 nm (canine brain homogenate)	No *in vitro* results reported	Increased synaptic transmission (ex vivo), clinical trial as memory enhancement	(Miura et al. 1997; Tanaka et al. 1994; Umemura et al. 1997)
ONO-1603		Ki= 12 nM	Protection against neuronal survival and neurite outgrowth, delayed age-induced apoptosis	Protection against scopolamine-induced learning and memory dysfunction	(Katsube et al. 1999; Katsube et al. 1996)
SUAM-1221		IC$_{50}$= 2.0 nM (porcine PREP) and 190 nM (bovine PREP)	Model inhibitor for SAR assessment	No in vivo studies reported	(Portevin et al. 1996; Wallén et al. 2002)
KYP-2047		IC$_{50}$= 0.2 nM (porcine PREP)	Reduced angiogenesis, reduced αSyn aggregation and increased clearance, increased interaction with PREP and αSyn leading to decreased αSyn dimerization, reduced toxicity caused by αSyn, increased PP2A activity	Improved memory performance in young scopolamine-treated rats, reduced angiogenesis, reduced αSyn aggregation and increased αSyn clearance via autophagy, restoration of behavior and reduced αSyn oligomers in AAV viral vector model, enhanced dopaminergic system activity in PD mouse model	(Jalkanen et al. 2014a; Jarho 2000; Myöhänen et al. 2012a; Myöhänen et al. 2017; Rostami et al. 2020; Savolainen et al. 2014; Svarcbahs et al. 2016; Svarcbahs et al. 2018; Wallén et al. 2003a; Venäläinen et al. 2006)
UAMC-00021		IC$_{50}$=1.6 nM (porcine PREP)	Decreased PREP induced αSyn aggregation	No *in vivo* studies reported	(Bal et al. 2003; Brandt et al. 2008)
SUAM-14746		IC$_{50}$=16 nM (porcine PREP)	Suppression of cancer cell growth	No *in vivo* studies reported	(Saito et al. 1991; Sakaguchi et al. 2011; Suzuki et al. 2013)
IPR19		IC$_{50}$= 80 nM (recombinant human PREP)	No *in vitro* results reported	Increased cognitive performance in schizophrenia mouse models	(Giralt et al. 2014; Prades et al. 2017)
Y-29794		IC$_{50}$= 0.95 nM (rat brain homogenate)	Inhibition of cancer cell growth	Increased Ach release, reduction of Aβ like deposits, inhibition of tumor growth	(Kato et al. 1997; Nakajima et al. 1992; Perez et al. 2020)
J94		Full inhibition at 100 nM (Cell assay)	No *in vitro* results reported	Suppression of colon cancerous tumors in mice	(Jackson et al. 2015)

26

2.3.3.14 Summary of PREP inhibitors

In summary, a wide variety of PREP inhibitors have been synthesized and tested *in vitro* and *in vivo* in several different disorders, mainly focusing on the CNS and cancer. Almost all PREP inhibitors have a peptide structure, but they may still have different biological activities. Some PREP inhibitors have managed to progress to clinical trials as modulators of neuropeptide levels and memory enhancers. However, to date, there is no PREP inhibitor available on the market despite the effort directed to the development of PREP inhibitors. Furthermore, surprisingly many of these promising PREP inhibitors lack further studies indicating that development of these compounds has not progressed. Many of these presented inhibitors are mainly used as reference compounds for PREP inhibition to evaluate the role of PREP in different processes, not as a lead compound for drug development. Overall, there is a need for development and design for more drug-like nonpeptidic compounds. Interestingly, studies with PREP inhibitors shifted gradually from memory enhancement by inhibition of neuropeptide cleavage to PPI-mediated functions of PREP inhibition. One reason for this might be the improved methods measuring protein levels *in vivo*. Microdialysis and mass spectrometry methods are more powerful and accurate methods for evaluating changes in neuropeptide levels compared to IHC of short lived neuropeptides. Moreover, PREP is mainly an intracellular enzyme, and it seems rather complex for intracellular enzymes to degrade neuropeptides that are released to extracellular space. In addition, in 2012 it was shown that 4-day inhibition with KYP-2047 did not alter the levels of several intact neuropeptides in mice using peptidomic approach (Tenorio-Laranga et al. 2012). However, many proteins that are not substrates of PREP had altered levels. For example, mitochondrial proteins in kidneys and hormone precursors in hypothalamus. This data suggests that PREP acts as a regulator protein for other proteins rather than by degrading active peptides and hormones.

2.3.5 Relationships of inhibitory activity and biological response

As PREP inhibition shifts the conformation of the protein to a closed form (López et al. 2016; Szeltner et al. 2013), it is hypothesized that conformational changes in PREP might have a more important physiological role than the inhibition of the proteolytic activity itself. This is supported by the finding that binding of KYP-2047 stabilizes the conformations of B and His-loops in PREP, which are both flexible structures located near the entry site of the catalytic cavity (Tsirigotaki et al. 2017). These loops could also have an effect on PPIs, indicating that different PREP inhibitors could stabilize the loops in slightly different conformations. To support this hypothesis, the point mutation T590C in the external B loop at the surface of PREP removed the regulatory effect of PREP on PP2A (Svarcbahs et al. 2020). Furthermore, ZPP and KYP-2047 gave slightly different spectra in a quantum relaxation dispersion assay when incubated with PREP although both inhibitors have very high affinity to the enzyme and a low nanomolar IC_{50}-value (López et al. 2016).

Interestingly, different PREP inhibitors are reported to have different biological effects even though their inhibitory activity and pharmacokinetic properties are similar. In a study where extracellular Ach and DA levels were measured by microdialysis in rats, JTP-4819 decreased Ach levels significantly after systemic (50 µmol/kg) and intrastriatal (12.5, 37.5 or 125 uM at 1.5 ul/min for 60 min) administration but KYP-2047 had an effect only after intrastriatal injection (Jalkanen et al. 2012). Since both compounds have a low nanomolar IC_{50}-value and have proven to be orally active, these results indicate that this effect may be mediated by something else other than mere inhibition

of the proteolytic activity of PREP. In the hippocampus, 50 µmol/kg i.p administration of JTP-4819 significantly decreased Ach levels but KYP-2047 did not have the same effect (Jalkanen et al. 2014b). However, in the cortex, KYP-2047 decreased the levels but JTP-4819 did not.

A study where the effect of PREP inhibitors on GAPDH translocation was studied using 6-OHDA-treated neuroblastoma cells showed that JTP-4819 did not prevent translocation of GAPDH in 6-OHDA-treated neuroblastoma cells, but ZPP was able to prevent the translocation of GAPDH (Puttonen et al. 2006). Notably, the doses of PREP inhibitors used in the study were such that PREP was fully inhibited. However, both inhibitors were able to block ROS production. Again, both PREP inhibitors are highly potent, but they have a different effect on this PPI-mediated function of PREP. This supports the hypothesis that different PREP inhibitors stabilize different conformations in PREP and result in different PPIs. The main difference in the structure of these inhibitors is in the electrophilic group. ZPP has a more reactive aldehyde and JTP-4819 has a hydroxyacetyl group that, in addition to the electrophilic ketone functionality, has a hydroxyl group next to it. This may lead to different binding and different conformation stabilization of the enzyme.

On the other hand, there has been inconsistency in the dose responses of different PREP inhibitors. In a study, an acute 1 mg/kg i.p injection of the non-specific PREP inhibitor benzyloxycarbonyl-methionyl-2(S)-cyanopyrrolidine in rats prevented the development of behavioral despair but a 2 mg/kg dose did not (Krupina et al. 2013). However, both doses decreased the PREP and DPP4 activities in the striatum. In another study, S17092 was administered to MPTP-treated monkeys in doses of 1, 3, and 10 mg/kg and their cognitive deficits were measured by different tasks (Schneider et al. 2002). Interestingly, the most efficacious dose was 3 mg/kg which improved performance in all tasks. The 1 mg/kg dose was ineffective in all tests whereas the 10 mg/kg dose significantly improved the performance only in one task.

Some surprisingly weak PREP inhibitors have also shown promising results in different models. ZTTA (N-benzyloxycarbonyl-thioprolyl-thioprolinal-dimetylacetal) is a weak PREP inhibitor having K_i-value of 2.9 µM but showed promising results in the passive avoidance test in rats with a basal forebrain lesion (Shishido et al. 1998). However, later on, ZTTA did not have an effect on delayed neuronal death in rats having four-vessel-occlusion transient ischemia but more potent inhibitor ZPP was able to protect neurons from cell death (Shishido et al. 1999).

3 AIMS OF THE STUDY

The current available therapeutic options for NDD are only to alleviate symptoms. Thus, there is an urgent need for a disease-modifying therapy. Current studies have shown that PREP inhibitors have potential in decreasing harmful protein aggregates and increasing autophagy in *in vivo* models of PD. The aim of this study was to clarify the ability of PREP inhibitors to modulate PPI-mediated functions of PREP such as inducing autophagy and reducing formation of αSyn aggregates. This study also aimed to find novel PREP-ligands as a potential drug therapy for NDD. The specific aims of the study were:

1. To test a series of peptidic PREP inhibitors in novel PPI-related functions of PREP such as autophagy induction and αSyn dimerization (I). A further aim was to confirm the observed disconnected SARs for modulating the different functions of PREP, showing that their effect on induction of autophagy or decrease of αSyn dimerization are not dependent on the magnitude of inhibition of proteolytic activity (I-II).

2. Optimizing the structure of atypical PREP ligands for generating a more selective effect on the decrease of αSyn dimerization over the inhibition of the proteolytic activity (II). A further aim was also to invent new types of PREP ligands for modulating its PPIs.

3. To characterize A30P*A53T αSyn transgenic mouse line as a model of PD and to evaluate the effect of a novel PREP inhibitor *in vivo* in this model (III).

4 MATERIALS AND MAIN METHODS

4.1 REAGENTS

Reagents were purchased from commercial suppliers if not specified otherwise. The PREP inhibitors in study I and compound 7a (SUAM-1221), 7b and 14a (KYP-2047) in study II were received from the compound library from University of Kuopio (current University of Eastern Finland (UEF). The novel PREP-ligand HUP-55 used in study III, was synthesized during the doctoral project, but its structure and synthesis are not part of the doctoral thesis.

4.2 PLASMIDS AND PROTEINS

pMRX-IP-GFP-LC3-RFP plasmid (Noboru Mizushima Lab; RRID:Addgene_84573) used in study I is described in (Kaizuka et al. 2016) and was obtained from Adgene. The split *Gaussia princeps* luciferase (GLuc) expression plasmids used in study I and II were previously described in (Nykänen et al. 2012). Henri Huttunen lab at the University of Helsinki provided αSyn-GLuc1 and αSyn-GLuc2 constructs for the studies. GLuc constructs used in studies I and II have the GLuc reporter fragment placed at the N terminus separated by a (GGGGS)2SG linker. Human PREP expression plasmid used in study I was described in (Savolainen et al. 2015) Recombinant porcine PREP (Study I) was purified as previously described in (Venäläinen et al. 2002). Human PREP cDNA (pOT7_hPREP vector) used in study I was obtained from GE Dharmacon (Diegem, Belgium). Human PREP was expressed in BL21(DE3) cells and purified using immobilized co-chelating chromatography (GE Healthcare, Diegem, Belgium) followed by anion exchange chromatography on a 1 mL Mono-Q column (GE Healthcare). αSyn was expressed and purified as described by (Gerard et al. 2006). Mice brain homogenates used in study II were prepared from cortices of C57BL/6 mice. Brains were dissected and frozen in -80 °C. The brain cortex samples were homogenized in ten volumes of assay buffer (0.1 M Na-K-phosphate buffer, pH 7.0). The homogenate was centrifuged at $10,000 \times g$ at 4 °C, for 20 min. Aliquots of supernatant were frozen and stored at -80 °C until assayed. The protein concentrations of the supernatants were determined with Bio-Rad BCA-protein assay kit.

4.3 CELL CULTURES AND TRANSFECTIONS

Mouse Neuro-2A (N2A) neuroblastoma cells used in studies I and II were cultured in Dulbecco's modified Eagle's medium (DMEM) Glutamax^{TM} with pyruvate supplement (gibco), with an additional 10% (v/v) FBS (Invitrogen), 1 % (v/v) non-essential aminoacids solution (gibco), 1% (v/v penicillin-streptomycin solution (Thermo Fischer). HEK-293 cell used in study I were cultured in full DMEM with an additional 10% (v/v) FBS (Invitrogen), 1% (v/v) penicillin-streptomycin solution (Lonza). The HEK-293 PREPko cell line used in study I is described in (Svarcbahs et al. 2018) and was cultured in DMEM with an additional 20% (v/v) FBS (Invitrogen), and 1% (v/v) penicillin-streptomycin solution (Lonza). All used cell lines were cultured at 37 °C and 5% CO_2, water-saturated air. Transfection of N2A cells in study I was done with JetPei (Polyplus) according to the

manufacturer's instructions. Transfections of PREPko and HEK-293 cells in study I and N2A cells in study II was done with Lipofectamine 3000 (Thermo Fischer) according to the manufacturer's instructions.

4.3.1 Creation of stably expressing GFP-LC3B-RFP cell line

HEK-293 cells stably expressing GFP-LC3B-RFP construct was created according to the protocol described in Svarcbahs et al. (Svarcbahs et al. 2020). Shortly, HEK-293 cells were seeded at a density of 400 000 cells per well on a 6-well plate and transfected with pMRX-IP-GFP-LC3-RFP plasmid (2500 ng/well; #84573, Addgene, Noboru Mizushima Lab; RRID:Addgene_84573) using Lipofectamine 3000 (#L3000015, ThermoFisher Scientific) transfection reagent according manufacturer's protocol. 48 hours selection with 3 µg/ml puromycin was done 24 hours post-transfection. After selection cells were seeded on 96-well plate in single cell suspension, and the growth of the cells was followed based on their GFP expression. Cell colonies expressing GFP-LC3B-RFP were selected and they were cultured for further use in experiments.

4.3.2 Determination of autophagic flux

Autophacgic flux was measured as described in (Svarcbahs et al. 2020). Shortly, GFP-LC3B-RFP expressing HEK-293 cells were plated at a density of 35 000 cells/well on a black poly-L-lysine coated 96-well. Cells were treated for 24 hours at 10 µM concentration of PREP inhibitors. 0.5 µM rapamycin (BML-A275, Enzo Life Sciences) was used as a positive control for autophagy induction and 20 nM bafilomycin 1A (ML1661) as an autophagy inhibitor. After the treatment, cells were washed twice with warm PBS and GFP-signal was read by Victor2 multilabel counter (PerkinElmer; excitation/emission 485nm/535nm). For each experimental condition, 4 replicate wells were used in each experiment, and at least 3 of independent experiments were performed. Analysis was performed for only GFP signal since RFP signal was not reliably detectable in well-plate format as RFP in this construct may be degraded by lysosomes to a certain degree (Kaizuka et al. 2016). Representative pictures from GFP-LC3-RFP expressing cells were taken by Leica DMi8 fluorescence microscope (Leica Microsystems, Wetzlar, Germany).

4.4 WESTERN BLOT

To determine autophagy marker LC3B-II levels by Western Blot (WB) in study I, 400 000/cells per well were seeded on 6-well plates, and 24 h post plating, cells were treated for 4 h with tested compounds at 1 µM concentration. Followed by the treatment, cells were lysed with mRIPA buffer (Tris-HCl 50 mM, NaCl (150 mM, 0.25% sodium deoxycholate, 1% NP-40, pH 7.4) with 1:100 protease inhibitor cocktail (Product# P8340, Sigma) and HALT phosphate inhibitor cocktail (Product# 87786, Thermo Fisher Scientific). Lysates were sonicated and centrifuged at 13,300 rpm for 15 min at 4 °C. Supernatants were collected and protein amounts were determined by the BCA method. Procedure for WB is described earlier in (Svarcbahs et al. 2018). Shortly, samples (20 µg protein/sample) were loaded onto a 12% polyacrylamide-SDS gel. β-actin was used as the loading

control. Standard transfer and blocking techniques were used. Goat anti-rabbit horse-radish peroxidase (HRP) -conjugated secondary antibody (dilution 1:2000 in 5% milk; #31460, RRID:AB228341, Thermo Fischer Scientific) was used for β-actin (dilution 1:2000 in 5% milk; ab8227, RRID:AB2305186, AbCam) and LC3BI–II (1:1000 in 5% milk; #L7543, RRID:AB796155, Sigma). The images were captured using the C-Digit imaging system (Licor, Lincoln, USA) and 4-7 independent WB experiments were performed. Optical density (OD) was analyzed with ImageJ (version 1.48; National Institute of Health, Bethesda, MD), and the values were normalized to the OD values of loading control bands.

4.5 PROTEIN-FRAGMENT COMPLEMENTATION ASSAY

PCA in studies I and II was performed according to (Savolainen et al. 2015) with small modifications. N2A or PREPko cells were seeded on poly-L-lysine-coated 96-well plates at a density of 13 000 cells/well (PerkinElmer Life Sciences, white wall). 24 h post-plating, reporter plasmids were transfected with 100 ng of total plasmid DNA per well. In study I, N2A cells and PREPko cells were transfected with 25 ng of both αSyn-Gluc1 and αSyn-Gluc2 and 50 ng mock-plasmid or non-tagged human PREP expression plasmid 50 ng/well. In study II, N2A cells were transfected with αSyn-Gluc1 and αSyn-Gluc2 (25 ng/well) and 50 ng mock-plasmid (50 ng/well). 48 hours post-transfection medium was changed to phenol red free DMEM without serum containing the tested compounds at 10 μM concentration or proteasome inhibitor lactacystin (AG scientific) as a positive control. The PCA signal was detected by injecting 25 μl of native coelenterazine (Nanolight Technology) per well (final concentration of 20 μM). The emitted luminescence was read using Varioskan Flash multiplate reader (Thermo Scientific). For each experimental condition, 4 replicate wells were used in each experiment; 3–4 independent experiments with N2A cells and 2-4 with PREPko cells were performed. A 10 mM stock solution of compounds was prepared in DMSO and further diluted to phenol red free DMEM at 10 μM concentration. The corresponding amount of DMSO was used as the vehicle control.

4.6 *IN VITRO* ALPHA-SYNUCLEIN AGGREGATION ASSAY

Samples which consisted of 98 μM αSyn, 25 nM hPREP, 1 μM PREP inhibitors and 50 uM thioflavin-T in 100 μl buffer (20 mM HEPES, pH 7.40, 150 mM NaCl, 1 mM DTT) were pre-incubated for 15 min at room temperature. The plate was covered with plate sealer and placed in a microtiter plate reader (Tecan Infinite M200, Tecan Group Ltd.) at 37 °C. The plate was put to the shaker (200 rpm) for 999 seconds followed by an absorbance reading (350 nm) and fluorescence reading (Ex/Em 446 nm/482 nm, gain 100 and 80, 40 flashes). The turbidity and fluorescence course were monitored kinetically every 20 min during 200 h. Magellan software was used to process the experimental data.

4.7 NATIVE GEL ELECTROPHORESIS

For detection of different PREP conformations, native gel electrophoresis was performed as described in (Savolainen et al. 2015). 10% separating gel (40 % acrylamide/bis 2.5 mL, H_2O 4.8 mL 1.5 M Tris-HCl pH 7.9, 2.5 mL, 10 % SDS, 100 μL, 10 % ammonium persulfate, 50 μL, TEMED, 10 μL) with stacking gel (40 % acrylamide/bis, 334 μL, H_2O, 2.1 mL, 0.5 M Tris-HCl pH 6.8, 830 μL, 20% SDS 33 μL, 10 % ammonium persulfate 13.5 μL, TEMED 6.5 μL) were used. The samples containing 1 μM concentration of PREP inhibitor and 0.5 μg of purified recombinant porcine PREP in native sample buffer (#1610738, Biorad) were incubated for 30 min at 25 °C to and 15 μL was loaded on a native gel. After electrophoresis, the gel was stained with Coomassie blue (0.1% Coomassie Blue R250, 45 % ethanol and 10 % glacial acetic acid) for 2 h at room temperature. For destaining solution containing 45% methanol and 10 % glacial acetic acid was added for 2 × 30 min to get a clear background before it was scanned.

4.8 SYNTHESIS OF PREP LIGANDS

4.8.1 General information

All synthesized compounds were characterized by ^1H and ^{13}C NMR spectroscopy using a Bruker Avance III 400 MHz or Varian Mercury 300 MHz spectrometer. Chemical shifts are reported in parts per million (ppm), and spectra were calibrated using residual solvent signals (CDCl$_3$: δ_H = 7.26 ppm and δ_C = 77.16 ppm; CD$_3$OD: δ_H = 3.31 ppm and δ_C = 49.00 ppm). The progress of the reactions was monitored by thin‑layer chromatography on silica gel 60‑F$_{254}$ plates. Purification was performed with flash chromatography using silica gel (SiO$_2$) 60 (230–400 mesh). Mass spectrometric analysis was carried out with a Waters Synapt G2 HDMS mass spectrometer using electrospray ionization (ESI). The purity was determined by UPLC-MS with diode-array. Melting points were determined for non-amorphous solids by Stuart SMP40 automatic melting point instrument.

4.8.2 Synthetic procedures

The implemented synthesis procedures for compounds of study II are presented in the Results section. The solution phase synthesis was performed as the following: the connecting amide bonds were synthesized using activation of carboxylic acid groups to the corresponding acid chlorides or mixed anhydrides. For non-N-alkylated chiral amino acids, a milder activation to hydroxysuccinimide esters were used due to their susceptibility for racemization. The 4-phenylbutanoylaminoacyl-L-prolinamides were dehydrated to the corresponding nitriles with trifluoroacetic anhydride and then further reacted to form the corresponding tetrazoles with sodium azide. Experimental details and characterization of the tested compounds are presented in the Results section.

4.9 DOCKING STUDIES

Docking studies were done by using Schrödinger Maestro molecular modeling software (LLC, New York 2019). The crystal structure of PREP (PDB:3DDU) (Haffner et al. 2008) was selected for these studies as it had a good resolution of 1.56 Å and it included a co-crystallized ligand, which helped in determining the binding site. The protein structure was prepared with Maestro Protein Preparation Wizard. Preprocessing was done with the default settings with few exceptions: missing loops and sidechains were constructed with Prime, and heteroatom states were generated with Epik using pH of 7.4. Acetate ions and glycerol were removed from the structure. H-bonds were assigned with default settings using PROPKA pH of 7.4. Waters with less than 3 H-bonds to non-waters were removed and the structure was minimized with default settings using OPLS3e force field.

4.10 *IN VITRO* ASSAY FOR PROTEOLYTIC ACTIVITY OF PREP

The IC_{50}-values for compounds in study II were determined in the microplate assay procedure. The enzyme dilution or brain homogenate (10 μL) was preincubated with 0.1 M sodium–potassium phosphate buffer (65 μL, pH 7.0) containing the compounds at desired concentrations at 30 °C for 30 min. The final concentration of the compounds in the assay mixture varied from 1 mM-1 nM and the final concentration of the enzyme measured by Bradford´s method was approximately 2 nM. The enzyme reaction was carried out by incubating the mixture with 25 μL of 4 mM Suc-Gly-Pro-AMC substrate dissolved in 0.1 M sodium– potassium phosphate buffer (pH 7.0) at 30° C for 60 min. The reaction was terminated by adding 100 μL of 1 M sodium acetate buffer (pH 4.2). Formation of AMC was measured with Victor2 multilabel counter (PerkinElmer; excitation/emission 360 nm/ 460 nm). All activity measurements were made at least in triplicate. The inhibitory activities (percent of control) were plotted against the log concentration of the compound, and the IC_{50}-value was determined by non-linear regression utilizing GraphPad Prism 7.0 software.

4.11 ANIMALS

For study III, male C57BL/6J-Tg(Th-SNCA*A30P*A53T)39Eric/J (The Jackson Laboratory, USA) mice were used. Mouse line is originally described in (Richfield et al. 2002). In study III, mice were 3-18 months of age. For seven days i.p treatment with HUP-55, 15-month-old male and female C57BL/6J-Tg(Th-SNCA*A30P*A53T)39Eric/J mice were used. For these mice, HUP-55 (10 mg/kg) or vehicle (5% tween20 in 0,9 % NaCl (Braun)) were administered i.p every 12 hours for seven days. All animals used in this study were housed at 20-22 °C room temperature with 12 hours light/dark cycle and had access to food and water *ad libitum* in individually ventilated cages with bedding, nesting material, and Aspen brick. Mice had access to chow food and filtered and irradiated water *ad libitum*. The experiments were performed according to European Communities Council Directive 86/609/EEC and were approved by the Finnish National Animal Experiment Board (ESAVI/441/04.10.07/2016).

4.12 BEHAVIORAL EXPERIMENTS

In study III, locomotor activity was measured from 3, 6, 9, 12 and 18-months-old mice using automated open field locomotor activity chambers (Activity monitor, SOF-812, Med Associates inc, Georgia, USA). Total photobeam breaks were recorded for 22 h (starting at 10:00) for horizontal, vertical, and ambulatory movements. In the seven days HUP-55 treatment, 22 h locomotor measurements were carried out once before and after drug treatment. Amphetamine induced locomotor activity was assessed every third month in study III. Before administration of amphetamine (3 mg/kg i.p), mice were habituated in locomotor boxes for 30 min. Locomotor activity was recorded for 90 min. Grip strength was measured using grip strength meter (Columbus instruments, Ohio, USA). Animals were placed on the metal grid followed by gradual pull from tail until they grip and pull the grid. Three repeats were performed and the highest value was used in analysis.

4.13 MICRODIALYSIS

4.13.1 Surgical procedures

The stereotaxic operation was performed as described in (Julku et al. 2018). Guide cannula (AT4.9.iC, AgnTho's, Sweden) for microdialysis was inserted into the left STR at 0.6 mm anterior, 1.8 mm lateral, and 2.7 mm below the dura (stereotaxic coordinates according to (Franklin and Paxinos 1997)). The guide cannula was attached to the skull with dental cement (Aqualox, Voco, Germany) and two stainless steel screws (1.2×3 mm, DIN84, Helsingin Ruuvihankinta, Finland). The operation was performed under isoflurane anaesthesia (4 % induction, 1.5– 2.0 % maintenance; Attane vet 1000 mg/g, Piramal Healthcare, UK). Buprenorphine (0.1 mg/kg s.c.; Temgesic 0.3 mg/mL, Reckitt Benckiser Healthcare, UK) was given before the operation and 5-6 h after the surgery, and carprofen (5 mg/kg s.c.; Norocarp vet 50 mg/mL, Norbrook Laboratories Ltd, Ireland) was given immediately after the surgery and 24 h after the surgery for post-operative pain.

4.13.2 Microdialysis

Microdialysis was performed in the 12 and 18 months old mice as described earlier (Julku et al. 2018). In short, a microdialysis probe (1-mm cuprophan membrane, o.d. 0.2 mm, 6 kDa cut-off; AT4.9.1.Cu, AgnTho's) was inserted into the guide cannula 2 h before the experiment. The probe was perfused with a modified Ringer solution (147 mM NaCl, 1.2 mM $CaCl_2$, 2.7 mM KCl, 1.0 mM $MgCl_2$, and 0.04 mM ascorbic acid) at a flow rate of 2.0 μL/min. Four baseline samples were collected (20 min/40 μL/sample) after the stabilization period. After the collection of baseline samples, the probe was perfused 2×20 min with 10 μM and 30 μM d-amphetamine sulphate with 2×20 min recovery time between the concentrations. The concentrations of DA, its metabolites, dihydroxyphenylacetic acid (DOPAC) and homovanillic acid (HVA), gamma-aminobutyric acid (GABA) and 5-hydroxyindoleacetic acid (5-HIAA) which is a metabolite of 5-hydroxytryptamine (5-HT) in dialysates were measured using the HPLC methods that have been described earlier in (Julku et al. 2018).

4.14 TISSUE HPLC

Striatal tissue samples were punched below corpus callosum +0.74 mm from bregma to 2 mm depth by using sample corer (i.d. of 2 mm) with a plunger (Stoelting Co, Wood Dale, IL, USA) on a cryostat (Leica CM3050). Tissue processing was done as earlier described in (Julku et al. 2018). The concentration of DA, its metabolites, DOPAC and HVA, 5-HT, its metabolite 5-HIAA, GABA and glutamate in the tissue samples of striatum were analyzed with HPLC as earlier described in (Julku et al. 2018). The concentrations were calculated as nanograms per milligram of brain tissue.

4.15 IMMUNOHISTOCHEMISTRY

4.15.1 Tissue processing

At the age of 12- or 18-months mice were perfused using cold PBS under terminal pentobarbital anaesthesia (Mebunat Vet 60 mg/ml, Orion Finland) followed by dissection of the whole brain. The hemispheres were separated by using a brain matrix. The right hemispheres were post-fixed for 24 h in fresh 4 % paraformaldehyde (PFA) at 4 °C and transferred to 10 % sucrose in PBS (pH 7.4; 137 mM NaCl, 2.7 mM KCl, 10 mM Na_2HPO_4, 1.8 mM KH_2PO_4) for 24 h at 4 °C. After 24 h, brains were transferred to 30 % sucrose solution in PBS until they sank. Brains were frozen on dry ice and were kept at -80°C until sectioning. Frozen brains were sectioned as 30 μm free-floating sections on a cryostat (Leica CM3050) and kept in a cryoprotectant solution (30 % ethylene glycol and 30 % glycerol in 0.5 M phosphate buffer).

4.15.2 Staining procedure

TH IHC was done as described in (Svarcbahs et al. 2016). In short, after blocking endogenous peroxidase activity, sections were incubated for 30 min in 10 % normal goat serum to block nonspecific binding, after which the sections were incubated overnight in rabbit anti-TH primary antibody (1:2000; AB152, RRID:AB390204, Merck, Darmstadt, Germany). After that, the sections were placed in goat anti-rabbit biotin-conjugated secondary antibodies (1:500; BA1000, RRID:AB2313606, Vector Laboratories, Peterborough, UK). The signal was enhanced with the avidin–biotin complex method (Standard Vectastain ABC kit, RRID: AB2336819, Vector Laboratories, Peterborough, UK) and visualized using 3,3'-diaminobenzidine (DAB). Oligomer-specific -αSyn IHC was performed as described in Svarcbahs et al. 2016 (Svarcbahs et al. 2016) using the Basic Vector Mouse on Mouse (M.O.M.) Immunodetection Kit (BMK-2202, RRID:AB2336833, Vector Laboratories, Peterborough, UK). In short, after blocking endogenous peroxidase activity sections were incubated for 30 min in M.O.M. Mouse Ig Blocking Reagent to block nonspecific binding, and 5 min in M.O.M. diluent. The sections were transferred in mouse anti-human -αSyn oligomer-specific primary antibody (Brännström et al. 2014) (1:200 in M.O.M. diluent; AS132718, RRID: AB 2629502, Agrisera, Vännäs, Sweden) and incubated overnight. The total αSyn (1:600,

ab1903, Abcam) IHC was performed similarly to oligomer-specific αSyn staining. The sections were then incubated with goat- anti-mouse HRP-conjugated secondary antibody (dilution, 1:300 in M.O.M. diluent, catalogue #31430, RRID:AB228307, Thermo Fisher Scientific, Grand Island, NY, USA) and visualized using DAB.

4.15.3 Microscopy and optical density analysis

The ODs of TH and oligomer-specific αSyn from STR and SN were determined as described earlier(Svarcbahs et al. 2016). Digital images were scanned at 40x magnification with a Pannoramic Flash II Scanner (3DHISTECH, Budapest, Hungary). Three coronal sections from each mouse were processed for further analyses with Pannoramic Viewer (version 1.15.3. RRID:SCR 014424, 3DHISTECH). Images were converted to 8-bit grayscale and inverted. OD was analysed using line analysis tools for STR and freehand tool for SN in ImageJ (1.48b; RRID:SCR_003070, NIH). Background was substracted using OD of corpus callosum for each section and then normalized to the control mice.

4.16 STATISTICAL ANALYSIS

Statistical analysis for 22 h locomotor activity and amphetamine-induced locomotor activity in study III was conducted by IBM SPSS statistic software 25, using repeated measurements 2-way-ANOVA. All the other statistical analyses were conducted by GraphPad Prism 7.0 software using Student´s t-test or one-way ANOVA with suitable post-hoc-tests.

5 RESULTS

Several actions of PREP cannot be directly linked to its proteolytic activity, for example regulation of IP_3, modulation of neutrophilic inflammation, and neuronal cell development and differentiation (Di Daniel et al. 2009; Harwood 2011; Roda et al. 2014; Schulz et al. 2005). This has raised interest to study direct PPIs, and lately several interaction partners for PREP such as tubulin, GAPDH, and GAP-43 have been identified (Di Daniel et al. 2009; Matsuda et al. 2013; Schulz et al. 2005). PREP has also been shown to be involved in the αSyn aggregation process, although αSyn is not a substrate of PREP (Brandt et al. 2008; Myöhänen et al. 2012a). Inhibition of PREP with the small molecule KYP-2047 has been shown to decrease αSyn dimerization and increase autophagy, the latter of which is the main route for cells to degrade aggregated proteins *in vivo* and *in vitro* (Myöhänen et al. 2012a; Savolainen et al. 2014; Savolainen et al. 2015). However, only very few PREP inhibitors have been tested in PPI-related functions. Therefore, in study I we wanted to explore different PREP inhibitors in αSyn dimerization and autophagy. Based on the results, we synthesized novel PREP ligands and assessed their ability to decrease αSyn dimerization in study II. Furthermore, there is a lack of a well-characterized early onset mouse model for PD so in the final study we wanted to assess behavioral and DAercgic changes of A30P*A53T tg mice and test if novel PREP inhibitor HUP-55 could modify the PD pathology of these tg mice.

5.1 INHIBITION OF PROTEOLYTIC ACTIVITY OF PREP DOES NOT CORRELATE WITH ITS PROTEIN-PROTEIN INTERACTION-MEDIATED FUNCTIONS (I)

To investigate how a set of PREP inhibitors with different structures and IC_{50}-values affects on PREP's ability to increase autophagy and decrease αSyn dimerization we measured autophagy marker LC3B-II levels using WB and αSyn-αSyn interaction using PCA. In addition, a GFP-LC3-RFP expressing cell line was used to evaluate if PREP inhibitors have an effect on autophagic flux. Results of the assays are presented in **Fig. 4**. 3 out of 12 tested compounds had a statistically significant increase in LC3B-II levels (**Fig. 4A**). These compounds were KYP-2091 with 104 % increase to DMSO control (p = 0.002, 1-way ANOVA with Dunnett´s multiple comparison), KYP-2047 with 89 % increase to DMSO control, (p = 0.001, 1-way ANOVA with Dunnett´s multiple comparison) and KYP-2189 with 86 % increase to DMSO control (p = 0.0017, 1-way ANOVA with Dunnett´s multiple comparison). In addition, KYP-2001, KYP-2087, KYP-2117, KYP-2153, ZPP, and S17092 had an increasing trend ranging from 38% to 64 % increase compared to DMSO on LC3B-II levels. KYP-2101, KYP-2108, and KYP-2112 did not have an effect on LC3B-II levels. As measurements of LC3B-II levels shows only formation of autophagosomes, not the whole autophagy process we used GFP-LC3-RFP expressing HEK-293 cells to monitor autophagic flux. After 24 h 10 µM treatment with these PREP inhibitors, no accumulation of LC3B-II vesicles were observed and most of the compounds induced a small decrease in GFP signal indicating increased autophagic flux (**Fig. 4B**). In αSyn-αSyn PCA 6 out of 12 compounds, were able to decrease formation of αSyn dimers in the PCA (**Fig. 4C**). The most potent compound in this assay was KYP-2047 with 25% reduction of luminescence signal (p=0.0001, t=5.45, df=12, Student's t-test). Interestingly, KYP-2001, KYP-2087, KYP-2091, KYP-2108, and KYP-2117 decreased αSyn dimerization 12-17% compared to the control cells. Compounds KYP-2101, KYP-2112 KYP-2153, KYP-2189, ZPP, and S17092 did not reduce αSyn dimerization in the PCA. To ensure that the observed effect on αSyn dimerization was PREP-mediated, we treated PREPko cells for 4 h with 10 µM concentration of PREP inhibitors (**Fig. 4D**). No statistically significant changes in luminescence signal were observed with PREP inhibitors. However, when hPREP was restored with transient transfection, the reduction of αSyn dimers was seen with KYP-2091 (luminescence signal 72 % from DMSO control, 1-way ANOVA with Dunnett´s multiple comparisons, p=0.0097) and KYP-2047 (luminescence signal 89 % from DMSO control, not significant). Interestingly, KYP-2112 caused a small increasing effect on αSyn dimerization in this assay (luminescence signal 125 % compared to DMSO control, 1-way ANOVA with Dunnett´s multiple comparisons, p=0.028). Lactacystin (luminescence signal 160% compared to DMSO control, 1-way ANOVA with Dunnett´s multiple comparisons, p=0.0044) and hPREP transfection (50 ng/well blank) were used as positive control for αSyn dimerization.
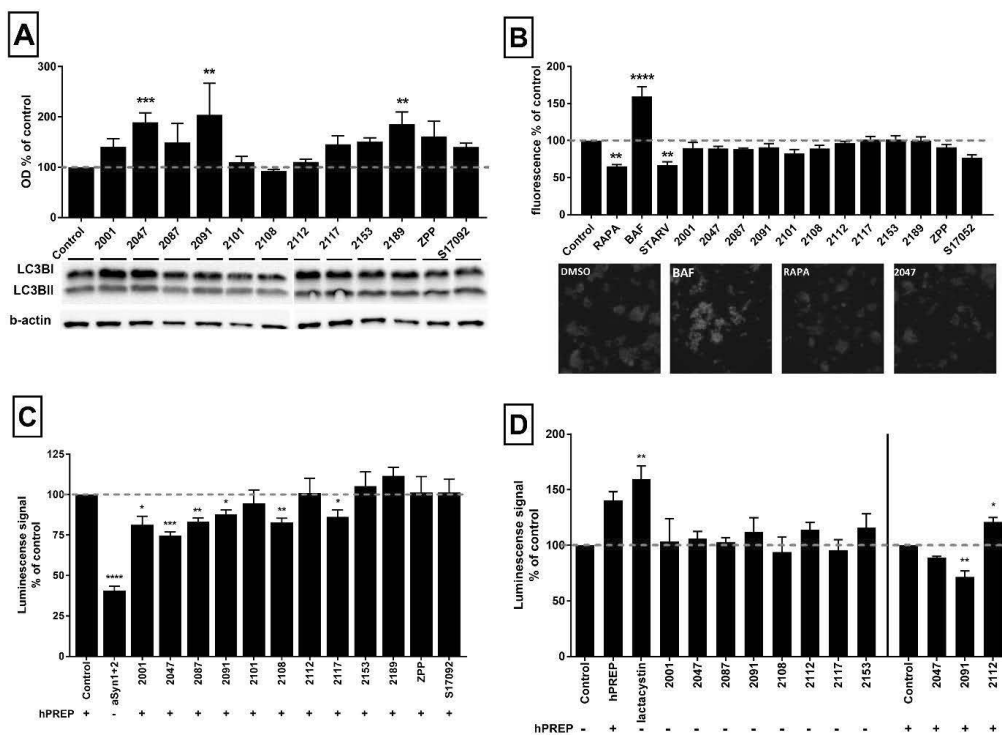
Figure 4A-D. **A**. The effect of tested PREP inhibitors on LC3B-II levels in HEK-293 cells at 1 μM concentration and with 4 h treatment. Compounds KYP-2047, KYP-2091, and KYP-2189 had statistically significant increases in the levels of LC3B-II: 197 %, 231 %, and 181 %, respectively, compared to DMSO control (1-way ANOVA with Dunnett´s multiple comparison to DMSO control, * p<0.05, ** p<0.005). **B**. The effect of 24 h treatment of studied PREP inhibitors at 10 μM concentration on autophagic flux in GFP-LC3-RFP expressing HEK-293 cells. None of the tested PREP inhibitors showed accumulation of LC3-II protein whereas 20 nM bafilomycin 1A (BAF) increased accumulation of LC3B and inhibited autophagic flux. 0.5 μM rapamycin (RAPA) treatment and serum starvation (STARV) induced autophagic flux significantly after 24 h treatment. (1-way ANOVA with Dunnett´s multiple comparison to DMSO control, ** p<0.005, *** p<0.001, **** p<0.0001). **C**. αSyn dimerization in N2A cells determined by protein-fragment complementation assay (PCA) with PREP overexpression (PREP inhibitors added at 10 μM final concentration for 4 h). Compounds KYP-2001, KYP-2047, KYP-2087, KYP-2091, KYP-2108, and KYP-2117 reduced αSyn dimer formation 12-25 % compared to control. Compound KYP-2047 showed the most potent effect on αSyn dimerization with 25 % reduction, while KYP-2091 being the least potent with 12 % reduction in αSyn dimerization. αSyn1+αSyn2+mock cells served as a negative control for αSyn dimerization as there is no PREP overexpression (*** p<0.001, **p< 0.01, *p<0.05; Student´s t-test compared to DMSO control). **D**. αSyn dimerization in PREPko cells in PCA assay. PREP inhibitors did not have an effect on αSyn dimerization when PREP was not present in the cells. Transfection of hPREP increased αSyn dimerization and PREP inhibitor KYP-2047 (not statistically significant) and KYP-2091 were able to decrease this compared to DMSO control (1-way ANOVA with Dunnett´s multiple comparison to DMSO control, *p<0.05, ** p<0.005). All data are presented as mean+SEM, n≥3. Hatched red line indicates the level of DMSO control.

Based on the αSyn dimerization assay results, we investigated how selected PREP inhibitors with distinct structures and IC$_{50}$-values, KYP-2047, KYP-2112, and KYP-2091, modulated αSyn aggregation in cell-free conditions. There was a difference in the results compared to αSyn PCA as all of the tested inhibitors reversed the accelerating effect of PREP on αSyn aggregation (**Fig. 5A**). Then again, no differences between weak (KYP-2091) and strong (KYP-2047 and KYP-2112) inhibitors were found. As the IC$_{50}$-values did not predict the impact in αSyn dimerization and

autophagy, we tested the effect of PREP inhibitors on PREP conformations in native gel to see if weak and potent inhibitors can cause different conformational changes. The assay revealed that all tested strong inhibitors locked PREP into one conformation but weaker inhibitors with IC_{50}-values higher than 100 nM did not have the same effect (**Fig. 5B**). Thus, a conformational change in PREP seen in native gel does not explain the discrepancy between IC_{50}-value and biological effect in αSyn dimerization and autophagy.
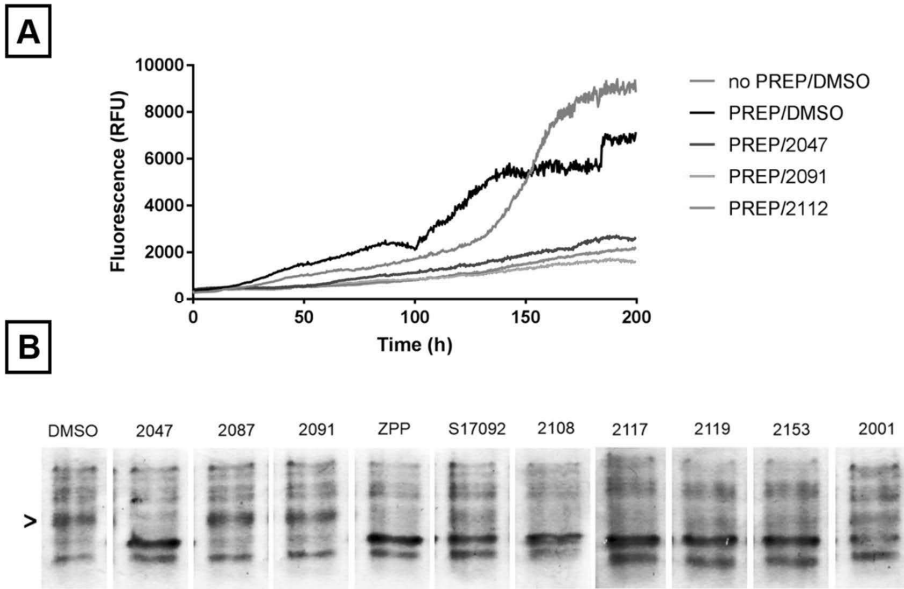

Figure 5A-B. **A.** Results of the *in vitro* αSyn aggregation assay. αSyn aggregation assay (β-sheet formation followed by thioflavin-T) was performed in the presence or absence of PREP and PREP inhibitors in a cell-free assay. All tested PREP inhibitors reduced the aggregation of αSyn in the presence of PREP. **B**. Conformation changes in PREP after treatment with 10 μm concentration of different PREP inhibitors. Potent PREP inhibitors lock the conformation while the weaker inhibitors do not lock one conformation leaving also the two other conformations visible in gel.

5.2 TETRAZOLE GROUP AS A REPLACMENT OF ELECTROPHILE IN TYPICAL PREP INHIBITORS (II)

5.2.1 IC$_{50}$-values of synthesized compounds

To evaluate if 4-phenylbutanoyl-aminoacyl-tetrazolyl-pyrrolidines have the same SAR against the proteolytic activity of PREP compared to 4-phenylbutanoyl-aminoacyl-pyrrolidines, a typical PREP inhibitor structure, we synthesized a series of compounds having different natural and unnatural amino acids (Pro, Ala, MeAla, Sar, D-Ala, Aib, B-Ala and Gly) at the P2-site and different substituents (H, CONH$_2$, COOH, CN and CH$_2$N$_4$) at the P1-site. We selected the most prominent amino acids for different P1 substituents. IC$_{50}$-values of all tested compounds are shown in Table 3. As expected, Pro and Ala were the most favorable aminoacids in all groups. Interestingly, MeAla also gave potent compounds (**7c, 14c**), except in combination with tetrazaole (**15c**). Overall, prolinamide intermediates **13a-13e** had only weak inhibitory activities and the nitrile intermediates **14a-14e** were highly potent inhibitors. However, introduction of tetrazole group gave similar IC$_{50}$-values than unsubstituted pyrrolidines. The most potent inhibitors were **15a** and **15b**, with IC$_{50}$-values of 12 and 129 nM, respectively. The only exception was MeAla where addition of the tetrazole group lowered the activity over 200-fold. The carboxylic acid analogues **10a** and **10b** of the most potent tetrazoles **15a** and **15b**, respectively, had only weak inhibitory activities.

Table 3. Structures and IC$_{50}$-values of synthesized compounds. Modifications were made on P2 aminoacid and R-group in the P1 pyrrolidine ring. Values with itlaics were measured using mouse brain homogenate, other values were obtained using recombinant purified porcine PREP.
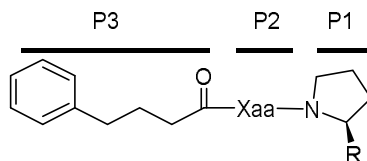
Compound	P2	R	IC$_{50}$ (nM)
7a (SUAM-1221)	Pro	H	12
7b	Ala	H	147
7c	MeAla	H	*298*
7e	Sar	H	*5141*
7f	D-Ala	H	*35180*
7g	Aib	H	*13510*
7h	βAla	H	*12080*
13a	Pro	CONH$_2$	4371
13b	Ala	CONH$_2$	*6213*
13c	MeAla	CONH$_2$	*28 800*
13d	Gly	CONH$_2$	*153 800*
13e	Sar	CONH$_2$	*457 000*
14a (KYP-2047)	Pro	CN	0.86
14b	Ala	CN	4.06
14c	MeAla	CN	5.4
14d	Gly	CN	220
14e	Sar	CN	269
15a	Pro	tetrazolyl	12
15b	Ala	tetrazolyl	129
15c	MeAla	tetrazolyl	27 180
15d	Gly	tetrazolyl	205 400
15e	Sar	tetrazolyl	10 640
10a	Pro	CO$_2$H	3626
10b	Ala	CO$_2$H	17 540

Values with italics were measured with mouse brain homogenate

5.2.3 4-Phenylbutanoyl-α-aminoacyl-tetrazolyl-pyrrolidines reduce αSyn dimerization in PCA-assay and might bind differently to the active site of PREP

To evaluate the ability of tetrazoles to reduce αSyn dimerization we used the PCA method; the nitrile intermediates and carboxylic acid compounds were also tested as a comparison. Lactacystin was used as a positive control for αSyn dimerization. Results of the assay are shown in **Fig. 6**. Notably, all 4-Phenylbutanoyl-α-aminoacyl-tetrazolyl-pyrrolidines (**15a-e**) decreased αSyn dimerization. Potent inhibitors **14c** (KYP-2047) and **14b** with nitrile group at R did not reduce αSyn dimerization but compounds **14a**, **14d**, and **14e** were able to reduce dimerization. Statistical significances were found using Student´s t-test compared to DMSO control with compounds, **15b** (75%, $p<0.05$), **15c** (75%, $p<0.05$), **15d** (77%, $p<0.05$), **14c** (KYP-2047, 89 % $p<0.005$) and **14d** (81% $p<0.05$). Carboxylic acid

analogues **10a** and **10b** of the most potent tetrzaoles **15a** and **15b** did not have an effect on αSyn dimerization.
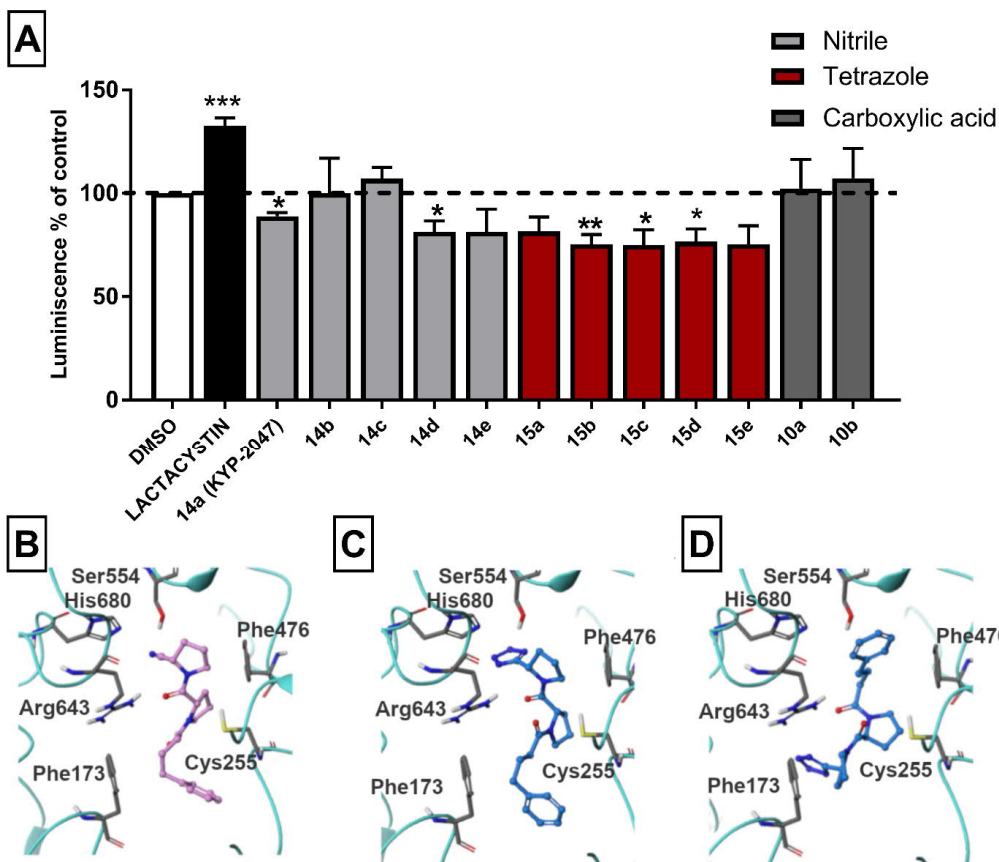

Figure 6A-D. Results of the αSyn-αSyn2 dimerization in PCA (protein-fragment complementation assay) with 4 h treatment and 10 μM concentration (**A**). Tetrazoles **15a-e** reduced the amount of αSyn dimers 18-25% compared to control. **14a** (KYP-2047), **14d**, and **14e** were the only compounds from the nitrile group which were able to reduce αSyn dimerization. Carboxyl acids **10a** and **10b** were not able to reduce formation of αSyn dimers. Lactacystin serves as a positive control for αSyn dimerization. Data are presented as means+SEM (n≥3, *** p<0.001, **p< 0.01, *p<0.05). Putative binding sites of the compounds (**B-D**). **14a** at the inhibitor-binding site (**B**). The nitrile points towards Ser554 and forms hydrogen bond to it (not shown in the figure). Compound **15a** at the inhibitor-binding site in the commonly known binding mode (**C**). A suggested hypothetical binding mode for the tetrazoles with compound **15a** as a representative compound (**D**).

Binding of these compounds to PREP were evaluated using molecular docking. Tetrazoles could place the tetrazole ring at S1 but they did not form an interaction with Ser554. The comparison with the poses of nitrile compounds at S1 revealed that the tetrazole ring might be positioned in the binding pocket slightly differently than the nitrile group. The most prominent difference were seen when compounds with proline (**14a** and **15a**) and glycine (**14d** and **15d**) at P2 were evaluated. The two most potent tetrazoles **15a** and **15b** formed an interaction between their negatively charged tetrazole group and the positively charged Arg643 instead of Ser554. Notably, the docking results also proposed other putative binding pose for all tetrazoles, where the phenyl group at P3 was oriented

toward S1. All nitriles oriented the nitrile group at S1 and the phenyl group at S3. The most potent nitriles **14a**, **14b**, and **14c** directed the nitrile group toward Ser554. However, in docking studies **14d** and **14e** could not orient the nitrile group toward the Ser554 residue.

5.2.2 Synthesis of compounds

The implemented synthetic routes and used reagents are presented in **Fig. 7**. The overall yields of products and number of steps are presented in **Table 4**. Overall yields varied from 13 % to 71 % over 2-6 steps depending on used amino acids. However, the formation of nitrile and tetrazole products had good yields from 58 % to 94 %, and 60 % to 89 %, respectively. The purity of all *in vitro* tested compounds was 95 % or higher, except for **15b** for which the purity was only 90 % due to the difficulties in purification. The yield from the last step, purification and characterization, for all tested products is presented below. Amide bonds of secondary amines, such as pyrrolidine and N-alkylated amino acids, have cis and trans isomers of almost the same stability, and these rotamers usually give separate signals in NMR spectra. The full experimental details are presented in the supplementary information of study II.
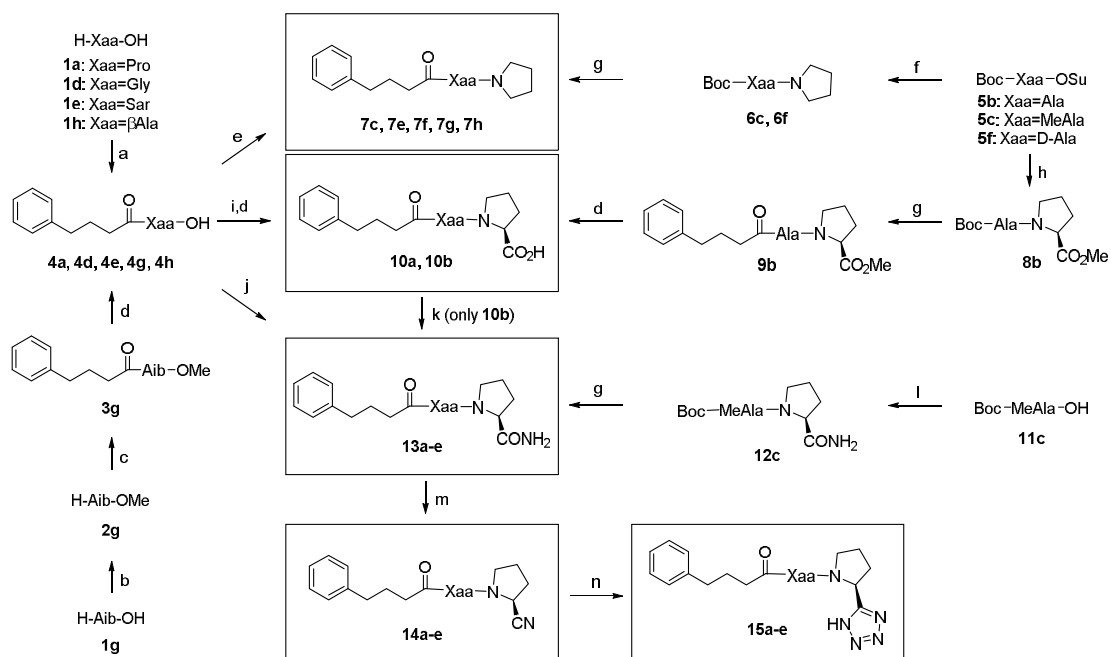

Figure 7. Synthesis of the compounds, where a specific aminoacyl group is always with the same lower-case letter in compound numbering. Reagents and conditions (a) 1. 10% aqueous Na_2CO_3, 4-phenylbutanoyl chloride / Et_2O; (b) $SOCl_2$ / MeOH, reflux; (c) 4-phenylbutanoyl chloride, DIPEA / DCM; (d) LiOH / water, MeOH; (e) 1. pivaloyl chloride (or in its place ethyl chloroformate for 4g), Et_3N / DCM, 0 °C, 2. pyrrolidine, Et_3N / DCM; (f) pyrrolidine / DCM; (g) 1. TFA / DCM, 0 °C, 2. 4-phenylbutanoyl chloride, Et_3N / DCM (or alternatively for 6f, 2. 1 M NaOH, 4-phenylbutanoyl chloride, / Et_2O); (h) L-proline methyl ester, DIPEA / DCM; (i) 1. ethyl chloroformate, Et_3N / DCM, 0 °C, 2. L-proline methyl ester, Et_3N / DCM; (j) 1. pivaloyl chloride, Et_3N / DCM, 0 °C, 2. L-prolinamide, Et_3N, / DCM; (k) 1. ethyl chloroformate,

Et₃N / THF, -10 °C, 2. NH₃ (7 M in MeOH); (l) 1. ethyl chloroformate, Et₃N / DCM, 0 °C, 2. L-prolinamide, Et₃N / DCM; (m) TFAA, Et₃N / THF; (n) NaN₃, NH₄Cl / DMF, 100 °C.

Table 4. Overall yields and number of steps for each tested compound.

Compound	Number of steps	Overall yield
7c	3	41 %
7e	2	71 %
7f	3	27 %
7g	2	23 %
7h	2	24 %
13a	2	52 %
13b	4	33 %
13c	2	44 %
13d	2	37 %
13e	2	43 %
14a (KYP-2047)	3	49 %
14b	5	26 %
14c	3	40 %
14d	3	21 %
14e	3	29 %
15a	4	44 %
15b	6	17 %
15c	4	37 %
15d	4	13 %
15e	4	26 %
10a	3	47 %
10b	3	46 %

4-Phenylbutanoyl-N-methyl-L-alanyl-pyrrolidine (7c). Flash chromatography (EtOAc/MeOH 9:1) gave colorless amorphous compound (0.40 g, 79 %). ^{1}H NMR (300 MHz, CDCl₃) δ 7.37–7.10 (m, 5H), 5.44 (q, J = 7.0 Hz, 1H), 3.50–3.38 (m, 4H), 2.89 (s, 3H), 2.68 (t, J = 7.5 Hz, 2H), 2.32 (t, J = 7.5 Hz, 2H), 2.10–1.68 (m, 6H), 1.27 (d, J = 7.0 Hz, 3H). ^{13}C NMR (75 MHz, CDCl₃) δ 172.72, 170.13, 141.78, 128.60, 128.50, 126.06, 50.06, 46.44, 46.12, 35.42, 32.87, 30.50, 26.49, 26.34, 24.22, 14.51. HRMS (ESI-QTOF) m/z [M+H]$^+$ calcd for C₁₈H₂₆N₂O₂: 303.2073, found: 303.2068.

4-Phenylbutanoyl-sarcosyl-pyrrolidine (7e) Flash chromatography (EtOAc/MeOH 9:1) gave a colorless amorphous compound (1.25 g, 87 %). ^{1}H NMR (300 MHz, CDCl₃) δ 7.35–7.12 (m, 5H), 4.10 (s, 1.8H), 3.88 (s, 0.2H) 3.50-3.38 (m, 4H), 3.06 (s, 2.6H), 2.97 (s, 0.4H) 2.71–2.61 (m, 2H), 2.39 (t, J = 7.5 Hz, 1.8H), 2.21 (t, J = 7.5 Hz, 0.2H) 2.09–1.77 (m, 6H) (two rotamers 9:1). ^{13}C NMR (75 MHz, CDCl₃) δ 173.52, 166.72, 141.93, 128.62, 128.39, 125.88, 50.01, 45.95, 45.76, 36.96, 35.27, 32.33, 26.47, 26.25, 24.16 (and an additional set of signals with lower intensity from minor rotamer). HRMS (ESI-QTOF) m/z [M+H]$^+$ calcd for C₁₇H₂₄N₂O₂: 289.1916, found: 289.1920.

4-Phenylbutanoyl-D-alanyl-pyrrolidine (7f) Flash chromatography (EtOAc/MeOH 99:1) gave a colorless amorphous compound (0.50 g, 66 %). ^{1}H NMR (300 MHz, CDCl₃) δ 7.33–7.09 (m, 5H), 6.49 (d, J = 7.0 Hz, 1H), 4.80–4.62 (m, 1H), 3.68–3.34 (m, 4H), 2.70–2.53 (m, 2H), 2.25–2.14 (m, 2H), 2.03–1.80 (m, 6H), 1.31 (d, J = 6.6 Hz, 3H). ^{13}C NMR (75 MHz, CDCl₃) δ 171.97, 171.06, 141.65, 128.63, 128.49, 126.04, 46.85, 46.50, 46.16, 36.02, 35.38, 27.25, 26.17, 24.25, 18.61. HRMS (ESI-QTOF) m/z [M+H]$^+$ calcd for C₁₇H₂₄N₂O₂: 289.1916, found: 289.1916.

4-Phenylbutanoyl-2-aminoisobutyl-pyrrolidine (7g). Flash chromatography (EtOAc/MeOH 9:1) gave a white hygroscopic powder (0.33 g, 44 %). ^{1}H NMR (300 MHz, CD$_3$OD) δ 7.35–7.07 (m, 5H), 3.44 (t, J = 6.7 Hz, 4H), 2.62 (t, J = 7.6 Hz, 2H), 2.21 (t, J = 7.6 Hz, 2H), 1.99–1.65 (m, 6H), 1.43 (s, 6H). ^{13}C NMR (75 MHz, CD$_3$OD) δ 174.52, 173.89, 142.87, 129.39, 129.37, 126.96, 57.57, 48.93, 48.63, 36.33, 35.91, 28.45, 28.07, 25.53, 23.95. HRMS (ESI-QTOF) m/z [M+H]$^+$ calcd for C$_{18}$H$_{26}$N$_2$O$_2$: 303.2073, found: 303.2071.

4-Phenylbutanoyl-β-alanyl-pyrrolidine (7h). Flash chromatography (EtOAc/MeOH 19:1) gave a colorless amorphous compound (0.61 g, 41.0 %)^{1}H NMR (300 MHz, CDCl$_3$) δ 7.33–7.11 (m, 5H), 6.48 (s, 1H), 3.54 (dd, J = 11.2, 5.8 Hz, 2H), 3.44 (t, J = 6.8 Hz, 2H), 3.35 (t, J = 6.7 Hz, 2H), 2.63 (t, J = 7.5 Hz, 2H), 2.45 (t, J = 5.6 Hz, 2H), 2.18–2.11 (m, 2H), 2.02 –1.76 (m, 6H). ^{13}C NMR (75 MHz, CDCl$_3$) δ 172.73, 170.45, 141.72, 128.59, 128.44, 126.00, 46.62, 45.69, 36.21, 35.41, 34.91, 34.30, 27.34, 26.11, 24.47. HRMS (ESI-QTOF) m/z [M+H]$^+$ calcd for C$_{17}$H$_{24}$N$_2$O$_2$: 289.1916, found: 289.1920.

4-Phenylbutanoyl-L-prolyl-L-proline (10a). Colorless amorphous compound (0.192 g, 76 %). ^{1}H NMR (400 MHz, CDCl$_3$) δ 7.40–7.11 (m, 5H), 6.28 (s, 1H), 4.69–4.51 (m, 2H), 3.85 (q, J = 8 Hz, 1H), 3.71 – 3.49 (m, 2H), 3.43 (dt, J = 9.7, 6.9 Hz, 1H), 2.77–2.55 (m, 2H), 2.45–1.70 (m, 12H). ^{13}C NMR (101 MHz, CDCl$_3$) δ 173.52, 172.93, 172.07, 141.79, 128.65, 128.45, 126.00, 59.94, 57.68, 47.55, 47.45, 35.21, 33.56, 28.70, 27.61, 26.05, 25.16, 24.99. HRMS (ESI-QTOF) m/z [M+H]$^+$ calcd for C$_{20}$H$_{26}$N$_2$O$_4$: 359.1971, found: 359.1971.

4-Phenylbutanoyl-L-alanyl-L-proline (10b). White powder (1.33 g 95 %). mp: 128-130 °C. ^{1}H NMR (300 MHz, CDCl$_3$) δ 7.33–7.10 (m, 5H), 6.45 (d, J = 7.5 Hz, 1H), 4.78 (p, J = 7.1 Hz, 1H), 4.57 (dd, J = 7.6, 4.6 Hz, 1H), 3.83–3.41 (m. 2H), 2.73–2.54 (m, 2H), 2.39–1.82 (m, 8H), 1.35 (d, J = 6.9 Hz, 2.4H), 1.31 (d, J = 6.9 Hz, 0.6H) (two rotamers 4:1). ^{13}C NMR (75 MHz, CDCl$_3$) δ 173.17, 173.16 172.56, 141.58, 128.63, 128.54, 126.11, 59.48, 47.46, 46.69, 35.82, 35.34, 28.32, 27.14, 25.03, 18.07 (and an additional set of lower intensity signals from minor rotamer). HRMS (ESI-QTOF) m/z [M+H]$^+$ calcd for C$_{18}$H$_{24}$N$_2$O$_4$: 333.1814, found: 333.1811.

4-Phenylbutanoyl-L-prolyl-L-prolineamide (13a) Flash chromatography (EtOAc/MeOH 9:1) gave a colorless amorphous compound (0.910 g, 66 %). ^{1}H NMR (400 MHz, CDCl$_3$) δ 8.19 (s, 0.5H), 7.32–7.13 (m, 5H), 6.90 (s, 0.5H), 5.71 (s, 0.5H), 5.41 (s, 0.5H), 4.67–4.59 (m, 1H), 4.45–4.33 (m, 0.5H), 4.28 (d, J = 7.9 Hz, 0,5H), 3.89–3.78 (m, 0,5H), 3.66–3.49 (m, 2.5H), 2.74–2.51 (m, 2H), 2.62–1.71 (m, 13H) (two rotamers 1:1). ^{13}C NMR (400 MHz, CDCl$_3$) δ 173.97, 173.80, 172.53, 172.19, 171.68, 170.80, 141.80, 141.63, 128.64, 128.63, 128.45, 128.43, 126.03, 125.97, 60.92, 59.57, 58.77, 57.81, 47.81, 47.41, 47.37, 46.84, 35.27, 35.20, 33.75, 33.62, 31.63, 28.88, 28.67, 27.02, 26.16, 26.05, 25.41, 25.15, 24.98, 22.27 (two rotamers). HRMS (ESI-QTOF) m/z [M+H]$^+$ calcd for C$_{20}$H$_{27}$N$_3$O$_3$: 358.2131, found: [M+H]$^+$ 358.2129.

4-Phenylbutanoyl-L-alanyl-L-prolineamide (13b). Flash chromatography (EtOAc/MeOH 9:1) gave a white hygroscopic powder (0.94 g, 71 %). ^{1}H NMR (300 MHz, CDCl$_3$) δ 7.58 (s, 0.2 H), 7.37–6.99 (m, 5H), 6.67 (s, 0.8 H), 6.53 (d, J = 7.7 Hz, 1H), 6.02 (s, 0.2 H), 5.88 (s, 0.8H), 4.80–4.67 (m, 1H), 4.59–4.47 (m, 1H), 3.80–3.50 (m, 2H), 2.64 (t, J = 7.5 Hz, 2H), 2.37–1.85 (m, 8H), 1.33 (d, J = 6.9 Hz, 2.4H), 1.28 (d, J = 6.9 Hz, 0.6 H) (two rotamers 4:1). ^{13}C NMR (75 MHz, CDCl$_3$) δ 173.51, 172.91, 172.29, 141.57, 128.58, 128.48, 126.05, 59.71, 47.42, 46.65, 35.77,

35.33, 27.58, 27.14, 25.16, 18.22 (and an additional set of lower intensity signals from minor rotamer). HRMS (ESI-QTOF) *m/z* [M+H]$^+$ calcd for $C_{18}H_{25}N_3O_3$: 332.1974, found: 332.1969.

4-Phenylbutanoyl-*N*-methyl-L-alanyl-L-prolineamide (13c). Flash chromatography (EtOAc/MeOH 9:1) gave a white hygroscopic powder (1.51 g, 66 %). ^{1}H NMR (400 MHz, CDCl$_3$) δ 7.23 (m, 5H), 6.80 (s, 0.2 H), 6.75 (s, 0,8 H) 5.60 (s, 1H), 5.39 (q, *J* = 7.1 Hz, 0.8H), 5.39 (q, *J* = 7.1 Hz, 0.2H) 4.59–4.35 (m, 1H), 3.73–3.50 (m, 2H), 2.95 (s, 2.4H), 2.85 (s, 0.6H), 2.65 (m, 2H), 2.29 (m, 3H), 2.19–1.78 (m, 5H), 1.32 (d, *J* = 7.1 Hz, 2,4H), 1.28 (d, *J* = 7.2 Hz, 0.6H) (two rotamers 4:1). ^{13}C NMR (400 MHz, CDCl$_3$) δ 173.59, 173.22, 172.36, 141.67, 128.58, 128.49, 126.07, 59.66, 50.06, 47.32, 35.32, 32.95, 30.77, 27.47, 26.36, 25.18, 14.65 (and an additional set of lower intensity signals from minor rotamer). HRMS (ESI-QTOF) *m/z* [M+Na]$^+$ calcd for $C_{19}H_{27}N_3O_3$: 368.1945, found: 368.1936.

4-Phenylbutanoyl-glycyl-L-prolineamide (13d) Flash chromatography (EtOAc/MeOH 6:1) gave a white hygroscopic powder (0.97 g, 45 %). ^{1}H NMR (400 MHz, CDCl$_3$) δ 7.39–7.04 (m, 5H), 6.75 (s, 1H), 6.48 (s, 1H), 5.67 (s, 1H), 4.55 (dd, J=7.6, 2.4 Hz, 1H), 4.07 – 3.99 (m, 1H), 3.69–3.49 (m, 1H), 3.49–3.36 (m, 1H), 2.66 (t, J=7.6 Hz, 2H), 2.41–2.29 (m, 1H), 2.29–2.18 (m, 2H), 2.11 (m, 1H), 2.06–1.86 (m, 4H). ^{13}C NMR (101 MHz, CDCl$_3$) δ 173.28, 173.22, 168.57, 141.56, 128.62, 128.53, 126.10, 60.06, 46.63, 42.19, 35.69, 35.35, 27.99, 27.21, 24.88. HRMS (ESI-QTOF) *m/z* calcd for $C_{17}H_{23}N_3O_3$: 318.1818, found: 318.1820.

4-Phenylbutanoyl-sarcosyl-L-prolineamide (13e). White hygroscopic powder (0.330 g, 52 %). ^{1}H NMR (400 MHz, CDCl$_3$) δ 7.44–7.23 (m, 5H), 7.07 (s, 1H), 5.59 (s, 1H), 4.69–4.63 (m, 1H), 4.26 (d, *J* = 15.8 Hz, 1H), 4.05 (d, *J* = 15.8 Hz, 1H), 3.85–3.73 (m, 1H), 3.66–3.52 (m, 1H), 3.19 (s, 2,6H), 3.18 (s, 0,4H), 2.77 (t, *J* = 7.5 Hz, 2H), 2.51–2.40 (m, 2H), 2.15–2.00 (m, 6H) (two rotamers 5:1). ^{13}C NMR (101 MHz, CDCl$_3$) δ 174.14, 173.77, 168.60, 141.74, 128.61, 128.49, 126.04, 60.05, 50.80, 46.85, 37.64, 35.29, 32.35, 28.18, 26.45, 24.86 (and an additional set of lower intensity signals from minor rotamer). HRMS (ESI-QTOF) *m/z* [M+H]$^+$ calcd for $C_{18}H_{25}N_3O_3$: 332,1974, found: 332,1974.

4-Phenylbutanoyl-L-prolyl-2(*S*)-cyanopyrrolidine (14a) Colorless amorphous product (0.58 g, 94 %), the crude product was used without further purifications in the next step and not as the tested KYP-2047 ^{1}H NMR (400 MHz, CDCl$_3$) δ 7.37–7.07 (m, 5H), 4.89–4.76 (m, 1H), 4.56 (dd, *J* = 8.2, 4.0 Hz, 1H), 3.95–3.81 (m, 1H), 3.70–3.53 (m, 2H), 3.49–3.37 (m, 1H), 2.66 (t, *J* = 7.5 Hz, 2H), 2.38–2.07 (m, 8H), 2.03–1.87 (m, 4H) . ^{13}C NMR (101 MHz, CDCl$_3$) δ 171.78, 171.49, 141.75, 128.63, 128.44, 125.99, 118.77, 57.48, 47.35, 46.61, 46.47, 35.21, 33.55, 29.81, 28.86, 26.04, 25.49, 25.01.

4-Phenylbutanoyl-L-alanyl-2(*S*)-cyanopyrrolidine (14b). Flash chromatography (*n*-heptane/EtOAc 1:1) gave a colorless amorphous compound (0.25 g, 80 %). ^{1}H NMR (300 MHz, CDCl$_3$) δ 7.43–6.98 (m, 5H), 6.53-6.25 (m, 1H), 4.82–4.52 (m, 2H), 3.91–3.42 (m, 2H), 2.80–2.52 (m, 2H), 2.34–2.10 (m, 6H), 2.02–1.90 (m, 2H), 1.43 (d, *J* = 6.9 Hz, 0.3 H), 1.36 (d, *J* = 6.9 Hz, 2.3H), 1.31 (d, *J* = 6.9 Hz, 0.5H) (three rotamers 15:3:2) ^{13}C NMR (75 MHz, CDCl$_3$) δ 172.39, 171.97, 141.51,128.60, 128.51, 126.09, 118.20, 46.63, 46.61, 46.49, 35.69, 35.25, 29.92, 27.09, 25.35, 18.15 (and two additional sets of lower intensity signals from minor rotamers). HRMS (ESI-QTOF) *m/z* [M+H]$^+$ calcd for $C_{18}H_{23}N_3O_2$: 314.1869, found: 314.1872. (NB. This compound gave three rotamers although only one amide bond is N-alkylated)

4-Phenylbutanoyl-*N*-methyl-L-alanyl-(*S*)-cyanopyrrolidine (14c). Flash chromatography (gradient *n*-heptane/EtOAc 9:1 → EtOAc) gave a colorless amorphous compound (1.04 g, 91 %).

^{1}H NMR (400 MHz, CDCl$_3$) δ 7.56–6.90 (m, 5H), 5.56 (q, J = 7.2 Hz, 0.4H), 5.35 (q, J = 7.2 Hz, 0.6H), 4.76 (d, J = 6.7 Hz, 0.4H), 4.73–4.65 (m, 0.6H), 3.69–3.46 (m, 2H), 2.94 (s, 1.8H), 2.83 (s, 1.2H), 2.80–2.53 (m, 2H), 2.40–1.90 (m, 8H), 1.35 (d, J = 7.1 Hz, 1.8H), 1.27 (d, J = 6.8 Hz, 1.2H) (two rotamers 3:2). ^{13}C NMR (101 MHz, CDCl$_3$) δ 173.27, 171.31, 141.62, 128.57, 128.50, 126.09, 118.44, 49.98, 46.65, 46.47, 35.30, 32.90, 30.72, 29.97, 26.36, 25.40, 14.48 (and an additional set of lower intensity signals from minor rotamer). HRMS (ESI-QTOF) m/z [M+H]$^+$ calcd for C$_{19}$H$_{25}$N$_3$O$_2$: 328.2025, found: 328.2028.

4-Phenylbutanoyl-glycyl-2(S)-cyanopyrrolidine (14d). Flash chromatography (EtOAc) gave a colorless amorphous compound (0.364 g, 58 %). ^{1}H NMR (400 MHz, CDCl$_3$) δ 7.32–7.15 (m, 5H), 6.39 (s, 1H), 4.77–4.69 (m, 1H), 4.16-4.06 (m, 2H), 3.75–3.58 (m, 1H), 3.53–3.41 (m, 1H), 2.66 (t, J = 7.6 Hz, 2H), 2.39–2.09 (m, 6H), 2.04–1.95 (m, 2H). ^{13}C NMR (101 MHz, CDCl$_3$) δ 173.06, 167.63, 141.52, 128.63, 128.53, 126.11, 118.01, 46.70, 45.64, 42.13, 35.70, 35.34, 30.03, 27.18, 25.16. HRMS (ESI-QTOF) m/z [M+H]$^+$ calcd for C$_{17}$H$_{21}$N$_3$O$_2$: 300.1712, found: 300.1713.

4-Phenylbutanoyl-sarcocyl-2(S)-cyanopyrrolidine (14e). Flash chromatography (EtOAc/MeOH 19:1) gave a colorless amorphous compound (0.780 g, 69 %). ^{1}H NMR (400 MHz, CDCl$_3$) δ 7.31–7.16 (m, 5H), 4.96 (dd, J = 8.4, 1.9 Hz, 0.2H), 4.79–4.73 (m, 0.8H), 4.50 (m, 1H), 3.96–3.84 (m, 0.2H), 3.73 (d, J = 16.1 Hz, 0.8H), 3.67–3.40 (m, 2H), 3.10 (s, 0.6H), 3.08 (s, 2.4H), 2.68 (t, J = 7.5 Hz, 2H), 2.46–2.05 (m, 6H), 2.04–1.93 (m, 2H) (two rotamers 4:1). ^{13}C NMR (101 MHz, CDCl$_3$) δ 173.82, 167.87, 141.82, 128.65, 128.49, 126.02, 118.42, 49.92, 46.39, 45.90, 37.08, 35.32, 32.29, 29.93, 26.44, 25.37 (and an additional set of lower intensity signals from minor rotamer). HRMS (ESI-QTOF) m/z [M+H]$^+$ calcd for C$_{18}$H$_{23}$N$_3$O$_2$: 314.1869, found: 314.1869.

4-Phenylbutanoyl-prolyl-2(S)-tetrazolyl-pyrrolidine (15a). Flash chromatography (EtOAc/MeOH 4:1) gave a brown amorphous compound (0.564 g, 89 %). ^{1}H NMR (400 MHz, CD$_3$OD) δ 7.43–7.03 (m, 5H), 5.40 (dd, J = 8.2, 3.5 Hz, 1H), 4.70–4.60 (m, 1H), 3.97–3.88 (m, 1H), 3.87–3.37 (m, 3H), 2.73–2.57 (m, 2H), 2.47–2.09 (m, 6H), 2.09–1.66 (m, 6H). ^{13}C NMR (101 MHz, CD$_3$OD) δ 174.01, 173.38, 159.79, 143.07, 129.53, 129.37, 126.93, 59.38, 52.94, 48.67, 48.23, 36.08, 34.38, 32.00, 29.58, 27.57, 25.82, 25.67 (and an additional set of lower intensity signals (ca. 10 %) from minor rotamer). HRMS (ESI-QTOF) m/z [M+H]+ calcd for C$_{20}$H$_{26}$N$_6$O$_2$: 383,2195 found: 383,2196.

4-Phenylbutanoyl-L-alanyl-2(S)-tetrazolyl-pyrrolidine (15b). Flash chromatography (EtOAc/MeOH/AcOH 749:250:1) gave a yellowish amorphous compound (64 %, 0.182 g). ^{1}H NMR (300 MHz, CD$_3$OD) δ 7.30–7.06 (m, 5H), 5.49–5.33 (m, 1H), 4.71–4.33 (m, 1H), 4.01–3.46 (m, 2H), 2.66–2.54 (m, 2H), 2.48–2.00 (m, 6H), 1.95–1.79 (m, 2H), 1.33 (m, 0.7H), 1.28 (d, J = 7.0, 2.3H) (two rotamers 3:1). ^{13}C NMR (75 MHz, CD$_3$OD) δ 175.58, 173.82, 160.95, 142.98, 129.47, 129.34, 126.89, 53.43, 48.43, 48.23, 36.24, 35.96, 32.17, 28.57, 25.75, 16.72 (and an additional set of lower intensity signals from minor rotamer). HRMS (ESI-QTOF) m/z [M+H]+ calcd for C$_{18}$H$_{24}$N$_6$O$_2$: 357.2039, found: [M+H]+ 357.2036. Purity 90 % according UPLC-MS

4-Phenylbutanoyl-N-methyl-L-alanyl-2(S)-tetrazolyl-pyrrolidine (15c). Flash chromatography (gradient EtOAc/MeOH 9:1 → 3:1) gave a brown amorphous compound (0.706 g, 93 %). ^{1}H NMR (400 MHz, CD3OD) δ 7.32–7.12 (m, 5H), 5.50–5.40 (m, 0.4 H), 5.39–5.34 (m, 0.8 H), 5.28 (q, J = 7.0 Hz, 0.8H) 3.85–3.50 (m, 2H), 2.90 (s, 2.3 H), 2.81 (s, 0.2H), 2.60 (s, 0.5H) 2.71–2.63 (m, 2H), 2.46–2.30 (m, 3H), 2.20–1.85 (m, 5H), 1.30 (d, J = 6.8 Hz, 0.2H),1.25 (d, J = 6.8 Hz, 2.3H) 1.20 (d, J = 6.8 Hz, 0.5H) (three rotamers 77:17:6). 13C NMR (101 MHz, CD3OD) δ 175.47, 172.73, 159.71,

143.01,129.60, 129.49, 126.99, 53.32, 52.79, 48.13, 36.18, 33.63, 32.15, 31.30, 27.82, 25.67, 14.14 (and two additional sets of lower intensity signals from other rotamers). HRMS (ESI-QTOF) m/z [M+H]+ calcd for $C_{19}H_{26}N_6O_2$: 371.2195, found: [M+H]+ 371.2198.

4-Phenylbutanoyl-glycyl-2(S)-tetrazolyl-pyrrolidine (15d). Flash chromatography (EtOAc/MeOH 20:7) gave a white powder (0.154 g, 60 %). ^{1}H NMR (400 MHz, CD3OD) δ 7.33–7.06 (m, 5H), 5.50-3.59 (m, 1 H), 4.18-4.08 (m, 1H), 3.98 (d, J = 16.8 Hz, 0.6H), 3.83-3.70 (m, 1H), 3.69–3.53 (m, 1H), 3.35 (d, J = 16,8, 0.4 H), 2.72–2.53 (m, 2H), 2.46–1,85 (m, 8H) (two rotamers 3:2). ^{13}C NMR (101 MHz, CD3OD) δ 176.38, 169.79, 162.65, 142.98, 129.49, 129.36, 126.90, 54.40, 47.90, 42.91, 36.22, 34.95, 32.51, 28.61, 23.16 (and an additional set of lower intensity signals from minor rotamer). HRMS (ESI-QTOF) m/z [M+H]+ calcd for $C_{17}H_{22}N_6O_2$: 343.1882, found: [M+H]+ 343.1883.

4-Phenylbutanoyl-sarcosyl-2(S)-tetrazolyl-pyrrolidine (15e). Flash chromatography (EtOAc/MeOH 3:1) gave a brown amorphous compound (0.345 g, 88 %). ^{1}H NMR (400 MHz, CD3OD) δ 7.34–7.08 (m, 5H), 5.49–5.30 (m, 1H), 4.40–4.09 (m, 2H), 3.90–3.47 (m, 2H), 3.01 (s, 1.6H), 2.93 (s, 0.5H), 2.89 (s, 0.6H), 2.81 (s, 0.3H), 2.70–2.49 (m, 2H), 2.49–2.20 (m, 3H), 2.20–1.71 (m, 5H) (four rotamers 53:20:17:10).^{13}C NMR (101 MHz, CD3OD) δ 176.33, 169.66, 160.33, 143.11, 129.51, 129.37, 126.92, 53.67, 51.33, 47.45, 37.51, 36.14, 33.17, 32.27, 27.87, 25.52 (and three additional sets of lower intensity signals from minor rotamers). HRMS (ESI-QTOF) m/z [M+Na]+ calcd for $C_{18}H_{24}N_6O_2$: 379.1853, found: 379.1850.

5.3 CHARACTERIZATION OF A30P*A53T ALPHASYNUCLEIN TRANSGENIC MOUSE MODEL OF PARKINSON´S DISEASE (III)

5.3.1 A30P*A53T transgenic mice have altered locomotor activity

22 h locomotor activity measurements were done to asses differences in locomotor behavior between transgenic (tg) C57BL/6J-Tg(Th-SNCA*A30P*A53T)39Eric/J mice and wt littermates in 3-, 6-, 9- 12- and 15- moths old mice (**Fig.8A-F**). All age group had differences in locomotor activity between tg and wt animals. However, 3-month-old mice did not have a statistically significant difference but, -tg mice were slightly less active compared to wt littermates (**Fig.8A**, genotype effect: $F_{1,16}$ = 3.705, p = 0.072, repeated measures 2-way ANOVA) , between the second and fifth hour (11-14). In 6-month-old mice, statistically significant differences were found between 12:00 and 14:00, and 22:00 and 00:00 when tg mice were less active compared to wt littermates (**Fig.8B**, 12:00-14:00 genotype effect: $F_{1,26}$ = 9.982, p = 0.004; 22:00-00:00 genotype effect: $F_{1,26}$ = 12.986, p = 0.001, repeated measures 2-way ANOVA). Similar but more robust effects were also seen in 9-month-old mice. Tg mice had lower activity between 12:00 and 14:00, and between 22:00 and 02:00 compared to wt littermates (**Fig.8C**, 12:00-14:00 genotype effect: $F_{1,28}$ = 9.725, p = 0.004; 22:00-02:00 genotype effect: $F_{1,28}$=19.213, p = 0.0001, repeated measures 2-way ANOVA). However, between 18:00 and 20:00 tg mice were more active compared to wt littermates (**Fig. 8C**, genotype effect: $F_{1,28}$ = 8.924, *p* = 0.006, repeated measures 2-way ANOVA). 12-month-old mice also had similar behavioral profile as 6- and 9-month-old animals. Tg mice were more active compared to wt littermates during 18:00 and 20:00 period (**Fig. 8D,** genotype effect: $F_{1,35}$ = 6.620, p = 0.014, repeated measures 2-way

ANOVA), but between 12:00 and 15:00, and between 22:00 and 02:00 tg mice had decreased activity compared to wt littermates (**Fig. 8D**, 12:00–15:00 genotype effect: $F_{1,35} = 5.911$, $p = 0.029$; 22:00-02:00 genotype effect: $F_{1,35} = 6.540$, $p = 0.015$, repeated measures 2-way ANOVA). Interestingly, the roles shifted at 18 months as during the night time tg mice were more active compared to wt littermates (**Fig. 8E** genotype effect: $F_{1,14} = 20.753$, $p = 0.0004$, repeated measures 2-way ANOVA).
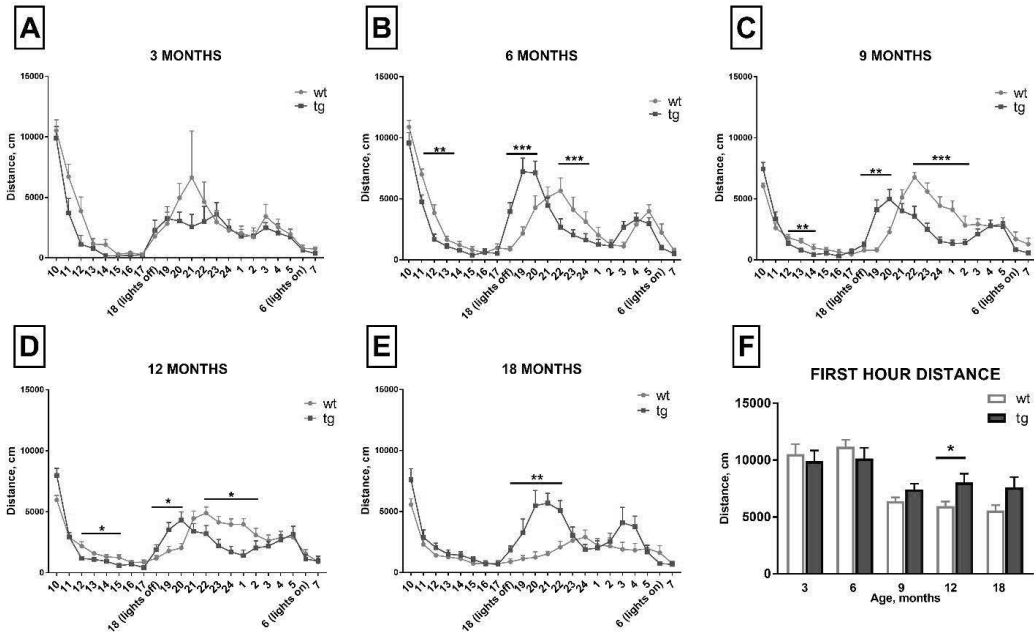
Figure 8A-F. 22 h locomotor activity was measured every 3 months in A30P*A53T transgenic mice (tg) and wild-type littermates (wt) (**A**). Dark time locomotor activity was altered in the 6- (**B**), 9- (**C**), 12- (**D**) and 18- (**E**) month-old mice but not in the young 3-month-old mice (**A**). Average speed was decreased in tg mice at all timepoints (**F**). n = 8-22, *$p <$ 0.05, $p** < 0.01$, $p*** < 0.001$, $p**** < 0.0001$, repeated measures ANOVA (**A-E**), Student´s t-test (**F**).

In addition, grip strength was altered in 6-month-old tg mice compared to wt littermates (**Fig. 9A** t=2.989, df=31, p=0.0054, Student´s t-test). Other parameters measured during 22 h revealed differences in total distance traveled, vertical activity, jump count, and average speed between tg and wt mice (**Fig. 9B-D**). Tg mice had decreased vertical activity as vertical counts (**Fig. 9B,** 3 months t = 2.54, p = 0.0218, Student´s t-test, 6 months t = 4.409, p = 0.0002, Student´s t-test) and vertical time (**Fig. 9C**, 3 months, t=2.46, p=0.026, 6 months t=2.81, p=0.009, Student´s t-test) were lower in 3- and 6-month-old tg mice compared to wt mice. However, 12-month-old tg mice had more vertical counts compared to wt littermates (**Fig. 9B**, t = 2.068, p = 0.045, Student´s t-test) but no differences in vertical time was found. Tg mice also had a significantly lower jump count at 3 (**Fig. 9D**, t = 3.835, p = 0.0013, Student´s t-test), 6 (**Fig. 9D**, t = 7.062, p<0.0001, Student´s t-test) and 9 months (**Fig. 9D**, t = 2.785, p = 0.0093, Student´s t-test). Furthermore, average speed was significantly lower during the ambulatory episodes in tg mice compared to wt mice in all age groups (**Fig. 9E**, 3 (t=6.028), 6 (t=7.356), 12 (t=8.311) and 18 (t=5.718) months p < 0.0001; 9 months, t = 3.328, p = 0.0023, Student´s t-test).
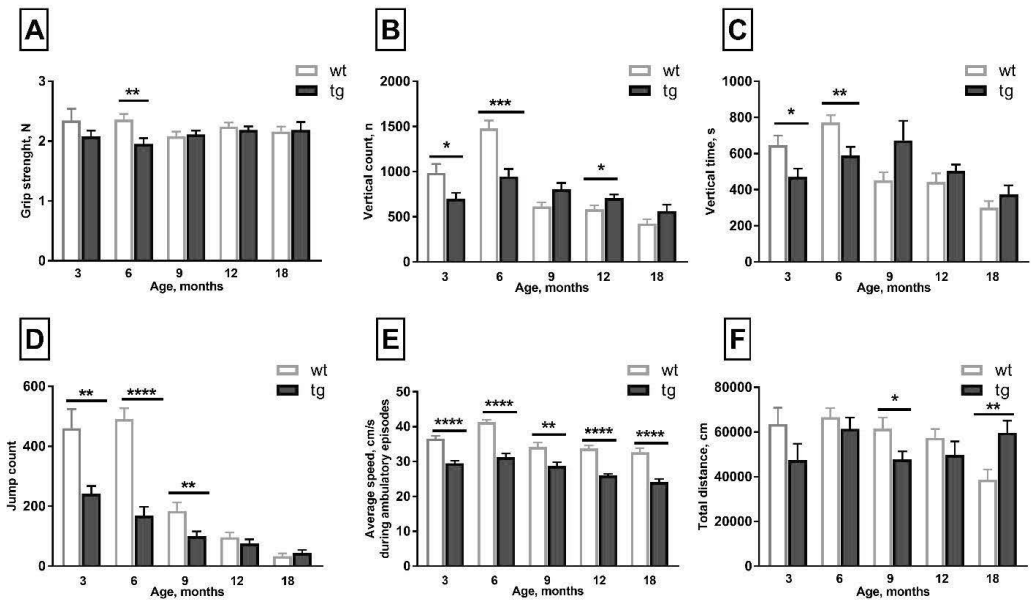
Figure 9A-F. Comparison of grip strength (**A**) (this data is not found in the article) and parameters measured during the 22 h locomotor activity monitoring (**B-F**) A30P*A53T transgenic mice (tg) and wild-type littermates (wt). Grip strength were altered in 6-month-old tg mice compared to wt littermates (**A**). Differences in vertical activity was seen in 3-, 6- and 12-month-old animals where tg mice had decreased vertical activity compared to wt mice at 3 and 6 months (**B** and **C**), but tg mice were more active at 12 months (**B**). 3- and 6-month-old tg mice showed significantly fewer vertical counts compared to littermates (**B**). 12-month-old tg mice had more vertical counts compared to wt mice (**B**). Jump counts were significantly lower in 3-, 6-, and 9-month-old tg mice compared to wt littermates (**D**). Average speed of tg mice was significantly lowered in all age groups (**E**). Total distance traveled was decreased in 9-month-old and increased in 18-month-old tg mice compared to wt mice (**F**). Data are expressed as mean ± SEM, n = 7–23. Student's t-test, *p < 0.05, **p < 0.005, ***p < 0.001, ****p < 0.0001.

To evaluate differences in systemic amphetamine administration in tg mice, 90 min amphetamine-induced locomotor activity was measured. Tg and wt mice did not have statistically significant differences at 3 and 12 months while at the 9-month time-point tg animals were more active compared to wt littermates only during the first 15 minutes after amphetamine administration (**Fig. 10C**, genotype effect: $F_{1,30}$ = 4.790, p = 0.037, repeated measures 2-way ANOVA). In addition, 6-month-old tg animals were significantly more active during the whole 90 minute period compared to wt littermates (**Fig. 10B**, genotype effect: $F_{1,32}$ = 9.649, p = 0.004, repeated measures 2-way ANOVA). In 18-month-old mice, a similar effect was observed (**Fig. 10F**, genotype effect: $F_{1,15}$ = 4.632, p = 0.047, repeated measures 2-way ANOVA). Interestingly, total traveled distance during the first 5 minutes, when mice are exploring their new surroundings, was significantly increased in 3 (**Fig. 10A**, t = 2.879, p = 0.01, Student's t-test), 6- (**Fig. 10B**, t = 3.701, p = 0.0008, Student's t-test), 12- (t=2.306, p = 0.026, Student's t-test) and 18-month-old (**Fig. 10F**, t=2.429, p = 0.028, Student's t-test) tg mice compared to wt littermates.
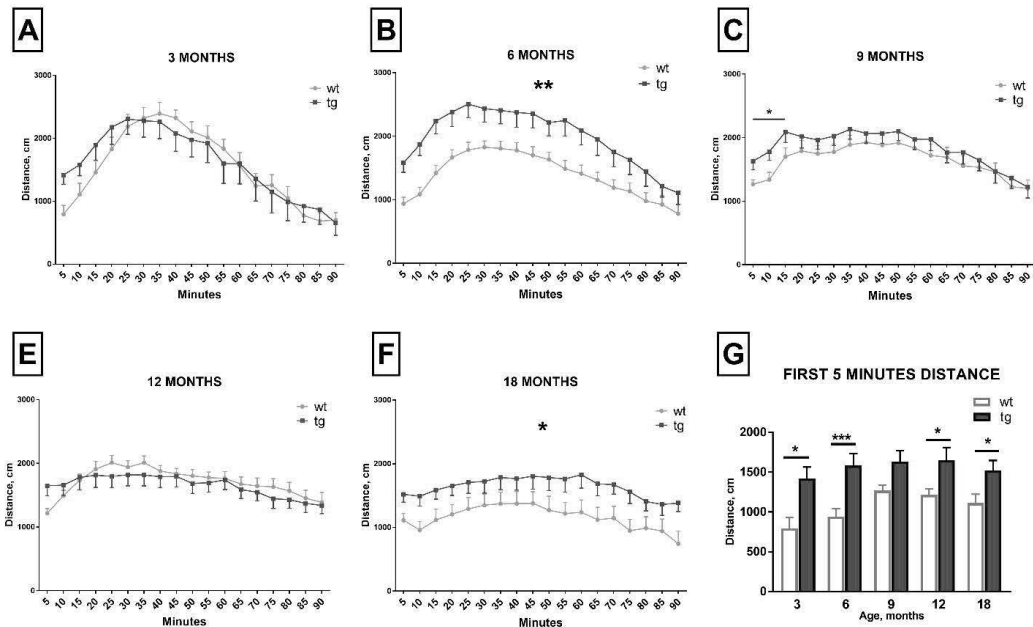
Figure 10A-G. Amphetamine induced locomotor activity was increased in A30P*A53T transgenic mice (tg) and wild-type littermates (wt). Increased activity in tg mice was seen at 6- and 18-month-old mice throughout the measurement, while only initial locomotor activity was increased in 9-month-old tg animals, after the amphetamine administration (**A-E).** Distance travelled during the initial 5 minutes of the locomotor activity test was increased in tg mice in all age groups compared to wt littermates (**F**). Data are expressed as mean ± SEM; n = 7-23. Repeated measures two-way ANOVA (**A-E**), Student´s t-test (F); *p < 0.05, ** p < 0.01, ***p<0.001

5.3.2 A30P*A53T transgenic mice have age-dependent changes in striatal dopamine

The impact of the double mutant A30P*A53T transgene in the striatal DAergic function was studied in 12- and 18-month-old tg mice and their wt littermates by microdialysis and HPLC analysis. In microdialysis, the baseline levels of extracellular striatal DA, its metabolites DOPAC and acid HVA, or GABA were not changed statistically significantly in the 12- or 18-month-old tg mice compared to wt littermates. However, the extracellular concentration of 5-HIAA was increased in the 12- and 18-month-old tg mice **(Fig. 11C)**. Amphetamine-induced DA release elevated striatal extracellular DA concentration less in 12-month old tg mice than in wt littermates with 30 μM d-amphetamine sulphate concentration (**Fig. 11A**, $F_{1, 20} = 4.988$, p = 0.037, repeated measures ANOVA), and there was a similar trend with the 10 μM dose (**Fig. 11A**, $F_{1, 20} = 3.286$, p = 0.085, repeated measures ANOVA). A similar difference was not observed in the 18-month group (**Fig.11B**, 10 μM d-amphetamine sulphate: $F_{1, 12} = 0.573$, p = 0.463; 30 μM d-amphetamine sulphate: $F_{1, 12} = 0.470$, p = 0.506, repeated measures ANOVA).

HPLC analysis revealed that striatal tissue concentrations of DA, its metabolites DOPAC and HVA, and 5-HT and its metabolite 5-HIAA and glutamate were not significantly altered in the 12-month-old tg mice compared to wt littermates. However, striatal concentration of DA was lower in the 18-month-old tg mice compared to wt littermates (**Fig.12A**, t=2.639, p = 0.019, Student´s t-test).

Additionally, 5-HT (**Fig. 12D**, t=4.283, p = 0.0008, Student´s t-test), GABA (**Fig.12C**, t=2.631, p = 0.020, Student´s t-test), and glutamate (**Fig.12B**, t=2.546, p = 0.023, Student´s t-test) were significantly elevated in the 18-month-old tg mice. Striatal GABA and glutamate were decreased in 18-month-old wt mice compared to 12-month-old wt mice (**Fig. 12C**, GABA: t = 2.647, p = 0.017; **Fig. 12B**, GLU: t = 2.508, p = 0.023, Student´s t-test), but a similar phenomenon was not observed in the tg mice.
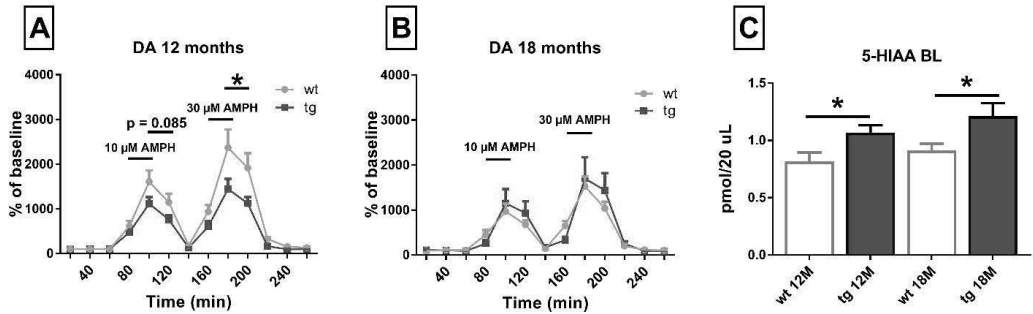
Figure 11A-B. Amphetamine-induced dopamine (DA) release was decreased in the 12-month-old A30P*A53T transgenic mice (tg) compared to wild-type littermates (wt) in striatal microdialysis (**A**) but a similar difference was not observed in the 18-month-old mice (**B**). 5-HIAA was increased in both 12-month-old and 18-month-old tg mice (**C**). n = 7-12. *p < 0.05, repeated measures ANOVA (**A-B**), Student´s t-test (**C**).
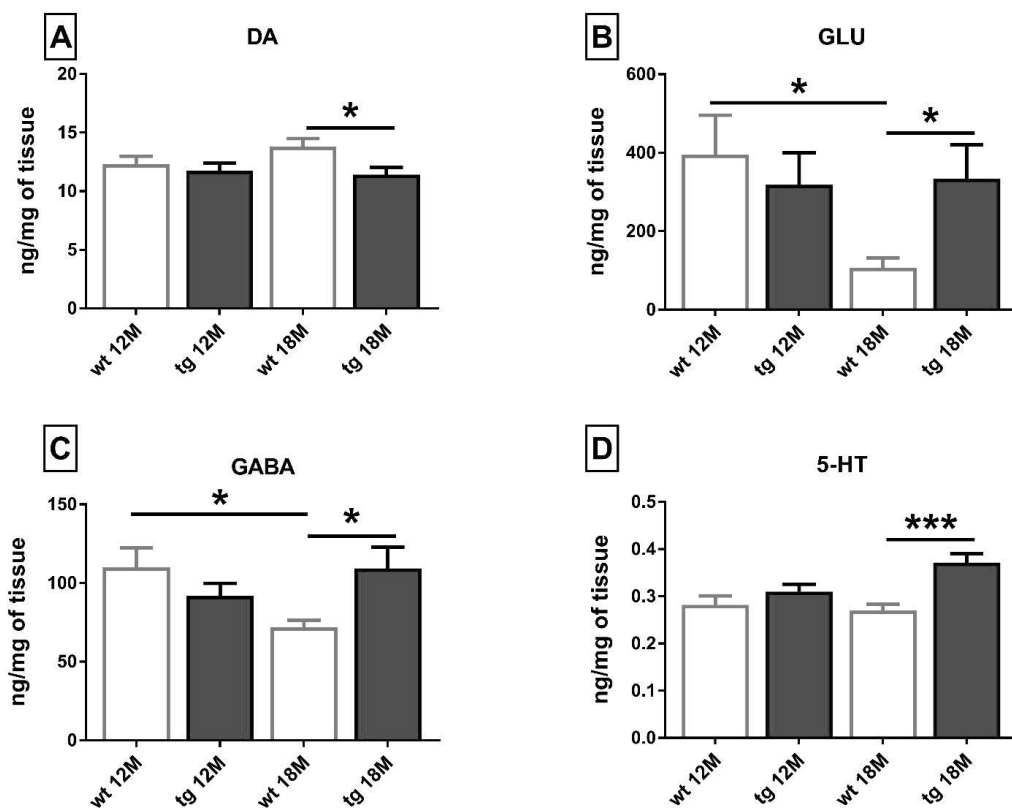
Figure 12A-D. 18-month-old A30P*A53T transgenic mice (tg) showed changes in DA, 5-HT, GABA and glutamate in the striatum compared to wild-type littermates (wt). DA was decreased in the striatum of 18-month-old tg mice compared to wt littermates (**A**). Glutamate (**B**), GABA (**C**), and 5-HT (**D**) had an age-dependent decrease in wt mice, but a similar phenomenon was not observed for other neurotransmitters in tg mice. Data are expressed as mean ± SEM; 12 months: n = 10–12/group, 18 months: n = 8/group. Student's t-test, *p < 0.05; ***p < 0.001.

5.3.3 A30P*A53T transgenic mice have reduced TH positive cells and increased αSyn oligomers in SN and STR

OD analyses of TH and αSyn oligomer-specific immunoreactivity was done by IHC from the nigrostriatal tract of 12- and 18-month-old wt and tg mice (**Fig.13 A–E**). Both 12- and 18-month-old tg mice had decreased TH positive immunoreactivity in STR (**Fig. 13B**, 12 months: t = 3.625, p = 0.0012; 18 months: t = 3.139, p = 0.0072, Student's t-test) and SN (**Fig. 13C,** 12 months: t = 2.499, p = 0.019; 18 months: t = 3.175, p=0.0067, Student's t-test) compared to wt littermates. Furthermore, tg mice had a significant accumulation of αSyn oligomers in the SN and STR. Both 12- and 18-month-old tg mice had significantly increased immunoreactivity for αSyn oligomers in striatum (immunostained by αSynO5 antibody; **Fig.13A, D**, 12 months: t = 6.36, p < 0.0001; 18 months: t = 7.716, p < 0.0001) and in SN (immunostained by αSynO5 antibody; **Fig. 13A,E**, 12 months: t = 8.084, p < 0.0001; 18 months: t = 11.53, p < 0.0001). OD analysis for total αSyn was also performed from

the STR but interestingly, no significant differences in OD in 12- and 18-month-old tg mice compared to wt mice were found (**Fig. 13F**).
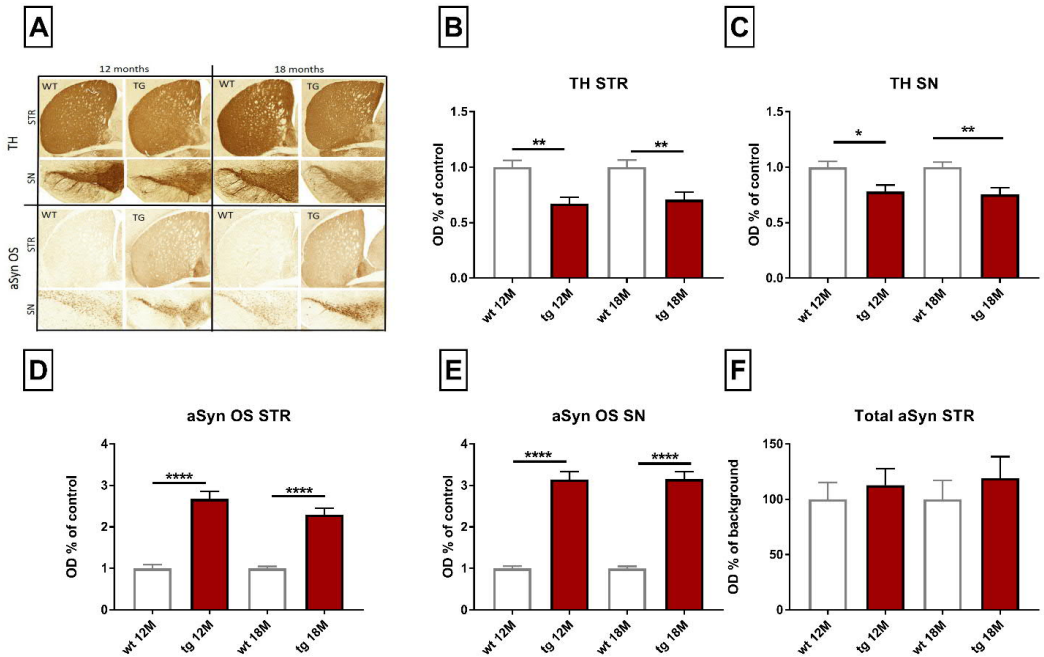

Figure 13A-F. Nigrostriatal TH+ cells and αSyn oligomers were studied by immunohistochemistry (**A**). Optical density of TH positive fibers in the striatum (**B**) and TH positive cells in the substantia nigra (**C**) were decreased in A30P*A53T transgenic mice (tg) compared to wild-type littermates (wt). Oligomeric αSyn was increased in the striatum (**D**) and in the substantia nigra of tg mice (E). n = 7-12. *p < 0.05, **p < 0.01, p**** < 0.0001, Student´s t-test. Data are presented as mean+SEM.

5.3.4 Seven days i.p. treatment with HUP-55 reduces αSyn oligomers in striatum in A30P*A53T transgenic mice (unpublished)

To test the effect of seven days i.p. treatment (10 mg/kg every 12 hours) of novel PREP inhibitor HUP-55 in the A30P*A53T transgenic mice we measured OD of nigrostriatal oligomeric αSyn. Results are shown in **Fig. 14A-C**. Vehicle-treated tg mice (n=6) had significantly higher OD of αSyn05 in STR (One way ANOVA with Tukey's multiple comparisons, VEH: p=0.0014, HUP-55: p=0.098) and in SN (One way ANOVA with Tukey's multiple comparisons, VEH: p=0.01, HUP-55: p=0.011) compared to vehicle- (n=5) and HUP-55-treated wt mice (n=5). However, HUP-55-treated tg mice (n=8) had significantly reduced OD of oligomeric αSyn in STR compared to vehicle-treated tg mice (47 % relative drop, Student´s t-test p=0.04, t=2.27,df=12). Similar trend was seen in SN with 38 % relative drop compared to vehicle-treated tg mice, with no statistical difference. OD of TH positive cells were also measured in STR and SN but only an effect of genotype in STR between HUP-55 treated tg and wt mice was found (One way ANOVA with Tukey's multiple comparison, p=0.023).
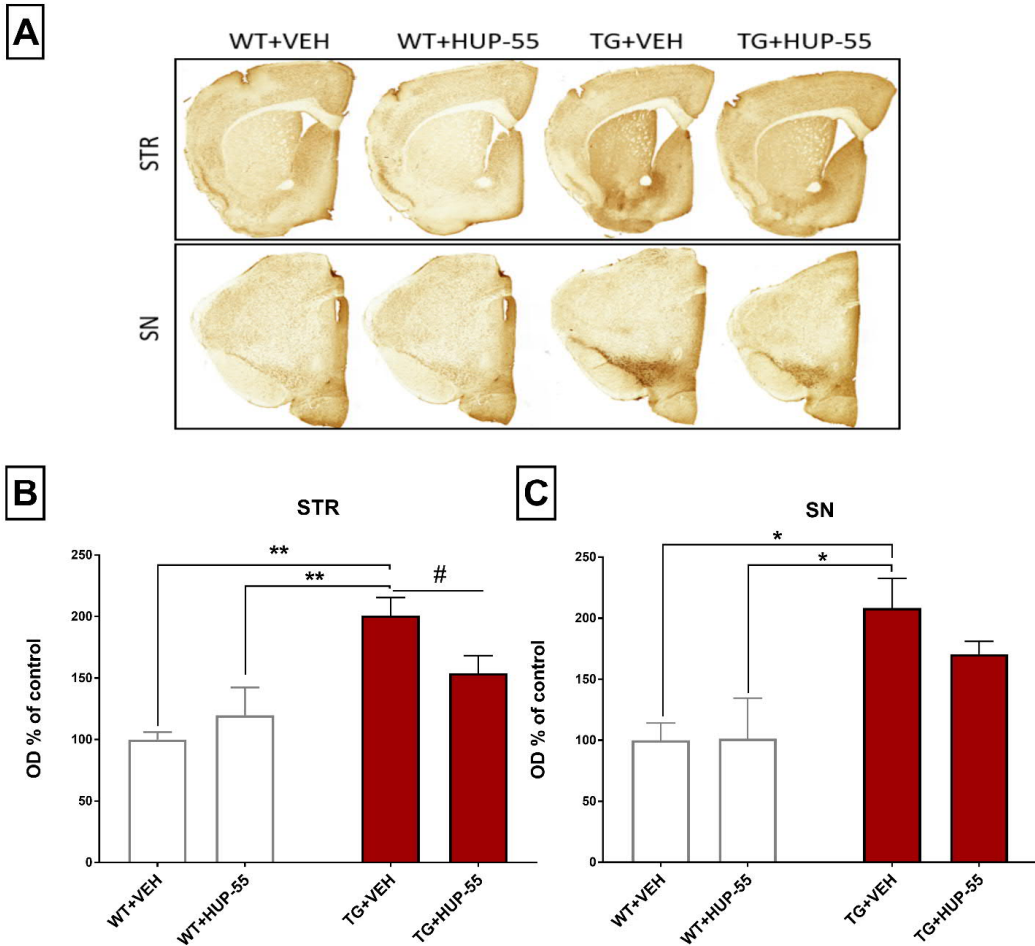
Figure 14A-C. Nigrostriatal αSyn oligomers were studied by immunohistochemistry (**A**). Optical density (OD) of oligomeric αSyn was increased in the STR (**B**) and in the SN (**C**) of vehicle treated A30P*A53T transgenic mice (tg) compared to both vehicle and HUP-55-treated wild-type littermates (wt). *p < 0.05, **p < 0.01 One-way ANOVA with Tukey´s multiple comparisons. 7-day treatment with HUP-55 (10 mg/kg i.p.) decreased the OD of striatal oligomeric αSyn. #p<0.05, Student´s t-test. n= 5-8. Data are presented as mean+SEM.

We also measured 22 h locomotor activity baseline and after 7-days treatment. Results are presented in **Fig. 15A-D**. There were no differences between groups except for one time point where vehicle-treated tg mice had higher activity compared to HUP-55-treated mice (two-way ANOVA with bonferron correction, p=0.0103). In addition, after treatment tg animals had a delay in the start of the dark time activity period compared to WT mice after treatment. Tissue concentrations of DA and its metabolites, GABA, glutamate and 5-HT were measured by HPLC after the treatment from SN and STR but no statistical differences were found between treatment group and vehicle-treated mice.
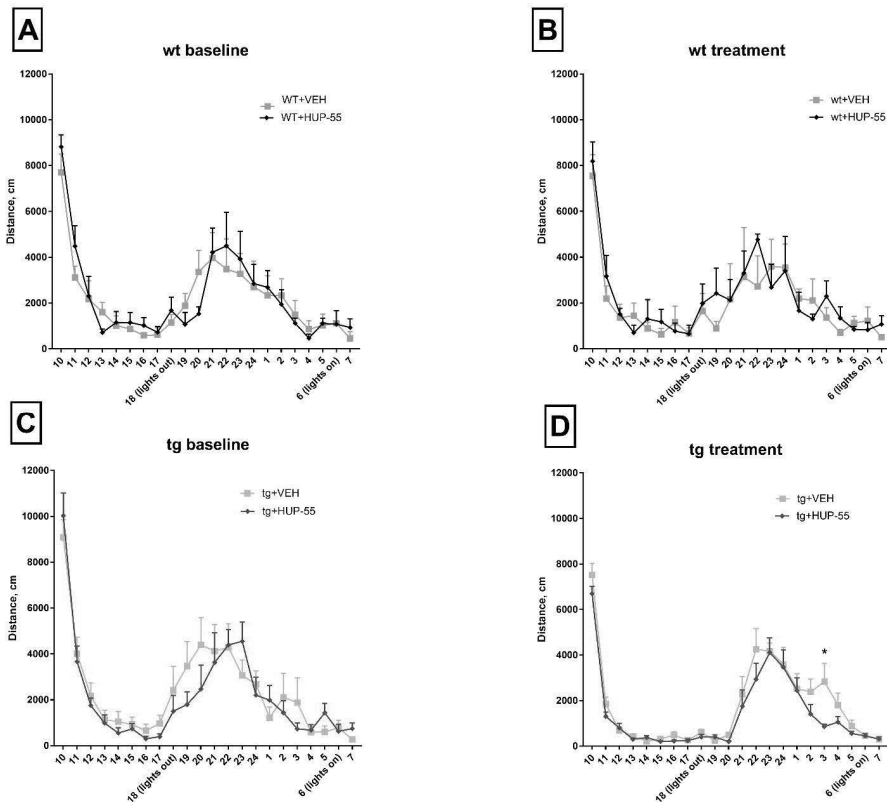
Figure 15A-D. Results of the 22 h locomotor activity measurements for wt mice baseline (**A**), wt mice after one week treatment with 10 mg/kg HUP-55 i.p injection (**B**), tg mice baseline, (**C**) tg mice treatment (**D**). There were no differences between groups except for one time point where vehicle-treated tg mice had higher activity compared to HUP-55-treated mice (two-way ANOVA with Bonferroni correction, p=0.0103). In addition, after treatment tg animals had a delay in the start of the dark time activity period compared to wt mice after treatment.

6 DISCUSSION

6.1 Structurally different PREP inhibitors have different effects on autophagy and αSyn dimerization (Study I)

This is the first study where a structurally diverse set of PREP inhibitors are characterized in αSyn aggregation and autophagy models. Interestingly, disconnected SARs are evident as structurally different inhibitors with similar IC$_{50}$-values had wide variations in their effects in these models. The weakest inhibitor of the proteolytic activity, KYP-2091, had a prominent effect on autophagy and αSyn dimerization in the cellular assays. Then again, some of the most potent inhibitors of proteolytic activity, such as KYP-2101 and KYP-2112, did not have any effect in αSyn PCA or LC3B-II levels in autophagy at the1000 nM concentration. KYP-2091 is around a 1000-fold weaker inhibitor with an IC$_{50}$-value of 1010 nM compared to KYP-2101 and KYP-2112 with IC$_{50}$-values of 1.2 and 0.32

nM, respectively. In addition, KYP-2189 increased LC3B-II levels but did not have an αSyn reducing effect in PCA. This indicates that autophagy is not the only factor affecting the quantity of αSyn dimers. As KYP-2047 is the only inhibitor which has gone through off-target analysis (Jalkanen et al. 2012), it cannot be excluded that some of the tested inhibitors have off-target effects. Off-targets for KYP-2047 were evaluated *in vitro* according to the general side effect profile II which contains a wide variety of important proteins involved in e.g., DAergic, GABAergic, and adrenergic systems, where no off-targets were found. In addition, 10 µM KYP-2047 did not show any significant inhibitory effect against other serine proteases and proline-specific proteases such as aminopeptidase P, dipeptidyl peptidases, and FAP. However, 15 % loss of activity was seen in prolyl carboxy peptidase. Taken together, our results with the αSyn dimerization assay in PREPko cells showed that the impact of PREP inhibitors on αSyn dimerization are PREP-related. It has been shown earlier that autophagy induction is also PREP-related as experiments on PREPko cells show that removal of PREP indeed induces autophagic flux, and that this is related to the interaction-based regulation of PREP on PP2A (Svarcbahs et al. 2020).

In the cell-free *in vitro* αSyn aggregation measurements, all tested inhibitors: KYP-2047, KYP-2091, and KYP-2112, did have an effect on the αSyn aggregation in the presence of PREP. This is not in line with the results in the αSyn PCA assay as KYP-2112 was able to reverse the induced aggregation caused by PREP. However, this might be due to a significantly more complex environment in the cell-based model than in *in vitro* model with purified proteins. The bioavailability of these three compounds were also tested (see original publication I) and found to be similar. Taken together, these findings suggest that in cells there are also other regulatory routes for αSyn aggregation than direct interaction between PREP and αSyn. Another interesting finding in the cell-free αSyn aggregation assay is that KYP-2091 had the best impact on reversing αSyn aggregation. However, KYP-2091 has over a 1000-fold higher IC_{50}-value compared to other tested compound. The concentration of PREP inhibitors used in the measurements were 1000 nM which means that with KYP-2091 approximately 50% of the PREP still had proteolytic activity. This indicates that the magnitude of inhibition of PREP's proteolytic activity does not correlate directly with the reduction of αSyn aggregation in the cell-free assay. To be noted, since the assay was not performed using αSyn and PREP inhibitors in absence of PREP, we cannot fully exclude the direct impact of PREP inhibitors on αSyn fibrillization.

This study suggests that ligands with a close structural similarity to SUAM-1221 (the inhibitor having only the 4-phenylbutanoyl-L-prolylpyrrolidine backbone) are preferred for the αSyn dimerization reducing effect. However, introduction of an electrophile at the P1 site seems to change the situation slightly for some compounds. For example, ZPP, with an aldehyde at the 2*S*-position of the pyrrolidine ring, was not able to decrease αSyn dimerization whereas KYP-2108, with a hydroxyacetyl group in the same position, had an effect on αSyn dimerization. A more reactive electrophilic group is likely to anchor in the known binding mode to the active site of the enzyme and thereby decreasing the opportunity for alternative binding modes, which may affect the conformational flexibility of PREP. The nitrile in KYP-2047, hydroxyacetyl group in KYP-2108, and ketone in KYP-2091 are less reactive electrophiles than the aldehyde in ZPP. Thus, it can be hypothesized that a strong electrophile might not be preferable for the αSyn dimerization reducing effect. This is supported by the fact that compounds SUAM-1221 and KYP-2087 lacking the electrophile have a reducing effect on αSyn dimerization in the PCA as well. On the other hand, adding an electrophile in some scaffolds might lead to decreased αSyn dimerization in PCA as seen when comparing compounds KYP-2101 and KYP-2117.

6.2 Novel tetrazole based PREP inhibitors modulates the oligomerization of αSyn despite the high IC$_{50}$-values and might bind differently compared to corresponding nitriles (Study II)

Tetrazole in the 2S-position of the pyrrolidine ring is an interesting group as it differs from typical substituents since it is not an electrophile and it has a negative charge in physiological conditions. This is a unique group of PREP inhibitors, however there are potent PREP inhibitors with 5 member aromatic heterocycles such as iso-oxazoles (Bal et al. 2003) and thiazoles (Tsutsumi et al. 1994) linked to the P1 pyrrolidine ring with a carbonyl group. This electrophilic carbonyl group is lacking from 4-phenylbutanoyl-aminoacyl-2(S)-tetrazolylpyrrolidines.

The synthetic route for the tested compounds was designed so that the desired nitrile products were also yielded during the route. The overall yields of the route ranged from 13-71 %. Low yields for some compounds could be explained by the properties of the amino acid in the P2 site. For example, Aib-derivative (**7g**) has two methyl groups in α-carbon which creates steric hindrance and reduces water solubility. In addition, there were slight differences in the yields depending on the selected synthesis route. Synthesis of 4-phenylbutanoyl-aminoacyl-2(S)-tetrazolylpyrrolidines was easily performed and conversion of the nitrile group to the tetrazole group gave good yields ranging from 60 % to 90 %. Lower yields with some compounds could be explained by difficulties in purification. As tetrazoles are polar compounds they need polar eluents in flash purification.

The SAR for inhibition of the proteolytic activity was greatly dependent on the aminoacyl group at the P2 site. As expected, the nitriles were the most potent ones and the IC$_{50}$-values increased significantly when the aminoacyl group was changed from Pro (**14a**), Ala (**14b**) or MeAla (**14c**) to Gly (**14d**) and Sar, which lacks the methyl group in α-carbon (**14e**). However, the tetrazoles did not have the same order in the potency for different aminoacyl groups as only Pro (**15a**) and Ala (**15b**) were nanomolar inhibitors. This indicates that the tetrazoles might have a different binding mode to the enzyme. Another interesting finding is that the compounds without 2-substituent in the pyrrolidine ring at the P1 site had comparable IC$_{50}$-values with the tetrazoles with a matching aminoacyl group. Compounds with L-prolinamide at the P1 site had the lowest IC$_{50}$-values in the range of 4-500 µM. An amino acid with its carboxylic acid group at the P1 site lowered the IC$_{50}$-value over 100-fold compared to tetrazoles. It cannot be excluded that some of these prolineamides are substrates for PREP.

The αSyn dimerization assay results for both nitriles and tetrazoles clearly indicate that the SAR for this function of PREP and inhibiting the proteolytic activity are disconnected. Remarkably, all PREP ligands having a tetrazole group at the P1 site and IC$_{50}$-values ranging from 12 to even 200 000 nM had a similar reducing effect on αSyn dimerization in PCA, while many more potent PREP inhibitors did not show the same effect. The used concentration of compounds in this assay was 10 µM. Thus, **15b** with an IC$_{50}$-value of 200 µM is speculated to have only a mild effect on proteolytic activity. The nitriles **14b** and **14c** with aminoacyl groups Ala and MeAla and IC$_{50}$-values of 4.1 and 5.4 nM, respectively, did not have an effect on the dimerization. This is not only due to the effect of nitrile group since, the nitriles **14d** and **14e** with aminoacyl groups Gly and Sar and IC$_{50}$-values of 220 and 269 nM, respectively, had an effect on αSyn dimerization. The amino acids did not have an effect on αSyn dimerization. Although the tetrazole group is a known common bioisostere for the carboxylic acid group, the tetrazole is clearly not a bioisostere of a carboxylic acid group in PREP inhibitors targeted in reducing αSyn dimerization.

Molecular docking studies explain why **14d** and **14e** are less potent inhibitors than other nitriles as they most likely do not orient the nitrile group toward the Ser554 residue. However, in the docking protocol the covalent interaction between the nitrile group and Ser554 was not assessed. Thus, the possible covalent bond formation could actually force the nitrile group to anchor to the active serine residue. Two possible binding poses for tetrazoles could be explained by the fact that tetrazoles prefer to position the lipophilic benzene ring rather than the hydrophilic tetrazole ring into the hydrophobic S1 pocket area. The tetrazole ring does not have a similar ability as the electrophilic nitrile to form a covalent bond to Ser554, which is an important interaction for at least some nitriles in anchoring them at S1. On the other hand, when the benzene ring is in the S1 pocket, the tetrazole ring does not orientate similarly to the S3 pocket but rather tilts toward Phe173. As a less hydrophilic moiety, the nitrile group might also be more easily placed into the S1 pocket than the tetrazole ring. Overall, these results suggest that the tetrazoles might have two putative binding poses: the phenyl group at S3 (**Fig. 6C**) or at S1 (**Fig. 6D**).

One has to remember that there are also limitations in αSyn PCA assay. A more robust positive control for reduction of αSyn dimers would give a better understanding to the magnitude of the effect with tested compounds. On the other hand, the effect of tetrazoles would also be informative to test also without PREP to see if the found effect is PREP mediated, especially when the IC$_{50}$-values for some compounds were high. These additional tests would support the hypothesis that tetrazoles bind to PREP differently compared to typical PREP inhibitors with the electrophile in the P1 site.

6.3 PREP inhibitors might modulate biological effects by changing the conformation of PREP to affect different protein-protein interactions (Studies I and II)

Different biological activity profiles by different PREP inhibitors in studies I and II most likely result from differences in how the PREP ligands stabilize one conformation or allow certain conformational flexibility to the enzyme. The conformation of loops around the active site should be most affected as they have been reported to be most affected in the stabilization of the conformation by KYP-2047 (Tsirigotaki et al. 2017). The native gel assay showed that conformational changes of PREP are in line with the IC$_{50}$-value of tested compounds, as molecules having an IC$_{50}$-value lower than 100 nM changed the equilibrium of conformations. However, the changes seen in the native gel did not follow the autophagy induction or αSyn dimerization reducing effect. Changes in native gel conformations are likely to be more drastic compared to the subtle movements of PREP loops which might modulate PPIs (Tsirigotaki et al. 2017). In fact, ZPP and KYP-2047 had slightly different spectra on PREP when measured by the multiple quantum relaxation assay (López et al. 2016), despite having the same effect on native gel. Other studies have shown that PREP adopts different conformational states which can be modified by PREP inhibitors (Kichik et al. 2011; Szeltner et al. 2004; Tarragó et al. 2009). However, PREP inhibitors cannot modulate the conformation of proteolytically inactive S554A mutant PREP. This explains why PREP inhibition by KYP-2047 is not able to reverse increased αSyn dimerization caused by S554 PREP (Savolainen et al. 2015). In addition, a mutation in the external loop B at the surface of PREP (T590C) removed the inhibitory activity of PREP on PP2A (Svarcbahs et al. 2020). Thus, loop B or the conformation this mutation stabilizes is critical for PREP interaction with the PP2A subunit indicating that slight movement on flexible loop structures plays a key role in PPIs.

Studies I and II showed that not all potent PREP inhibitors have an effect on αSyn dimerization. The hypothesis is that the required conformation of the enzyme for desired PPIs is not equivalent for an inhibitor-binding conformation. The desired conformation able to enhance PPIs is most likely acquired by a certain type of binding by the ligand (**Fig. 15**). This is supported by the molecular docking studies in study II which revealed that PREP ligands with a tetrazole group had an alternative binding mode to the enzyme compared to some more potent inhibitors, which did not have an αSyn dimer reducing effect. Another, even bit more exciting speculation, is that there is an alternative binding site in the enzyme, which regulates PPI-mediated functions and not the proteolytic activity. This would explain why a tetrazole compound with an IC_{50}-value of 200 µM (**15d**) had an effect on αSyn dimerization with a concentration of 10 µM. However, the existence of an alternative binding site cannot be postulated based on the current evidence. One option would be to use microscale thermophoresis to investigate the binding of these ligands to the purified PREP enzyme. If a ligand, having a high IC_{50}-value, binds to the enzyme with better affinity, it indicates that the ligand binds to the enzyme without changing the proteolytic activity. However, to investigate the conformational changes needed for different PPIs there is need for other tools such as cryogenic EM or advanced NMR techniques, but the large size of PREP enzyme limits the use of these methods.

Even though modulating PPIs is considered to be one of the most challenging fields of drug discovery, there are several PPI modulators in clinical trials. From the perspective of drug discovery, it would be beneficial to develop PREP ligands with an increased selectivity to affect certain PPI-mediated functions of PREP such as an autophagy inducing effect and/or an αSyn dimerization reducing effect. Knowing the SAR for the alternative binding mode or the speculated alternative binding site that stabilizes the conformation of PREP desirable for PPIs, would lead to more effective design of drugs targeted to autophagy and protein aggregation.
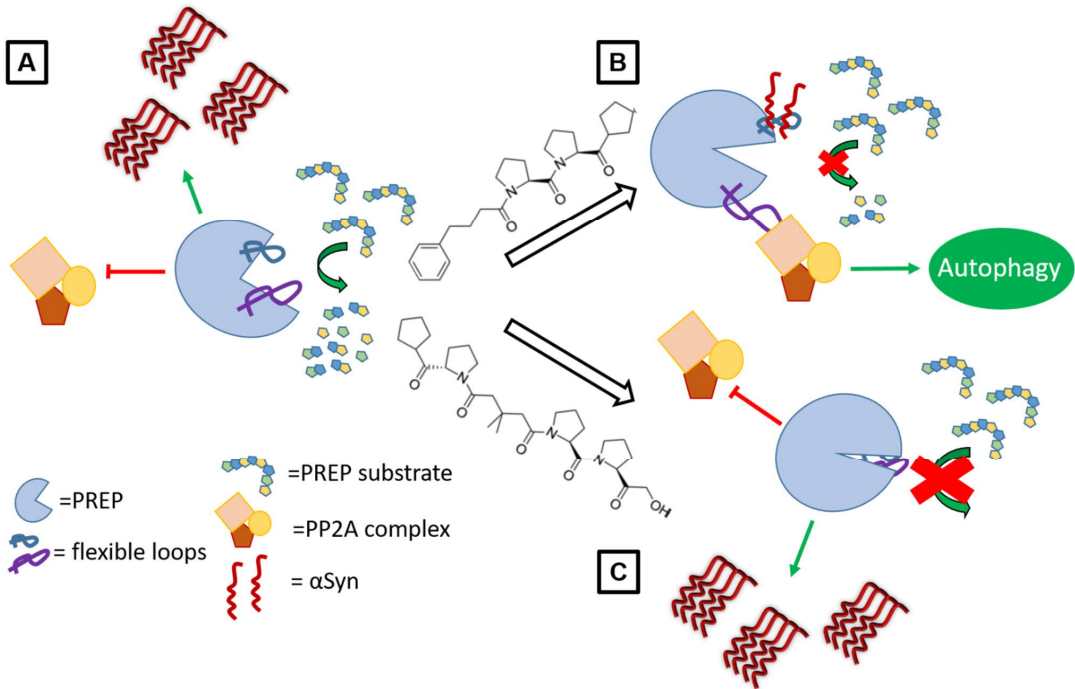
Figure 16. Schematic picture of the hypothesis for how PREP ligands modulates the interactions of PREP with other proteins. **A** Proteolytically active PREP in active conformations inhibits PP2A activity and increases αSyn dimerization and aggregation via direct interaction. **B** Binding of a certain type of PREP ligand (KYP-2091 as an example) causes a conformational change in PREP, providing different sites of the flexible loop structures to interact with other proteins leading to e.g., decreased αSyn dimerization and increased PP2A activity and autophagy. This action is not related to the proteolytic activity of PREP and there may be some proteolytic activity left. **C** Another PREP ligand (KYP-2112 as an example) causes a conformational change to PREP which leads to complete inhibition of proteolytic activity but not to enhanced PPIs. Ligands and interaction partners in this figure are examples, and this hypothesis may be applicable to other PREP-interacting proteins as well.

6.4 A30P*A53T αSyn tg mice is a useful tool to model early onset PD with familial SNCA mutations (Study III)

Results of study III show that homozygous C57BL/6J-Tg(TH-SNCA*A30P*A53T)39Eric/J tg mice had significant differences in locomotor activity in all age groups starting from 3-month-old animals, altered amphetamine response, and increased αSyn oligomer levels and decreased TH immunostaining in the SN and STR. Interestingly, the most distinct differences in dark time activity were observed in 6- and 9-month old animals. In the vertical and jump counts, the most prominent differences were observed in 3- and 6-month-old animals. These findings could be considered to model motor symptoms of early-onset PD. However, at 12 months of age, the difference was not as clear as at earlier time points, and at 18 months tg mice were actually hyperactive in the locomotor test compared to wt littermates. Hyperactivity in our study can also be explained by the elevated glutamate level in the STR of 18-month-old tg mice compared to wt littermates. Hyperactivity and reduced anxiety-like behavior has also been described before with A53T-αSyn mutant overexpressing

62

mice strains (Farrell et al. 2014; Graham and Sidhu 2010). This hyperactivity is due to D1 receptor and DAT-mediated alterations in DA neurotransmission as hyperactivity of A53T mutant mice could be reversed with a D1 antagonist (Unger et al. 2006). However, A30P αSyn is not linked to locomotor alternations (Unger et al. 2006). On the other hand, there are reports where wt C57BL/6 mice have reduced locomotor activity at 12 and 22 months of age compared to young animals (Fetsko et al. 2005).

Contrary to this study, Richfield et al. reported that tg mice had a reduced locomotor response to amphetamine compared to wt littermates (Richfield et al. 2002). We found that 6-, 9-, and 18-month-old tg mice had an increased response to amphetamine in the locomotor activity assay compared to wt littermates. Increased amphetamine-induced locomotor activity and decreased amphetamine-induced DA release in tg mice can indicate dysfunction of DAT. Interestingly, elevated amphetamine-induced DA release was only observed in 12-month-old tg mice compared to wt littermates, but not in 18-month-old tg mice. In addition, the observation that the wt mice had decreased amphetamine-induced DA release at 18 months compared to 12-months can explain differences in amphetamine induced locomotor activity. Age-related changes in DAergic function in wt mice could explain the difference that was observed between the 12-month-old wt and tg mice. As normal αSyn is known to negatively regulate the function of DAT and overexpression of αSyn modifies basal and amphetamine-induced DA-efflux, αSyn aggregation in this mouse model probably plays a key role in altered DA signaling and amphetamine response (Wersinger and Sidhu 2005).

According to the microdialysis results, striatal DA was not yet changed in 12-month-old tg mice compared to wt littermates, although striatal and nigral TH OD were already decreased at 12 months. Indeed, impairment in DAergic function of 12-month-old tg mice was observed in the microdialysis experiment as amphetamine-induced DA release was decreased and behavior altered in tg mice compared to wt mice. It has been reported that αSyn inhibits TH activity and decreases DA levels (Perez et al. 2002), but A53T αSyn and aggregation of αSyn disrupts αSyn's interaction with TH (Alerte et al. 2008; Lou et al. 2010). Thus, the elevated level of αSyn oligomers seen in tg mice could possibly explain reduced TH. Additionally, striatal tissue concentrations of 5-HT and GABA were increased which may arise from decreased DA regulation. This study also revealed decreased DOPAC and HVA levels in tg mice compared to wt mice which is in line with a previous study by Richfield et al.

Several mouse models overexpressing human αSyn with an A30P or A53T point mutation have been developed for PD research. However, the A30P mutation does not cause differences in locomotor activity and in DA and TH levels despite the accumulation of αSyn (Unger et al. 2006; Yavich et al. 2004). The A53T mutant αSyn-expressing mice usually have more severe motor impairments starting at an older age, but malfunction of the DAergic system has not been clearly determined (Giasson et al. 2002; Lee et al. 2002). The degeneration of the DAergic system would be one highly desired feature of a PD model. It is also important to note that these αSyn point mutations are a risk factor for early onset PD which occurs before the age of 40 to 50 years in humans (Schrag and Schott 2006), and generally behavioral deficits are seen only in aged tg animals (>12 months). Our study demonstrated that A30P*A53T αSyn tg mice did not only have early behavioral changes but also changes in their DAergic system and a decreased amount of TH positive cells compared to wt littermates. These effects are most likely caused by toxicity from increased αSyn oligomers that we reported here in the 12- and 18-month age groups. Differences between this study and the Richfield et al. study may arise from the fact that in this study tg mice were confirmed to be homozygous by using direct PCR-genotyping.

A30P and A53T double mutation in SNCA has not been described clinically and therefore, the relevance of this model in PD research could be criticized. However, this study indicates that double mutated αSyn tg mice models early onset PD better than other tg mouse models. In addition, this model displays loss of TH positive cells in SN and STR most likely due to increased toxicity from elevated αSyn oligomer levels, which is highly desirable for a model of PD. It would be interesting to study the changes in the TH immunoreactivity, αSyn accumulation, and DAergic function in younger animals (3-6 months old) when the behavioral differences were most prominent. In conclusion, there is a need for a PD model that displays motor and non-motor deficits, alternation in the DAergic system, and DAergic cell loss combined with αSyn propagation and formation of LB for development of novel disease-modifying therapies for PD. The homozygous double mutant A30P*A53T αSyn tg mouse does not fulfil all of these requirements but it has early onset and age-dependent changes in locomotor activity and in the striatal DAergic function together, with αSyn oligomer formation.

6.5 Seven days i.p. treatment with HUP-55 reduces αSyn oligomers in STR in A30P*A53T transgenic mice (unpublished)

The effect of seven day i.p. treatment by our novel HUP-55 compound as a reduction of oligomeric αSyn in the SN and STR, similarly to KYP-2047 in other αSyn tg mice (Savolainen et al. 2014). However, no differences in TH positive immunoreactivity were seen. As discussed in the previous chapter, αSyn negatively regulates TH, and αSyn aggregation is potentially toxic for DAergic neurons, but the same connection was not seen in this study. This might be explained by the fact that animals used were 15 months old with already reduced TH positive immunoreactivity in the nigrostriatal tract according to the study III. Thus, even if treatment reduced αSyn oligomers it was not able to restore TH positive cells during the 7-days treatment. This setup would be interesting to repeat by using younger animals that already have motor symptoms, but not advanced loss of TH positive cells, combined with longer treatment. In the 22 h locomotor experiment, the only difference was seen in one time point at 3:00 am in the dark time period. At this time point, HUP-55 treatment reduced the activity of tg mice compared to wt mice. Activity peak at the same time point was also seen in 22 h locomotor recordings in study III in 18-month old tg mice. As discussed above, hyperactivity might be caused by excess A53T mutant αSyn (Farrell et al. 2014; Unger et al. 2006). This might explain why HUP-55-treated mice did not have the hyperactivity peak at this time point.

HUP-55 is a novel PREP inhibitor having a structure differing from typical PREP inhibitors. Additional data cannot be presented here, due to patenting issues. However, it has also been tested successfully in cellular models of autophagy and αSyn dimerization, and in brain penetration studies *in vivo*. HUP-55 is able to pass the BBB and inhibit PREP in the mouse brain. 30 minutes after 10 mg/kg i.p. injection, approximately 50 % of PREP activity was reduced while the same dose of KYP-2047 reduced more than 80 % of brain PREP activity in the mouse. However, the effect of HUP-55 on αSyn oligomers seems similar as with KYP-2047 in earlier studies, further supporting the view that strong proteolytic inhibition of PREP is not required for αSyn or autophagy actions. In conclusion, HUP-55 might be a potential treatment for PD, but additional *in vivo* data in different models of PD are needed.

6.6 Future directions for PREP ligand design

After 40 years we know how to obtain a highly potent and specific PREP inhibitor, but as failures in clinical trials suggest, it may not be useful to put effort in developing an even more potent inhibitors. Despite this, most of the studies on PREP inhibitor design still aims to find highly potent PREP inhibitors. In a recent study, Plescia et al. discovered potent covalent PREP inhibitors having boronic esters as an electrophile at the P1 site (Plescia et al. 2020). These inhibitors had a similar backbone with carbonyl groups in the P2 site as with typical PREP inhibitors. Even though these kinds of novel compounds are interesting, only a small part of the physiological functions of PREP are explained by its proteolytic activity toward certain peptides. Thus, the highly potent inhibitors may not be the correct probes to address the PPI-derived functions of PREP.

Our studies show that there is still a lot to reveal on the role of PREP in several physiological functions and disease processes. PPIs regulated by conformational changes of PREP is the likely mechanism behind these effects. As aberrant PPIs play a role in, for example, cancer and neurodegeneration, modulation of PPIs by small molecules has gained more interest in drug development (Lu et al. 2020). Gaining the knowledge of how PPIs of PREP could be modulated by small molecular ligands can open a completely new world in drug discovery around PREP. Moreover, to find out the SAR behind modulation of PPIs would be highly beneficial and allow the design of drugs that would affect the pathophysiological factors behind NDD. This would require tools to study conformational changes of PREP such as SAXS or NMR experiments with different PREP ligands combined with computational modeling. On the other hand, confirming and identifying the speculated other binding site of PREP would allow the design of specific ligands to binding sites, which regulates the PPIs of PREP. Other binding sites could be confirmed with binding studies such as microscale thermophoresis for K_d determination. If comparison of the IC_{50}-value and K_d-value of a certain PREP ligand reveals significant differences between values, it can be speculated that the ligand also binds to the other binding site. In addition, this could be confirmed using a known PREP inhibitor which occupies the active site in combination with a PREP ligand which is hypothesized to bind to other site. As an example, if KYP-2047 and compound **15d** would be tested on such a setup seeing that **15d** binds to PREP when the active site is occupied by KYP-2047 would confirm the alternative binding site. However, the identification of the binding site would require biological assays with mutated PREP combined with computational modeling.

Another object to be considered in future PREP ligand design is to replace the peptide structure to improve the physicochemical properties, especially CNS-targeting. Even though some peptide structured PREP inhibitors are able to pass the BBB, they have higher inhibition in liver than in the brain (Venäläinen et al. 2006). This is not desirable when designing drugs for CNS as a high drug concentration in the periphery may increase the chance of adverse effects related to for example, hypertension or celiac disease (as discussed in chapter 2.1.4.3). On the other hand, all clinically tested PREP inhibitors have proven to be safe and tolerable.

When designing PREP inhibitors for NDD, the biological characterization of PREP ligands should not be directed by their inhibition of the proteolytic activity. As shown in this study, weak inhibitors may have beneficial effects that potent PREP inhibitors do not have. However, to characterize these PPI-related effects further, in the future it is important to use more variable assays for autophagy and protein aggregation. Different PCA setups for studying interactions between certain protein fragments and PREP or studying how certain mutations in PREP affects dimerization of proteins

would give more information about the site and nature of PPIs between PREP and the proteins of interest. In addition, different methods such as co-immunoprecipitation could also be applied to verify these results. Furthermore, since PREP regulates autophagy via direct PPI with PP2A, it would be interesting to test a set of PREP ligands in PP2A activity assays such as ELISA or phosphatase assay. On the other hand, PREP ligands could be studied in the aggregation and clearance of different NDD-related proteins such as tau, mHTT, and TDP-43. The effect of PREP inhibitors in the formation of ROS and oxidative stress is another NDD-related process should be studied more deeply.

7 CONCLUSIONS

The main conclusions from the studies are as follows:

1. For PREP inhibitors, high potency of inhibition of the proteolytic activity is not essential for the modulation of PPI mediated functions of PREP. Based on our results with a representative series of peptide-like PREP inhibitors, full inhibition of the proteolytic activity of PREP does not guarantee desired impact in biological functions such as decreased αSyn dimerization and induced autophagy.

2. Novel 4-phenylbutanoyl-α-aminoacyl-2(S)-tetrazolyl-pyrrolidines have another binding mode to PREP compared to 4-phenylbutanoyl-α-aminoacyl-2(S)-cyano-pyrrolidines. This was supported by the fact that the same amino acid at the P2 site of tetrazole did not have the same effect on the inhibition potency as with the nitriles. Furthermore, all tetrazoles were able to decrease αSyn dimerization while some potent nitrile compounds did not. This was supported with molecular docking studies where tetrazoles had another binding pose compared to nitriles. These findings indicate that the desired conformation able to enhance PPIs is most likely acquired by a certain type of binding mode by the ligand or binding to the alternative binding site.

3. Recharacterization of A30P*A53T αSyn tg mice showed that this mouse is a useful tool to model early onset PD with familial SNCA mutations. These mice display early behavioral alternations with differences in DAergic function and accumulation of αSyn leading to decreased TH positive immunoreactivity. In addition, we were able to reduce the accumulated αSyn in A30P*A53T αSyn mice after 7-day treatment with a novel PREP ligand.

Further studies investigating the conformational changes in PREP and identifying the possible other binding site or binding mode are highly needed for future development of efficient PREP ligands as a disease-modifying therapy for several different NDD. In addition, a novel PREP ligand family was discovered during the study, but additional data related to these compounds cannot be presented in this thesis. However, novel PREP ligands discovered during this thesis need further characterization in other models of NDD.

8 ACKNOWLEDGMENTS

9 REFERENCES

Agirregoitia N, Casis L, Gil J, Ruiz F, Irazusta J (2007) Ontogeny of prolyl endopeptidase and pyroglutamyl peptidase I in rat tissues. Regulatory Peptides 139: 52-58.

Alerte TN, Akinfolarin AA, Friedrich EE, Mader SA, Hong CS, Perez RG (2008) Alpha-synuclein aggregation alters tyrosine hydroxylase phosphorylation and immunoreactivity: lessons from viral transduction of knockout mice. Neurosci Lett 435: 24-9.

Arai H, Nishioka H, Niwa S, Yamanaka T, Tanaka Y, Yoshinaga K, Kobayashi N, Miura N, Iked Y (1993) Synthesis of Prolyl Endopeptidase Inhibitors and Evaluation of Their Structure-Activity Relationships: In Vitro Inhibition of Prolyl Endopeptidase from Canine Brain. Chemical and Pharmaceutical Bulletin 41: 1583-1588.

Arkin MR, Whitty A (2009) The road less traveled: modulating signal transduction enzymes by inhibiting their protein–protein interactions. Current Opinion in Chemical Biology 13: 284-290.

Atula S (2018) Parkinsonin tauti. Lääkärikirja Duodecim.

Bal G, Van der Veken P, Antonov D, Lambeir A-M, Grellier P, Croft SL, Augustyns K, Haemers A (2003) Prolylisoxazoles: potent inhibitors of prolyloligopeptidase with antitrypanosomal activity. Bioorganic & Medicinal Chemistry Letters 13: 2875-2878.

Ballatore C, Brunden KR, Trojanowski JQ, Lee VM, Smith AB, 3rd, Huryn DM (2011) Modulation of protein-protein interactions as a therapeutic strategy for the treatment of neurodegenerative tauopathies. Current topics in medicinal chemistry 11: 317-30.

Barelli H, Petit A, Hirsch E, Wilk S, De Nanteuil G, Morain P, Checler F (1999) S 17092-1, a highly potent, specific and cell permeant inhibitor of human proline endopeptidase. Biochemical and Biophysical Research Communications 257: 657-661.

Bellemère G, Morain P, Vaudry H, Jégou S (2003) Effect of S 17092, a novel prolyl endopeptidase inhibitor, on substance P and alpha-melanocyte-stimulating hormone breakdown in the rat brain. J Neurochem 84: 919-29.

Bellemère G, Vaudry H, Morain P, Jégou S (2005) Effect of prolyl endopeptidase inhibition on arginine-vasopressin and thyrotrophin-releasing hormone catabolism in the rat brain. Journal of neuroendocrinology 17: 306-13.

Braber S, Koelink PJ, Henricks PA, Jackson PL, Nijkamp FP, Garssen J, Kraneveld AD, Blalock JE, Folkerts G (2011) Cigarette smoke-induced lung emphysema in mice is associated with prolyl endopeptidase, an enzyme involved in collagen breakdown. American journal of physiology Lung cellular and molecular physiology 300: L255-65.

Brandt I, Gérard M, Sergeant K, Devreese B, Baekelandt V, Augustyns K, Scharpé S, Engelborghs Y, Lambeir AM (2008) Prolyl oligopeptidase stimulates the aggregation of a-synuclein. Peptides 29: 1472-1478.

Breen G, Harwood AJ, Gregory K, Sinclair M, Collier D, St Clair D, Williams RS (2004) Two peptidase activities decrease in treated bipolar disorder not schizophrenic patients. Bipolar disorders 6: 156-61.

Brännström K, Lindhagen-Persson M, Gharibyan AL, Iakovleva I, Vestling M, Sellin ME, Brännström T, Morozova-Roche L, Forsgren L, Olofsson A (2014) A generic method for design of oligomer-specific antibodies. PLoS One 9: e90857.

Bär JW, Rahfeld JU, Schulz I, Gans K, Ruiz-Carrillo D, Manhart S, Rosche F, Demuth HU (2006) Prolyl endopeptidase cleaves the apoptosis rescue peptide humanin and exhibits an unknown post-cysteine cleavage specificity. Advances in experimental medicine and biology 575: 103-8.

Casili G, Lanza M, Scuderi SA, Messina S, Paterniti I, Campolo M, Esposito E (2020) The Inhibition of Prolyl Oligopeptidase as New Target to Counteract Chronic Venous Insufficiency: Findings in a Mouse Model. Biomedicines 8.

Cavasin MA, Rhaleb NE, Yang XP, Carretero OA (2004) Prolyl oligopeptidase is involved in release of the antifibrotic peptide Ac-SDKP. Hypertension (Dallas, Tex : 1979) 43: 1140-5.

Chartier-Harlin M-C, Kachergus J, Roumier C, Mouroux V, Douay X, Lincoln S, Levecque C, Larvor L, Andrieux J, Hulihan M, Waucquier N, Defebvre L, Amouyel P, Farrer M, Destée A (2004) α-synuclein locus duplication as a cause of familial Parkinson's disease. The Lancet 364: 1167-1169.

Checler F, Amar S, Kitabgi P, Vincent JP (1986) Catabolism of neurotensin by neural (neuroblastoma clone N1E115) and extraneural (HT29) cell lines. Peptides 7: 1071-7.

Chen L, Jin J, Davis J, Zhou Y, Wang Y, Liu J, Lockhart PJ, Zhang J (2007) Oligomeric α-synuclein inhibits tubulin polymerization. Biochemical and Biophysical Research Communications 356: 548-553.

Collaborators GDaIIaP (2015) Global, regional, and national incidence, prevalence, and years lived with disability for 310 diseases and injuries, 1990-2015: a systematic analysis for the Global Burden of Disease Study 2015.

de Oliveira GAP, Silva JL (2019) Alpha-synuclein stepwise aggregation reveals features of an early onset mutation in Parkinson's disease. Communications Biology 2: 374.

DeMaagd G, Philip A (2015) Parkinson's Disease and Its Management: Part 1: Disease Entity, Risk Factors, Pathophysiology, Clinical Presentation, and Diagnosis. P T 40: 504-532.

Di Daniel E, Glover CP, Grot E, Chan MK, Sanderson TH, White JH, Ellis CL, Gallagher KT, Uney J, Thomas J, Maycox PR, Mudge AW (2009) Prolyl oligopeptidase binds to GAP-43 and functions without its peptidase activity. Molecular and Cellular Neuroscience 41: 373-382.

Dokleja L, Hannula MJ, Myöhänen TT (2014) Inhibition of prolyl oligopeptidase increases the survival of alpha-synuclein overexpressing cells after rotenone exposure by reducing alpha-synuclein oligomers. Neuroscience Letters 583: 37-42.

Dotolo R, Kim JD, Pariante P, Minucci S, Diano S (2016) Prolyl Endopeptidase (PREP) is Associated With Male Reproductive Functions and Gamete Physiology in Mice. J Cell Phsyiol 231: 551-557.

Dresdner K, Barker LA, Orlowski M, Wilk S (1982) Subcellular Distribution of Prolyl Endopeptidase and Cation-Sensitive Neutral Endopeptidase in Rabbit Brain. Journal of Neurochemistry 38: 1151-1154.

Dugger BN, Dickson DW (2017) Pathology of Neurodegenerative Diseases. Cold Spring Harb Perspect Biol 9: a028035.

Elgenaidi IS, Spiers JP (2019) Regulation of the phosphoprotein phosphatase 2A system and its modulation during oxidative stress: A potential therapeutic target? Pharmacology & Therapeutics 198: 68-89.

Emamzadeh FN (2016) Alpha-synuclein structure, functions, and interactions. Journal of research in medical sciences : the official journal of Isfahan University of Medical Sciences 21: 29.

Farrell KF, Krishnamachari S, Villanueva E, Lou H, Alerte TN, Peet E, Drolet RE, Perez RG (2014) Non-motor parkinsonian pathology in aging A53T α-synuclein mice is associated with progressive synucleinopathy and altered enzymatic function. J Neurochem 128: 536-46.

Fetsko LA, Xu R, Wang Y (2005) Effects of age and dopamine D2L receptor-deficiency on motor and learning functions. Neurobiology of Aging 26: 521-530.

Fiedorowicz A, Figiel I, Kamińska B, Zaremba M, Wilk S, Oderfeld-Nowak B (2001) Dentate granule neuron apoptosis and glia activation in murine hippocampus induced by trimethyltin exposure. Brain Research 912: 116-127.

Frake RA, Ricketts T, Menzies FM, Rubinsztein DC (2015) Autophagy and neurodegeneration. The Journal of Clinical Investigation 125: 65-74.

Franklin KBJ, Paxinos G (1997) The Mouse Brain in Stereotaxic Coordinates. Academic Press

Friedman TC, Orlowski M, Wilk S (1984) Prolyl endopeptidase: inhibition in vivo by N-benzyloxycarbonyl-prolyl-prolinal. J Neurochem 42: 237-41.

Friedman TC, Wilk S (1985) The effect of inhibitors of prolyl endopeptidase and pyroglutamyl peptide hydrolase on TRH degradation in rat serum. Biochemical and Biophysical Research Communications 132: 787-794.

Fülöp V, Böcskei Z, Polgár L (1998) Prolyl oligopeptidase: An unusual ß-propeller domain regulates proteolysis. Cell 94: 161-170.

Gaggar A, Jackson PL, Noerager BD, O'Reilly PJ, McQuaid DB, Rowe SM, Clancy JP, Blalock JE (2008) A novel proteolytic cascade generates an extracellular matrix-derived chemoattractant in chronic neutrophilic inflammation. J Immunol 180: 5662-5669.

Gallegos MEH, Zannatha MMI, Osornio EG, Sánchez AS, del Rio FAP (1999) The Activities of Six Exo- and Endopeptidases in the Substantia Nigra, Neostriatum, and Cortex of the Rat Brain. Neurochemical Research 24: 1557-1561.

Galpern WR, Lang AE (2006) Interface between tauopathies and synucleinopathies: a tale of two proteins. Annals of Neurology 59: 449-458.

García-Horsman JA, Männistö PT, Venäläinen JI (2007) On the role of prolyl oligopeptidase in health and disease. Neuropeptides 41: 1-24.

Gerard M, Debyser Z, Desender L, Kahle PJ, Baert J, Baekelandt V, Engelborghs Y (2006) The aggregation of alpha-synuclein is stimulated by FK506 binding proteins as shown by fluorescence correlation spectroscopy. FASEB Journal 20: 524-526.

Giasson BI, Duda JE, Quinn SM, Zhang B, Trojanowski JQ, Lee VM (2002) Neuronal alpha-synucleinopathy with severe movement disorder in mice expressing A53T human alpha-synuclein. Neuron 34: 521-33.

Giralt E, Tarragó T, Prades R, Royo S (2014) 1-[1(Benzoyl)-Pyrrolidine-2-Carbonyl]-Pyrrolodine-2-Carbonitrile Derivatives WO 2014/072498 A1

Goossens FH, De Meesler I, Vanhoofand G, Schärpe S (1996) Distribution of prolyl oligopeptidase in human peripheral tissues and body fluids. European Journal of Clinical Chemistry and Clinical Biochemistry 34: 17-22.

Graham DR, Sidhu A (2010) Mice expressing the A53T mutant form of human alpha-synuclein exhibit hyperactivity and reduced anxiety-like behavior. Journal of neuroscience research 88: 1777-1783.

Grellier P, Vendeville S, Joyeau R, Bastos IM, Drobecq H, Frappier F, Teixeira AR, Schrével J, Davioud-Charvet E, Sergheraert C, Santana JM (2001) Trypanosoma cruzi prolyl oligopeptidase Tc80 is involved in nonphagocytic mammalian cell invasion by trypomastigotes. The Journal of biological chemistry 276: 47078-86.

Haffner CD, Diaz CJ, Miller AB, Reid RA, Madauss KP, Hassell A, Hanlon MH, Porter DJT, Becherer JD, Carter LH (2008) Pyrrolidinyl pyridone and pyrazinone analogues as potent inhibitors of prolyl oligopeptidase (POP). Bioorganic & Medicinal Chemistry Letters 18: 4360-4363.

Hagihara M, Nagatsu T (1987) Post-proline cleaving enzyme in human cerebrospinal fluid from control patients and parkinsonian patients. Biochemical Medicine and Metabolic Biology 38: 387-391.

Hannula MJ, Myöhänen TT, Tenorio-Laranga J, Männistö PT, Garcia-Horsman JA (2013) Prolyl oligopeptidase colocalizes with α-synuclein, β-amyloid, tau protein and astroglia in the post-mortem brain samples with Parkinson's and Alzheimer's diseases. Neuroscience 242: 140-150.

Harwood AJ (2011) Prolyl oligopeptidase, inositol phosphate signalling and lithium sensitivity. CNS and Neurological Disorders - Drug Targets 10: 333-339.

Höfling C, Kulesskaya N, Jaako K, Peltonen I, Männistö PT, Nurmi A, Vartiainen N, Morawski M, Zharkovsky A, Võikar V, Roßner S, García-Horsman JA (2016) Deficiency of prolyl oligopeptidase in mice disturbs synaptic plasticity and reduces anxiety-like behaviour, body weight, and brain volume. European Neuropsychopharmacology 26: 1048-1061.

Irazusta J, Larrinaga G, González-Maeso J, Gil J, Meana JJ, Casis L (2002) Distribution of prolyl endopeptidase activities in rat and human brain. Neurochemistry International 40: 337-345.

Ishiura S, Tsukahara T, Tabira T, Shimizu T, Arahata K, Sugita H (1990) Identification of a putative amyloid A4-generating enzyme as a prolyl endopeptidase. FEBS Letters 260: 131-134.

Iwai A, Masliah E, Yoshimoto M, Ge N, Flanagan L, de Silva HA, Kittel A, Saitoh T (1995) The precursor protein of non-A beta component of Alzheimer's disease amyloid is a presynaptic protein of the central nervous system. Neuron 14: 467-75.

Jaako K, Waniek A, Parik K, Klimaviciusa L, Aonurm-Helm A, Noortoots A, Anier K, Van Elzen R, Gérard M, Lambeir A-M, Robner S, Morawski M, Zharkovsky A (2016) Prolyl endopeptidase is involved in the degradation of neural cell adhesion molecules in vitro Journal of Cell Science 129: 3792-3802.

Jackson KW, Christiansen VJ, Yadav VR, Silasi-Mansat R, Lupu F, Awasthi V, Zhang RR, McKee PA (2015) Suppression of tumor growth in mice by rationally designed pseudopeptide inhibitors of fibroblast activation protein and prolyl oligopeptidase. Neoplasia 17: 43-54.

Jalkanen AJ, Leikas JV, Forsberg MM (2014a) KYP-2047 penetrates mouse brain and effectively inhibits mouse prolyl oligopeptidase. Basic and Clinical Pharmacology and Toxicology 114: 460-463.

Jalkanen AJ, Leikas JV, Forsberg MM (2014b) Prolyl oligopeptidase inhibition decreases extracellular acetylcholine levels in rat hippocampus and prefrontal cortex. Neurosci Lett 579: 110-113.

Jalkanen AJ, Piepponen TP, Hakkarainen JJ, De Meester I, Lambeir AM, Forsberg MM (2012) The effect of prolyl oligopeptidase inhibition on extracellular acetylcholine and dopamine levels in the rat striatum. Neurochemistry International 60: 301-309.

Jalkanen AJ, Puttonen KA, Venäläinen JI, Sinervä V, Mannila A, Ruotsalainen S, Jarho EM, Wallén EA, Männistö PT (2007) Beneficial effect of prolyl oligopeptidase inhibition on spatial memory in young but not in old scopolamine-treated rats. Basic & clinical pharmacology & toxicology 100: 132-8.

Jalkanen AJ, Savolainen K, Forsberg MM (2011) Inhibition of prolyl oligopeptidase by KYP-2047 fails to increase the extracellular neurotensin and substance P levels in rat striatum. Neuroscience Letters 502: 107-111.

Jankovic J, Goodman I, Safirstein B, Marmon TK, Schenk DB, Koller M, Zago W, Ness DK, Griffith SG, Grundman M, Soto J, Ostrowitzki S, Boess FG, Martin-Facklam M, Quinn JF, Isaacson SH, Omidvar O, Ellenbogen A, Kinney GG (2018) Safety and

Tolerability of Multiple Ascending Doses of PRX002/RG7935, an Anti-α-Synuclein Monoclonal Antibody, in Patients With Parkinson Disease: A Randomized Clinical Trial. JAMA neurology 75: 1206-1214.

Jarho EM (2000) Uusien Prolyyli oligopeptidaasi inhibiittoreiden synteesi Department of Pharmaceutical Chemistry. University Of Kuopio

Jarho EM, Wallén EAA, Christiaans JAM, Forsberg MM, Venäläinen JI, Männistö PT, Gynther J, Poso A (2005) Dicarboxylic acid azacycle L-prolyl-pyrrolidine amides as prolyl oligopeptidase inhibitors and three-dimensional quantitative structure-activity relationship of the enzyme-inhibitor interactions. Journal of Medicinal Chemistry 48: 4772-4782.

Jarho EM, Venäläinen JI, Juntunen J, Yli-Kokko AL, Vepsäläinen J, Christiaans JAM, Forsberg MM, Järvinen T, Männistö PT, Wallén EAA (2006) An introduction of a pyridine group into the structure of prolyl oligopeptidase inhibitors. Bioorganic and Medicinal Chemistry Letters 16: 5590-5593.

Jiang D-X, Zhang J-B, Li M-T, Lin S-Z, Wang Y-Q, Chen Y-W, Fan J-G (2020) Prolyl endopeptidase gene disruption attenuates high fat diet-induced nonalcoholic fatty liver disease in mice by improving hepatic steatosis and inflammation. Annals of Translational Medicine 8: 218.

Julku UH, Panhelainen AE, Tiilikainen SE, Svarcbahs R, Tammimäki AE, Piepponen TP, Savolainen MH, Myöhänen TT (2018) Prolyl Oligopeptidase Regulates Dopamine Transporter Phosphorylation in the Nigrostriatal Pathway of Mouse. Molecular Neurobiology 55: 470-482.

Kahyaoglu A, Haghjoo K, Kraicsovitsk F, Jordan F, Polgar L (1997) Benzyloxycarbonylprolylprolinal, a transition-state analogue for prolyl oligopeptidase, forms a tetrahedral adduct with catalytic serine, not a reactive cysteine. Biochemical Journal 322: 839-843.

Kaizuka T, Morishita H, Hama Y, Tsukamoto S, Matsui T, Toyota Y, Kodama A, Ishihara T, Mizushima T, Mizushima N (2016) An Autophagic Flux Probe that Releases an Internal Control. Molecular Cell 64: 835-849.

Kamori M, Hagihara M, Nagatsu T, Iwata H, Miura T (1991) Activities of dipeptidyl peptidase II, dipeptidyl peptidase IV, prolyl endopeptidase, and collagenase-like peptidase in synovial membrane from patients with rheumatoid arthritis and osteoarthritis. Biochem Med Metab Biol 45: 154-60.

Kaszuba K, Róg T, Danne R, Canning P, Fülöp V, Juhász T, Szeltner Z, St. Pierre JF, García-Horsman A, Männistö PT, Karttunen M, Hokkanen J, Bunker A (2012) Molecular dynamics, crystallography and mutagenesis studies on the substrate gating mechanism of prolyl oligopeptidase. Biochimie 94: 1398-1411.

Kato A, Fukunari A, Sakai Y, Nakajima T (1997) Prevention of amyloid-like deposition by a selective prolyl endopeptidase inhibitor, Y-29794, in senescence-accelerated mouse. The Journal of pharmacology and experimental therapeutics 283: 328-335.

Katsube N, Sunaga K, Aishita H, Chuang DM, Ishitani R (1999) ONO-1603, a potential antidementia drug, delays age-induced apoptosis and suppresses overexpression of glyceraldehyde-3-phosphate dehydrogenase in cultured central nervous system neurons. The Journal of pharmacology and experimental therapeutics 288: 6-13.

Katsube N, Sunaga K, Chuang DM, Ishitani R (1996) ONO-1603, a potential antidementia drug, shows neuroprotective effects and increases m3-muscarinic receptor mRNA levels in differentiating rat cerebellar granule neurons. Neuroscience letters 214: 151-154.

Kaushik S, Etchebest C, Sowdhamini R (2014) Decoding the structural events in substrate-gating mechanism of eukaryotic prolyl oligopeptidase using normal mode analysis and molecular dynamics simulations. 82: 1428-1443.

Kichik N, Tarragó T, Claasen B, Gairí M, Millet O, Giralt E (2011) 15N relaxation NMR studies of prolyl oligopeptidase, an 80 kDa enzyme, reveal a pre-existing equilibrium between different conformational states. ChemBioChem 12: 2737-2739.

King J, Keim M, Teo R, Weening KE, Kapur M, McQuillan K, Ryves J, Rogers B, Dalton E, Williams RS, Harwood AJ (2010) Genetic control of lithium sensitivity and regulation of inositol biosynthetic genes. PLoS One 5: e11151.

Klegeris A, Li J, Bammler T, Jin J, Zhu D, Kashima D, Pan S, Hashioka S, Maguire J, McGeer P, Zhang J (2008) Prolyl endopeptidase is revealed following SILAC analysis to be a novel mediator of human microglial and THP-1 cell neurotoxicity. Glia 56: 675-685.

Klimaviciusa L, Jain RK, Jaako K, Van Elzen R, Gerard M, van Der Veken P, Lambeir AM, Zharkovsky A (2012) In situ prolyl oligopeptidase activity assay in neural cell cultures. Journal of neuroscience methods 204: 104-110.

Koida M, Walter R (1976) Post-proline cleaving enzyme. Purification of this endopeptidase by affinity chromatography. The Journal of biological chemistry 251: 7593-9.

Kramer ML, Schulz-Schaeffer WJ (2007) Presynaptic alpha-synuclein aggregates, not Lewy bodies, cause neurodegeneration in dementia with Lewy bodies. The Journal of neuroscience : the official journal of the Society for Neuroscience 27: 1405-10.

Krupina NA, Bogdanova NG, Khlebnikova NN, Zolotov NN, Kryzhanovskii GN (2013) Benzyloxycarbonyl-Methionyl-2(S)-Cyanopyrrolidine, a Prolyl Endopeptidase Inhibitor, Modulates Depression-Like Behavior of Rats in Forced Swimming Test and Activities of Proline-Specific Peptidases in the Brain Structures. Bulletin of Experimental Biology and Medicine 154: 606-609.

Kumar N, Nakagawa P, Janic B, Romero CA, Worou ME, Monu SR, Peterson EL, Shaw J, Valeriote F, Ongeri EM, Niyitegeka JM, Rhaleb NE, Carretero OA (2016) The anti-inflammatory peptide Ac-SDKP is released from thymosin-β4 by renal meprin-α and prolyl oligopeptidase. American journal of physiology Renal physiology 310: 1026-34.

Larrinaga G, Perez I, Blanco L, López JI, Andrés L, Etxezarraga C, Santaolalla F, Zabala A, Varona A, Irazusta J (2010) Increased prolyl endopeptidase activity in human neoplasia. Regulatory Peptides 163: 102-106.

Larrinaga G, Perez I, Blanco L, Sanz B, Errarte P, Beitia M, Etxezarraga MC, Loizate A, Gil J, Irazusta J, López JI (2014) Prolyl endopeptidase activity is correlated with colorectal cancer prognosis. Int J Med Sci 11: 199-208.

Lawandi J, Gerber-Lemaire S, Juillerat-Jeanneret L, Moitessier N (2010) Inhibitors of prolyl oligopeptidases for the therapy of human diseases: Defining diseases and inhibitors. Journal of Medicinal Chemistry 53: 3423-3438.

Lee FJ, Liu F, Pristupa ZB, Niznik HB (2001) Direct binding and functional coupling of alpha-synuclein to the dopamine transporters accelerate dopamine-induced apoptosis. FASEB journal : official publication of the Federation of American Societies for Experimental Biology 15: 916-26.

Lee MK, Stirling W, Xu Y, Xu E, Qui D, Mandir AS, Dawson TM, Copeland NG, Jenkins NA, Price DL (2002) Human α-synuclein-harboring familial Parkinson's disease-linked Ala-53 → Thr mutation causes neurodegenerative disease with α-synuclein aggregation in transgenic mice. Proceedings of the National Academy of Sciences of the United States of America 99: 8968-8973.

Leprince J, Cosquer D, Bellemère G, Chatenet D, Tollemer H, Jégou S, Tonon M-C, Vaudry H (2006) Catabolism of the octadecaneuropeptide ODN by prolyl endopeptidase: Identification of an unusual cleavage site. Peptides 27: 1561-1569.

Leverenz JB, Umar I, Wang Q, Montine TJ, McMillan PJ, Tsuang DW, Jin J, Pan C, Shin J, Zhu D, Zhang J (2007) Proteomic identification of novel proteins in cortical lewy bodies. Brain pathology (Zurich, Switzerland) 17: 139-45.

Li X, James S, Lei P (2016) Interactions Between α-Synuclein and Tau Protein: Implications to Neurodegenerative Disorders. Journal of Molecular Neuroscience 60: 298-304.

Liu JM, Kusinski M, Ilic V, Bignon J, Hajem N, Komorowski J, Kuzdak K, Stepien H, Wdzieczak-Bakala J (2008) Overexpression of the angiogenic tetrapeptide AcSDKP in human malignant tumors. Anticancer Research 28: 2813-2817.

López A, Herranz-Trillo F, Kotev M, Gairí M, Guallar V, Bernadó P, Millet O, Tarragó T, Giralt E (2016) Active-Site-Directed Inhibitors of Prolyl Oligopeptidase Abolish Its Conformational Dynamics. ChemBioChem 17: 913-917.

López A, Tarragó T, Giralt E (2011) Low molecular weight inhibitors of Prolyl Oligopeptidase: a review of compounds patented from 2003 to 2010. Expert opinion on therapeutic patents 21: 1023-44.

Loregian A, Palù G (2005) Disruption of protein-protein interactions: towards new targets for chemotherapy. J Cell Physiol 204: 750-62.

Lou H, Montoya SE, Alerte TN, Wang J, Wu J, Peng X, Hong CS, Friedrich EE, Mader SA, Pedersen CJ, Marcus BS, McCormack AL, Di Monte DA, Daubner SC, Perez RG (2010) Serine 129 phosphorylation reduces the ability of alpha-synuclein to regulate tyrosine hydroxylase and protein phosphatase 2A in vitro and in vivo. The Journal of biological chemistry 285: 17648-61.

Lu H, Zhou Q, He J, Jiang Z, Peng C, Tong R, Shi J (2020) Recent advances in the development of protein–protein interactions modulators: mechanisms and clinical trials. Signal Transduction and Targeted Therapy 5: 213.

Maes M, Goossens F, Scharpé S, Calabrese J, Desnyder R, Meltzer HY (1995) Alterations in plasma prolyl endopeptidase activity in depression, mania, and schizophrenia: effects of antidepressants, mood stabilizers, and antipsychotic drugs. Psychiatry Res 58: 217-225.

Maes M, Goossens F, Scharpé S, Meltzer H, D'Hondt P, Cosyns P (1994) Lower serum prolyl endopeptidase enzyme activity in major depression: further evidence that peptidases play a role in the pathophysiology of depression. Biol Pshychiatry 35: 545-552.

Maes MB, Lambeir AM, Gilany K, Senten K, Van der Veken P, Leiting B, Augustyns K, Scharpé S, De Meester I (2005) Kinetic investigation of human dipeptidyl peptidase II (DPPII)-mediated hydrolysis of dipeptide derivatives and its identification as quiescent cell proline dipeptidase (QPP)/dipeptidyl peptidase 7 (DPP7). The Biochemical journal 386: 315-24.

Maggi CA (1995) The mammalian tachykinin receptors. General Pharmacology: The Vascular System 26: 911-944.

Maggi CA (1997) The effects of tachykinins on inflammatory and immune cells. Regulatory Peptides 70: 75-90.

Mantle D, Falkous G, Ishiura S, Blanchard PJ, Perry EK (1996) Comparison of proline endopeptidase activity in brain tissue from normal cases and cases with Alzheimer's disease, Lewy body dementia, Parkinson's disease and Huntington's disease. Clinica Chimica Acta 249: 129-139.

Marighetto A, Touzani K, Etchamendy N, Torrea CC, De Nanteuil G, Guez D, Jaffard R, Morain P (2000) Further evidence for a dissociation between different forms of

mnemonic expressions in a mouse model of age-related cognitive decline: effects of tacrine and S 17092, a novel prolyl endopeptidase inhibitor. Learning & memory (Cold Spring Harbor, NY) 7: 159-69.

Matsuda T, Sakaguchi M, Tanaka S, Yoshimoto T, Takaoka M (2013) Prolyl oligopeptidase is a glyceraldehyde-3-phosphate dehydrogenase-binding protein that regulates genotoxic stress-induced cell death. International Journal of Biochemistry and Cell Biology 45: 850-857.

Miura N, Shibata S, Watanabe S (1995) Increase in the septal vasopressin content by prolyl endopeptidase inhibitors in rats. Neurosci Lett 196: 128-130.

Miura N, Shibata S, Watanabe S (1997) Z-321, a prolyl endopeptidase inhibitor, augments the potentiation of synaptic transmission in rat hippocampal slices. Behavioural Brain Research 83: 213-216.

Morain P, Lestage P, De Nanteuil G, Jochemsen R, Robin JL, Guez D, Boyer PA (2002) S 17092: A prolyl endopeptidase inhibitor as a potential therapeutic drug for memory impairment. Preclinical and clinical studies. CNS Drug Reviews 8: 31-52.

Moreno-Baylach MJ, Puttonen K, Tenorio-Laranga J, Venäläinen JI, Storvik M, Forsberg M, García-Horsman JA (2011) Prolyl endopeptidase is involved in cellular signalling in human neuroblastoma SH-SY5Y cells. Neurosignals 19: 97-109.

Moriyama A, Nakanishi M, Sasaki M (1988) Porcine muscle prolyl endopeptidase and its endogenous substrates. Journal of biochemistry 104: 112-7.

Myöhänen TT, Hannula MJ, Van Elzen R, Gerard M, Van Der Veken P, García-Horsman JA, Baekelandt V, Männistö PT, Lambeir AM (2012a) A prolyl oligopeptidase inhibitor, KYP-2047, reduces a-synuclein protein levels and aggregates in cellular and animal models of Parkinson's disease. British Journal of Pharmacology 166: 1097-1113.

Myöhänen TT, Norrbacka S, Savolainen MH (2017) Prolyl oligopeptidase inhibition attenuates the toxicity of a proteasomal inhibitor, lactacystin, in the alpha-synuclein overexpressing cell culture. Neuroscience Letters 636: 83-89.

Myöhänen TT, Pyykkö E, Männistö PT, Carpen O (2012b) Distribution of Prolyl Oligopeptidase in Human Peripheral Tissues and in Ovarian and Colorectal Tumors. Journal of Histochemistry and Cytochemistry 60: 706-715.

Myöhänen TT, Tenorio-Laranga J, Jokinen B, Vázquez-Sánchez R, Moreno-Baylach MJ, García-Horsman JA, Männistö PT (2011) Prolyl oligopeptidase induces angiogenesis both in vitro and in vivo in a novel regulatory manner. Br J Pharmacol 163: 1666-78.

Myöhänen TT, Venäläinen JI, Garcia-Horsman JA, Piltonen M, Männistö PT (2008a) Cellular and subcellular distribution of rat brain prolyl oligopeptidase and its association with specific neuronal neurotransmitters. The Journal of comparative neurology 507: 1694-708.

Myöhänen TT, Venäläinen JI, García-Horsman JA, Piltonen M, Männistö PT (2008b) Distribution of prolyl oligopeptidase in the mouse whole-body sections and peripheral tissues. Histochemistry and Cell Biology 130: 993-1003.

Myöhänen TT, Venäläinen JI, Tupala E, Garcia-Horsman JA, Miettinen R, Männistö PT (2007) Distribution of immunoreactive prolyl oligopeptidase in human and rat brain. Neurochemical Research 32: 1365-1374.

Männisto PT, Vanäläinen J, Jalkanen A, García-Horsman JA (2007) Prolyl oligopeptidase: A potential target for the treatment of cognitive disorders. Drug News and Perspectives 20: 293-305.

Nakajima T, Ono Y, Kato A, Maeda J, Ohe T (1992) Y-29794--a non-peptide prolyl endopeptidase inhibitor that can penetrate into the brain. Neuroscience letters 141: 156-160.

Natunen TA, Gynther M, Rostalski H, Jaako K, Jalkanen AJ (2019) Extracellular prolyl oligopeptidase derived from activated microglia is a potential neuroprotection target. Basic and Clinical Pharmacology and Toxicology 124: 40-49.

Nolte WM, Tagore DM, Lane WS, Saghatelian A (2009) Peptidomics of Prolyl Endopeptidase in the Central Nervous System. Biochemistry 48: 11971-11981.

Norrbacka S, Lindholm D, Myöhänen TT (2019) Prolyl oligopeptidase inhibition reduces PolyQ aggregation and improves cell viability in cellular model of Huntington's disease. Journal of Cellular and Molecular Medicine 23: 8511-8515.

Nykänen NP, Kysenius K, Sakha P, Tammela P, Huttunen HJ (2012) γ-aminobutyric acid type A (GABA A) receptor activation modulates Tau phosphorylation. Journal of Biological Chemistry 287: 6743-6752.

O'Reilly P, Jackson PL, Noerager B, Parker S, Dransfield M, Gaggar A, Blalock JE (2009) N-alpha-PGP and PGP, potential biomarkers and therapeutic targets for COPD. Respiratory research 10: 38.

Ogen-Shtern N, Ben David T, Lederkremer GZ (2016) Protein aggregation and ER stress. Brain Res 1648: 658-666.

Ohta N, Takahashi T, Mori T, Park MK, Kawashima S, Takahashi K, Kobayashi H (1992) Hormonal modulation of prolyl endopeptidase and dipeptidyl peptidase IV activities in the mouse uterus and ovary. Acta endocrinologica 127: 262-6.

Park JE, Lenter MC, Zimmermann RN, Garin-Chesa P, Old LJ, Rettig WJ (1999) Fibroblast activation protein, a dual specificity serine protease expressed in reactive human tumor stromal fibroblasts. The Journal of biological chemistry 274: 36505-12.

Peltonen I, Jalkanen AJ, Sinervä V, Puttonen KA, Männistö PT (2010) Different effects of scopolamine and inhibition of prolyl oligopeptidase on mnemonic and motility functions of young and 8- to 9-month-old rats in the radial-arm maze. Basic & clinical pharmacology & toxicology 106: 280-7.

Perez RE, Calhoun S, Shim D, Levenson VV, Duan L, Maki CG (2020) Prolyl endopeptidase inhibitor Y-29794 blocks the IRS1-AKT-mTORC1 pathway and inhibits survival and in vivo tumor growth of triple-negative breast cancer. Cancer Biol Ther 21: 1033-1040.

Perez RG, Waymire JC, Lin E, Liu JJ, Guo F, Zigmond MJ (2002) A Role for α-Synuclein in the Regulation of Dopamine Biosynthesis. The Journal of Neuroscience 22: 3090.

Petit A, Barelli H, Morain P, Checler F (2000) Novel proline endopeptidase inhibitors do not modify Abeta40/42 formation and degradation by human cells expressing wild-type and swedish mutated beta-amyloid precursor protein. Br J Pharmacol 130: 1613-7.

Plescia J, Dufresne C, Janmamode N, Wahba AS, Mittermaier AK, Moitessier N (2020) Discovery of covalent prolyl oligopeptidase boronic ester inhibitors. European Journal of Medicinal Chemistry 185: 111783.

Polgar L (1992) Unusual secondary specificity of prolyl oligopeptidase and the different reactivities of its two forms toward charged substrates. Biochemistry 31: 7729-7735.

Polgár L (1992) Prolyl endopeptidase catalysis. A physical rather than a chemical step is rate-limiting. The Biochemical journal 282: 647-648.

Polymeropoulos MH, Lavedan C, Leroy E, Ide SE, Dehejia A, Dutra A, Pike B, Root H, Rubenstein J, Boyer R, Stenroos ES, Chandrasekharappa S, Athanassiadou A, Papapetropoulos T, Johnson WG, Lazzarini AM, Duvoisin RC, Di Iorio G, Golbe LI, Nussbaum RL (1997) Mutation in the a-synuclein gene identified in families with Parkinson's disease. Science 276: 2045-2047.

Portevin B, Benoist A, Rémond G, Hervé Y, Vincent M, Lepagnol J, De Nanteuil G (1996) New Prolyl Endopeptidase Inhibitors: In Vitro and in Vivo Activities of

Azabicyclo[2.2.2]octane, Azabicyclo[2.2.1]heptane, and Perhydroindole Derivatives. Journal of Medicinal Chemistry 39: 2379-2391.

Prades R, Munarriz-Cuezva E, Urigüen L, Gil-Pisa I, Gómez L, Mendieta L, Royo S, Giralt E, Tarragó T, Meana JJ (2017) The prolyl oligopeptidase inhibitor IPR19 ameliorates cognitive deficits in mouse models of schizophrenia. Eur Neuropsychopharmacol 27: 180-191.

Puttonen KA, Lehtonen S, Raasmaja A, Männistö PT (2006) A prolyl oligopeptidase inhibitor, Z-Pro-Prolinal, inhibits glyceraldehyde-3-phosphate dehydrogenase translocation and production of reactive oxygen species in CV1-P cells exposed to 6-hydroxydopamine. Toxicology in vitro : an international journal published in association with BIBRA 20: 1446-54.

Qian W, Shi J, Yin X, Iqbal K, Grundke-Iqbal I, Gong CX, Liu F (2010) PP2A regulates tau phosphorylation directly and also indirectly via activating GSK-3beta. Journal of Alzheimer's disease : JAD 19: 1221-9.

Rabey FM, Gadepalli RSVS, Diano S, Cheng Q, Tabrizian T, Gailani D, Rimoldi JM, Shariat-Madar Z (2012) Influence of a novel inhibitor (UM8190) of prolylcarboxypeptidase (PRCP) on appetite and thrombosis. Curr Med Chem 19: 4194-4206.

Rampon C, Jiang CH, Dong H, Tang Y-P, Lockhart DJ, Schultz PG, Tsien JZ, Hu Y (2000) Effects of environmental enrichment on gene expression in the brain. 97: 12880-12884.

Rea D, Fülöp V (2006) Structure-function properties of prolyl oligopeptidase family enzymes. Cell Biochemistry and Biophysics 44: 349-365.

Richfield EK, Thiruchelvam MJ, Cory-Slechta DA, Wuertzer C, Gainetdinov RR, Caron MG, Di Monte DA, Federoff HJ (2002) Behavioral and neurochemical effects of wild-type and mutated human a-synuclein in transgenic mice. Experimental Neurology 175: 35-48.

Roda MA, Sadik M, Gaggar A, Hardison MT, Jablonsky MJ, Braber S, Blalock JE, Redegeld FA, Folkerts G, Jackson PL (2014) Targeting prolyl endopeptidase with valproic acid as a potential modulator of neutrophilic inflammation. PLoS ONE 9.

Rostami J, Jäntti M, Cui H, Rinne MK, Kukkonen JP, Falk A, Erlandsson A, Myöhänen T (2020) Prolyl oligopeptidase inhibition by KYP-2407 increases alpha-synuclein fibril degradation in neuron-like cells. Biomedicine & Pharmacotherapy 131: 110788.

Rubinsztein DC (2006) The roles of intracellular protein-degradation pathways in neurodegeneration. Nature 443: 780-6.

Russell DW, Hardison M, Genschmer KR, Szul T, Bratcher PE, Abdul Roda M, Xu X, Viera L, Blalock JE, Gaggar A, Noerager BD (2019) Benzyloxycarbonyl-proline-prolinal (ZPP): Dual complementary roles for neutrophil inhibition. Biochemical and Biophysical Research Communications 517: 691-696.

Saito M, Hashimoto M, Kawaguchi N, Fukami H, Tanaka T, Higuchi N (1990) Synthesis and inhibitory activity of acylpeptidyl-prolinal derivatives toward post-proline cleaving enzyme as nootropic agents. Journal of Enzyme Inhibition and Medicinal Chemistry 3: 163-178.

Saito M, Hashimoto M, Kawaguchi N, Shibata H, Fukami H, Tanaka T, Higuchi N (1991) Synthesis and Inhibitory Activity of Acyl-Peptidyl-Pyrrolidine Derivatives Toward Post-Proline Cleaving Enzyme; A Study of Subsite Specificity. Journal of Enzyme Inhibition 5: 51-75.

Sakaguchi M, Matsuda T, Matsumura E, Yoshimoto T, Takaoka M (2011) Prolyl oligopeptidase participates in cell cycle progression in a human neuroblastoma cell line. Biochemical and Biophysical Research Communications 409: 693-698.

Salers P (1994) Evidence for the presence of prolyl oligopeptidase and its endogenous inhibitor in neonatal rat pancreatic beta-cells. Regul Pept 50: 235-45.

Santana JM, Grellier P, Schrével J, Teixeira AR (1997) A Trypanosoma cruzi-secreted 80 kDa proteinase with specificity for human collagen types I and IV. The Biochemical journal 325 (Pt 1): 129-37.

Savolainen MH, Richie CT, Harvey BK, Männistö PT, Maguire-Zeiss KA, Myöhänen TT (2014) The beneficial effect of a prolyl oligopeptidase inhibitor, KYP-2047, on alpha-synuclein clearance and autophagy in A30P transgenic mouse. Neurobiology of Disease 68: 1-15.

Savolainen MH, Yan X, Myöhänen TT, Huttunen HJ (2015) Prolyl oligopeptidase enhances a-Synuclein dimerization via direct protein-protein interaction. Journal of Biological Chemistry 290: 5117-5126.

Schlesinger K, Pelleymounter MA, Kamp Jvd, Bader DL, Stewart JM, Chase TN (1986) Substance P facilitation of memory: Effects in an appetitively motivated learning task. Behavioral and Neural Biology 45: 230-239.

Schneider JS, Giardiniere M, Morain P (2002) Effects of the prolyl endopeptidase inhibitor S 17092 on cognitive deficits in chronic low dose MPTP-treated monkeys. Neuropsychopharmacology : official publication of the American College of Neuropsychopharmacology 26: 176-82.

Schrag A, Schott JM (2006) Epidemiological, clinical, and genetic characteristics of early-onset parkinsonism. The Lancet Neurology 5: 355-63.

Schulz-Schaeffer WJ (2010) The synaptic pathology of alpha-synuclein aggregation in dementia with Lewy bodies, Parkinson's disease and Parkinson's disease dementia. Acta Neuropathol 120: 131-43.

Schulz I, Gerhartz B, Neubauer A, Holloschi A, Heiser U, Hafner M, Demuth H-U (2002) Modulation of inositol 1,4,5-triphosphate concentration by prolyl endopeptidase inhibition. European Journal of Biochemistry 269: 5813-5820.

Schulz I, Zeitschel U, Rudolph T, Ruiz-Carrillo D, Rahfeld JU, Gerhartz B, Bigl V, Demuth HU, Roßner S (2005) Subcellular localization suggests novel functions for prolyl endopeptidase in protein secretion. Journal of Neurochemistry 94: 970-979.

Scrivo A, Bourdenx M, Pampliega O, Cuervo AM (2018) Selective autophagy as a potential therapeutic target for neurodegenerative disorders. The Lancet Neurology 17: 802-815.

Serfozo P, Wysocki J, Gulua G, Schulze A, Ye M, Liu P, Jin J, Bader M, Myöhänen T, García-Horsman JA, Batlle D (2020) Ang II (Angiotensin II) Conversion to Angiotensin-(1-7) in the Circulation Is POP (Prolyloligopeptidase)-Dependent and ACE2 (Angiotensin-Converting Enzyme 2)-Independent. Hypertension (Dallas, Tex : 1979) 75: 173-182.

Shan L, Marti T, Sollid LM, Gray GM, Khosla C (2004) Comparative biochemical analysis of three bacterial prolyl endopeptidases: implications for coeliac sprue. The Biochemical journal 383: 311-318.

Shinoda M, Miyazaki A, Toide K (1999) Effect of a novel prolyl endopeptidase inhibitor, JTP-4819, on spatial memory and on cholinergic and peptidergic neurons in rats with ibotenate-induced lesions of the nucleus basalis magnocellularis. Behavioural Brain Research 99: 17-25.

Shinoda M, Okamiya K, Toide K (1995) Effect of a Novel Prolyl Endopeptidase Inhibitor, JTP-4819, on Thyrotropin-Releasing Hormone-Like Immunoreactivity in the Cerebral Cortex and Hippocampus of Aged Rats. Japanese Journal of Pharmacology 69: 273-276.

Shinoda M, Toide K, Ohsawa I, Kohsaka S (1997) Specific Inhibitor for Prolyl Endopeptidase Suppresses the Generation of Amyloid β Protein in NG108-15 Cells. Biochemical and Biophysical Research Communications 235: 641-645.

Shishido Y, Furushiro M, Tanabe S, Shibata S, Hashimoto S, Yokokura T (1999) Effects of prolyl endopeptidase inhibitors and neuropeptides on delayed neuronal death in rats. Eur J Pharmacol 372: 135-42.

Shishido Y, Furushiro M, Tanabe S, Taniguchi A, Hashimoto S, Yokokura T, Shibata S, Yamamoto T, Watanabe S (1998) Effect of ZTTA, a prolyl endopeptidase inhibitor, on memory impairment in a passive avoidance test of rats with basal forebrain lesions. Pharm Res 15: 1907-1910.

Singleton AB, Farrer M, Johnson J, Singleton A, Hague S, Kachergus J, Hulihan M, Peuralinna T, Dutra A, Nussbaum R, Lincoln S, Crawley A, Hanson M, Maraganore D, Adler C, Cookson MR, Muenter M, Baptista M, Miller D, Blancato J, Hardy J, Gwinn-Hardy K (2003) α-Synuclein Locus Triplication Causes Parkinson's Disease. 302: 841-841.

Sirviö J, Lehtimäki T (2005) Prolyl oligopeptidase inhibitors ameliorating recovery from brain trauma. In: Corporation O (ed), Finland

Spillantini MG, Schmidt ML, Lee VMY, Trojanowski JQ, Jakes R, Goedert M (1997) α-Synuclein in Lewy bodies. Nature 388: 839-840.

Suzuki K, Sakaguchi M, Tanaka S, Yoshimoto T, Takaoka M (2013) Prolyl oligopeptidase inhibition-induced growth arrest of human gastric cancer cells. BIchem Biophys Res commun 443: 91-6.

Svarcbahs R, Julku UH, Myöhänen TT (2016) Inhibition of prolyl oligopeptidase restores spontaneous motor behavior in the ÷-synuclein virus vector-based parkinson's disease mouse model by decreasing a-synuclein oligomeric species in mouse brain. Journal of Neuroscience 36: 12485-12497.

Svarcbahs R, Julku UH, Norrbacka S, Myöhänen TT (2018) Removal of prolyl oligopeptidase reduces alpha-synuclein toxicity in cells and in vivo. Scientific Reports 8.

Svarcbahs R, Jäntti M, Kilpeläinen T, Julku UH, Urvas L, Kivioja S, Norrbacka S, Myöhänen TT (2020) Prolyl oligopeptidase inhibition activates autophagy via protein phosphatase 2A. Pharmacological Research 151.

Szeltner Z, Juhász T, Szamosi I, Rea D, Fülöp V, Módos K, Juliano L, Polgár L (2013) The loops facing the active site of prolyl oligopeptidase are crucial components in substrate gating and specificity. Biochimica et Biophysica Acta (BBA) - Proteins and Proteomics 1834: 98-111.

Szeltner Z, Morawski M, Juhász T, Szamosi I, Liliom K, Csizmók V, Tölgyesi F, Polgár L (2010) GAP43 shows partial co-localisation but no strong physical interaction with prolyl oligopeptidase. Biochimica et Biophysica Acta (BBA) - Proteins and Proteomics 1804: 2162-2176.

Szeltner Z, Rea D, Juhász T, Renner V, Fülöp V, Polgár L (2004) Concerted structural changes in the peptidase and the propeller domains of prolyl oligopeptidase are required for substrate binding. J Mol Biol 340: 627-37.

Takahashi S, Kawano T, Nakajima N, Suda Y, Usukhbayar N, Kimura KI, Koshino H (2018) Synthesis of polyozellin, a prolyl oligopeptidase inhibitor, and its structural revision.

Tanaka S, Suzuki K, Sakaguchi M (2017) The prolyl oligopeptidase inhibitor SUAM-14746 attenuates the proliferation of human breast cancer cell lines in vitro. Breast cancer (Tokyo, Japan) 24: 658-666.

Tanaka Y, Niwa S, Nishioka H, Yamanaka T, Torizuka M, Yoshinaga K, Kobayashi N, Ikeda Y, Arai H (1994) New Potent Prolyl Endopeptidase Inhibitors: Synthesis and

Structure-Activity Relationships of Indan and Tetralin Derivatives and Their Analogs. Journal of Medicinal Chemistry 37: 2071-2078.

Tarragó T, Kichik N, Claasen B, Prades R, Teixidó M, Giralt E (2008a) Baicalin, a prodrug able to reach the CNS, is a prolyl oligopeptidase inhibitor. Bioorg Med Chem 16: 7516-7524.

Tarragó T, Martín-Benito J, Sabidó E, Claasen B, Madurga S, Gairí M, Valpuesta JM, Giralt E (2009) A new side opening on prolyl oligopeptidase revealed by electron microscopy. FEBS Letters 583: 3344-3348.

Tarragó T, Masdeu C, Gómez E, Isambert N, Lavilla R, Giralt E (2008b) Benzimidazolium salts as small, nonpeptidic and BBB-permeable human prolyl oligopeptidase inhibitors. ChemMedChem 3: 1558-65.

Tenorio-Laranga J, Coret-Ferrer F, Casanova-Estruch B, Burgal M, García-Horsman JA (2010) Prolyl oligopeptidase is inhibited in relapsing-remitting multiple sclerosis. J Neuroinflammation 7: 23-23.

Tenorio-Laranga J, Montoliu C, Urios A, Hernández-Rabaza V, Ahabrach H, Garcia-horsman J, Felipo V (2015) The expression levels of prolyl oligopeptidase responds not only to neuroinflammation but also to systemic inflammation upon liver failure in rat models and cirrhotic patients. J Neuroinflammation 12.

Tenorio-Laranga J, Männistö PT, Storvik M, Van der Veken P, García-Horsman JA (2012) Four day inhibition of prolyl oligopeptidase causes significant changes in the peptidome of rat brain, liver and kidney. Biochimie 94: 1849-59.

Tenorio-Laranga J, Peltonen I, Keskitalo S, Duran-Torres G, Natarajan R, Männistö PT, Nurmi A, Vartiainen N, Airas L, Elovaara I, García-Horsman JA (2013) Alteration of prolyl oligopeptidase and activated α-2-macroglobulin in multiple sclerosis subtypes and in the clinically isolated syndrome. Biochem Pharmacol 85: 1783-94.

Tenorio-Laranga J, Venäläinen JI, Männistö PT, García-Horsman JA (2008) Characterization of membrane-bound prolyl endopeptidase from brain. The FEBS journal 275: 4415-27.

Toide K, Iwamoto Y, Fujiwara T, Abe H (1995a) JTP-4819: A novel prolyl endopeptidase inhibitor with potential as a cognitive enhancer. Journal of Pharmacology and Experimental Therapeutics 274: 1370-1378.

Toide K, Okamiya K, Iwamoto Y, Kato T (1995b) Effect of a Novel Prolyl Endopeptidase Inhibitor, JTP-4819, on Prolyl Endopeptidase Activity and Substance P- and Arginine-Vasopressin-Like Immunoreactivity in the Brains of Aged Rats. Journal of Neurochemistry 65: 234-240.

Toide K, Shinoda M, Fujiwara T, Iwamoto Y (1997a) Effect of a Novel Prolyl Endopeptidase Inhibitor, JTP-4819, on Spatial Memory and Central Cholinergic Neurons in Aged Rats. Pharmacology Biochemistry and Behavior 56: 427-434.

Toide K, Shinoda M, Iwamoto Y, Fujiwara T, Okamiya K, Uemura A (1997b) A novel prolyl endopeptidase inhibitor, JTP-4819, with potential for treating Alzheimer's disease. Behav Brain Res 83: 147-51.

Tsirigotaki A, Van Elzen R, Van Der Veken P, Lambeir AM, Economou A (2017) Dynamics and ligand-induced conformational changes in human prolyl oligopeptidase analyzed by hydrogen/deuterium exchange mass spectrometry. Scientific Reports 7.

Tsutsumi S, Okonogi T, Shibahara S, Ohuchi S, Hatsushiba E, Patchett AA, Christensen BG (1994) Synthesis and Structure-Activity Relationships of Peptidyl .alpha.-Keto Heterocycles as Novel Inhibitors of Prolyl Endopeptidase. Journal of Medicinal Chemistry 37: 3492-3502.

Umemura K, Kondo K, Ikeda Y, Kobayashi T, Urata Y, Nakashima M (1997) Pharmacokinetics and safety of JTP-4819, a novel specific orally active prolyl

endopeptidase inhibitor, in healthy male volunteers. Br J Clin Pharmacol 43: 613-618.

Umemura K, Kondo K, Ikeda Y, Nishimoto M, Hiraga Y, Yoshida Y, Nakashima M (1999) Pharmacokinetics and safety of Z-321, a novel specific orally active prolyl endopeptidase inhibitor, in healthy male volunteers. Journal of clinical pharmacology 39: 462-70.

Unger EL, Eve DJ, Perez XA, Reichenbach DK, Xu Y, Lee MK, Andrews AM (2006) Locomotor hyperactivity and alterations in dopamine neurotransmission are associated with overexpression of A53T mutant human alpha-synuclein in mice. Neurobiol Dis 21: 431-43.

Wallén EAA, Christiaans JAM, Jarho EM, Forsberg MM, Venäläinen JI, Männistö PT, Gynther J (2003a) New prolyl oligopeptidase inhibitors developed from dicarboxylic acid bis(L-prolyl-pyrrolidine) amides. Journal of Medicinal Chemistry 46: 4543-4551.

Wallén EAA, Christiaans JAM, Saarinen TJ, Jarho EM, Forsberg MM, Venäläinen JI, Männistö PT, Gynther J (2003b) Conformationally rigid N-acyl-5-alkyl-L-prolyl-pyrrolidines as prolyl oligopeptidase inhibitors. Bioorganic and Medicinal Chemistry 11: 3611-3619.

Wallén EAA, Christiaans JAM, Saario SM, Forsberg MM, Venäläinen JI, Paso HM, Männistö PT, Gynther J (2002) 4-Phenylbutanoyl-2(S)-acylpyrrolidines and 4-phenylbutanoyl-L-prolyl-2(S)-acylpyrrolidines as prolyl oligopeptidase inhibitors. Bioorganic and Medicinal Chemistry 10: 2199-2206.

Walter R, Shlank H, Glass JD, Schwartz IL, Kerenyi TD (1971) Leucylglycinamide released from oxytocin by human uterine enzyme. Science 173: 827-9.

Van Der Veken P, Fülöp V, Rea D, Gerard M, Van Elzen R, Joossens J, Cheng JD, Baekelandt V, De Meester I, Lambeir AM, Augustyns K (2012) P2-substituted N-acylprolylpyrrolidine inhibitors of prolyl oligopeptidase: Biochemical evaluation, binding mode determination, and assessment in a cellular model of synucleinopathy. Journal of Medicinal Chemistry 55: 9856-9867.

Vanhoof G, Goossens F, Hendriks L, De Meester I, Hendriks D, Vriend G, Van Broeckhoven C, Scharpé S (1994) Cloning and sequence analysis of the gene encoding human lymphocyte prolyl endopeptidase. Gene 149: 363-366.

Venditti M, Chemek M, Minucci S, Messaoudi I (2020a) Cadmium-induced toxicity increases prolyl endopeptidase (PREP) expression in the rat testis. Molecular reproduction and development 87: 565-573.

Venditti M, Fasano C, Minucci S, Serino I, Sinisi AA, Dale B, Di Matteo L (2020b) DAAM1 and PREP are involved in human spermatogenesis. Reproduction, fertility, and development 32: 484-494.

Venäläinen JI, Garcia-Horsman JA, Forsberg MM, Jalkanen A, Wallén EAA, Jarho EM, Christiaans JAM, Gynther J, Männistö PT (2006) Binding kinetics and duration of in vivo action of novel prolyl oligopeptidase inhibitors. Biochemical Pharmacology 71: 683-692.

Venäläinen JI, Juvonen RO, Forsberg MM, Garcia-Horsman A, Poso A, Wallen EAA, Gynther J, Männistö PT (2002) Substrate-dependent, non-hyperbolic kinetics of pig brain prolyl oligopeptidase and its tight binding inhibition by JTP-4819. Biochemical Pharmacology 64: 463-471.

Venäläinen JI, Juvonen RO, Männistö PT (2004) Evolutionary relationships of the prolyl oligopeptidase family enzymes. Eur J Biochem 271: 2705-15.

Wersinger C, Sidhu A (2005) Disruption of the interaction of alpha-synuclein with microtubules enhances cell surface recruitment of the dopamine transporter. Biochemistry 44: 13612-24.

Wilk S, Orlowski M (1983) Inhibition of Rabbit Brain Prolyl Endopeptidase by N-Benzyloxycarbonyl-Prolyl-Prolinal, a Transition State Aldehyde Inhibitor. Journal of Neurochemistry 41: 69-75.

Williams RS, Eames M, Ryves WJ, Viggars J, Harwood AJ (1999) Loss of a prolyl oligopeptidase confers resistance to lithium by elevation of inositol (1,4,5) trisphosphate. EMBO J 18: 2734-2745.

Wong P-M, Feng Y, Wang J, Shi R, Jiang X (2015) Regulation of autophagy by coordinated action of mTORC1 and protein phosphatase 2A. Nature Communications 6: 8048.

Yang W, Hamilton JL, Kopil C, Beck JC, Tanner CM, Albin RL, Ray Dorsey E, Dahodwala N, Cintina I, Hogan P, Thompson T (2020) Current and projected future economic burden of Parkinson's disease in the U.S. npj Parkinson's Disease 6: 15.

Yasuda Y, Mizutani S, Kurauchi O, Kasugai M, Narita O, Tomoda Y (1992) Induction by cortisol of aminopeptidases production from the human placenta in tissue culture. Horm Metab Res 24: 110-114.

Yasuhiko M (2011) Prolyl oligopeptidase inhibitor (Data in Japanese)

Yavich L, Tanila H, Vepsäläinen S, Jäkälä P (2004) Role of alpha-synuclein in presynaptic dopamine recruitment. The Journal of neuroscience : the official journal of the Society for Neuroscience 24: 11165-11170.

Yoshimoto T, Kado K, Matsubara F, Koriyama N, Kaneto H, Tsura D (1987) Specific inhibitors for prolyl endopeptidase and their anti-amnesic effect. Journal of pharmacobio-dynamics 10: 730-5.

Yoshimoto T, Tsukumo K, Takatsuka N, Tsuru D (1982) An inhibitor for post-proline cleaving enzyme; distribution and partial purification from porcine pancreas. Journal of pharmacobio-dynamics 5: 734-40.

Yoshimoto T, Tsuru D, Yamamoto N, Ikezawa R, Furukawa S (1991) Structure activity relationship of inhibitors specific for prolyl endopeptidase. Agric Biol Chem 55: 37-43.

Yoshimura Y, Hiramatsu Y, Sato Y, Homma S, Enomoto Y, Jikuya T, Sakakibara Y (2003) ONO-6818, a novel, potent neutrophil elastase inhibitor, reduces inflammatory mediators during simulated extracorporeal circulation. The Annals of thoracic surgery 76: 1234-9.

Zhou D, Li B-H, Wang J, Ding Y-N, Dong Y, Chen Y-W, Fan J-G (2016) Prolyl Oligopeptidase Inhibition Attenuates Steatosis in the L02 Human Liver Cell Line. PLOS ONE 11: e0165224.

Zhou D, Wang J, He LN, Li BH, Ding YN, Chen YW, Fan JG (2017) Prolyl oligopeptidase attenuates hepatic stellate cell activation through induction of Smad7 and PPAR-γ.